NEW EFFICIENT POWER ALLOCATION, CELL FORMATION, AND LOAD BALANCING PROTOCOLS FOR VISIBLE LIGHT COMMUNICATION NETWORKS

BY

MOHANAD ALI ABDULWAHID OBEED

A Dissertation Presented to the

DEANSHIP OF GRADUATE STUDIES

KING FAHD UNIVERSITY OF PETROLEUM & MINERALS

DHAHRAN, SAUDI ARABIA

In Partial Fulfillment of the
Requirements for the Degree of

DOCTOR OF PHILOSOPHY

In

ELECTRICAL ENGINEERING

MAY 2019

KING FAHD UNIVERSITY OF PETROLEUM & MINERALS
DHAHRAN 31261, SAUDI ARABIA

DEANSHIP OF GRADUATE STUDIES

This dissertation, written by **MOHANAD OBEED** under the direction of his dissertation adviser and approved by his dissertation committee, has been presented to and accepted by the Dean of Graduate Studies, in partial fulfillment of the requirements for the degree of **DOCTOR OF PHILOSOPHY IN ELECTRICAL ENGINEERING**.

Dissertation Committee

Prof. Salam A. Zummo (Adviser)

Dr. Anas M. Salhab (Co-Adviser)

Prof. Mohamed-Slim Alouini (Member)

Dr. Wessam Mesbah (Member)

Dr. Samir Al-Ghadhban (Member)

Dr. Abdallah S. Al-Ahmari
Department Chairman

Prof. Salam A. Zummo
Dean of Graduate Studies

21/7/2019
Date

To my parents, wife, siblings, my son, and my daughter

ACKNOWLEDGMENTS

TABLE OF CONTENTS

CHAPTER 5 DC-BIAS AND POWER ALLOCATION IN COOP-ERATIVE VLC NETWORKS FOR JOINT INFORMATION AND ENERGY TRANSFER 134

CHAPTER 6 CONCLUSION AND FUTURE WORK 171

LIST OF TABLES

LIST OF FIGURES

xiv

LIST OF ABBREVIATIONS

5G   fifth-generation

AC   alternating current

ACO-OFDM asymmetrically-clipped optical OFDM

AP   access point

APA   APs' assignment

BS   base station

CoMP   coordinated multi-point

Co-NOMA   cooperative non-orthogonal multiple-access

CSI   channel state information

DC   direct-current

DCO-OFDM DC-biased optical OFDM

DD   direct detection

EE   energy efficiency

EHUs   energy-harvesting users

FoV   field-of-view

GEE   global EE

H-FoV	half-FoV
IM	intensity modulation
IoT	internet-of-things
IUs	information-users
JT	joint transmission
KKT	Karush-Kuhn-Tucker
LB	load balancing
LiFi	light-fidelity
LoS	line-of-sight
MINLP	mixed-integer non-linear programming
MRC	maximal ratio combining
NOMA	non-orthogonal multiple access
OFDM	orthogonal frequency division multiplexing
PD	photo-detector
PDMA	pattern division multiple access
PD-NOMA	power domain NOMA
RF	radio-frequency
SCMA	sparse code multiple access
SIC	successive interference cancellation
UC	user-centric
VLC	Visible light communication

VT	vectored transmission
WiFi	wireless-fidelity
ZF	zero-forcing

DISSERTATION ABSTRACT

NAME: Mohanad Obeed

TITLE OF STUDY: New Efficient Power Allocation, Cell Formation, and Load Balancing Protocols for Visible Light Communication Networks

MAJOR FIELD: Electrical Engineering

DATE OF DEGREE: May 2019

Visible light communication (VLC) has emerged as a great potential solution, either in replacement of, or complement to, existing radio-frequency (RF) networks, to support the projected traffic demands. Despite the prolific advantages of VLC networks, VLC faces many challenges such as channel estimation and shadowing effects, small coverage area, and the noise or interference that may be generated by nearby lighting systems. Some common solutions to partially overcome these challenges are to optimize the parameters of VLC networks, supplement the VLC by RF networks, and coordinated transmission. In this dissertation, we first propose a new joint load balancing (LB) and power allocation scheme for a hybrid VLC/RF system consisting of one RF access point (AP) and multiple VLC APs. Second, we propose a joint AP

association and power allocation algorithms for energy efficiency (EE) maximization in standalone VLC networks. Based on the user-centric (UC) design, we propose a new algorithm for users' clustering and APs' association. We then propose two algorithms that jointly allocate the power, under quality-of-service (QoS) constraints, and decide which APs must be prevented from participating in communication. Third, we introduce a new transmission scheme based on the cooperative non-orthogonal multiple access (NOMA) scheme to improve the sum-rate and fairness in VLC systems. For a system model consisting of one VLC AP and multiple users, we formulate an optimization problem that jointly pairs the users, selects the optimal link for each weak user, and allocates the messages' power to maximize the weighted sum-rate function. Solutions for such mixed-integer non-covex optimization problem are presented and compared to the traditional optimal NOMA scheme. Finally, we consider the scenario where multiple cooperative APs serve both energy-harvesting users (EHUs) and information-users (IUs). We solve the problem of maximizing a network-wide utility, which consists of a weighted-sum of the IUs' sum-rate and the EHUs' harvested-energy, so as to jointly determine the direct-current (DC)-bias value at each AP, and the users' powers.

ملخص الرسالة

الاسم: مهند عبيد

عنوان الدراسة: تقنيات جديد لتوزيع الطاقة وموازنة الحمل و تصميم خلايا الاتصالات في اتصالات الضوء المرئية

التخصص: هندسة كهربائية

تاريخ الدرجة العلمية: رمضان 1440

تم انشاء اتصالات الضوء المرئية لمساعدة اتصالات الراديو اللاسلكية أو لتقوم مقامها وذلك لتلبية الاحتياجات المتوقعة من سرعة البيانات في الجيل الخامس والاجيال القادمة. على الرغم من ان اتصالات الضوء المرئية تتمتع بميزات عالية مقارنة باتصالات الراديو اللاسلكية الا انه لا يزال هناك عيوب مثل التغطية المحدودة و التظليل و التشويش النابع من مصادر الضوء القريبة وهذه العيوب من الضروري التخلص أو التقليل منها في المستقبل. يمكن التخلص من هذه العيوب اما كليا او جزئيا بتكامل اتصالات الضوء مع اتصالات الراديو اللاسلكية او بتعاون وتنسيق المرسلات في اتصالات الضوء المرئية مع بعضها البعض. في هذه الرسالة أولا: أقترحنا تقنية جديدة لموازنة الحمل (توزيع المستخدمين على المرسلات) وتوزيع الطاقة على المستخدمين في الشبكات المختلطة المكونة من اتصالات الضوء المرئية واتصالات الراديو اللاسلكية. ثانيا: اقترحنا تقنية جديدة لتجميع المستخدمين واختيار المرسلات المناسبة لكل مجموعة وايضا توزيع الطاقة للمستخدمين مع تعطيل المرسلات المضرة (التي تبعث تشويش اكثر من بيانات). ثالثا: اقترحنا تقنية جديدة للارسال بناءا على تقنية الوصول المتعدد الغير متعامد وذلك لتحسين سرعة البيانات ومراعاة المستخدمين الذين يستقبلون خدمة رديئة. أخيرا: أسسنا نظام في اتصالات الضوء المرئية لنقل البيانات لمستخدمي البيانات وايضا لنقل الطاقة لمحتاجي الطاقة من المستخدمين و قمنا بتعظيم مقدار البيانات المستقبلة ومقدار الطاقة المستقبلة.

CHAPTER 1

INTODUCTION

1.1 Motivation

With the dramatic increase in total data traffic (approximately 7.24 exabyte-per-month in 2016, predicted to be 48.95 exabyte-per-month in 2021 [2]), there is an urgent need to develop a fifth-generation (5G) of networks with a higher system-level spectral efficiency that will offer higher data rates, massive device connectivity, higher energy efficiency (EE), lower traffic fees, a more robust security, and ultra-low latency [3], [4], [5]. With the advent of the internet-of-things (IoT) era, the amount of the connected devices to the internet is increasing dramatically [6], [7], resulting in a significant increase in data traffic which makes the traditional radio-frequency (RF) or wireless-fidelity (WiFi) networks crowded [8]. Small cells or network densification have been proposed as a solution for 5G technologies [9], [10] in order to increase the system capacity and coverage, reduce the power consumption of mobile devices, and enhance the networks' EE. The continuity of dramatic growing in data traffic demand has motivated researchers to explore new spectrum, new techniques, and new

network architectures to meet these demands. Visible light communication (VLC) has been introduced as a promising solution for 5G and beyond. The motivation behind emerging the VLC technology is the great invention of the energy-efficient light emitting diode (LED) [11]. White LEDs outperform the other light sources with their high electrical-to-optical conversion efficiency, long life span, small size and light weight, low cost, and operational speed [12], [13], [14]. LED lamps consume approximately 20% of the power consumed by fluorescent bulbs and approximately 0.5% of the power consumed by traditional light sources [15].

VLC uses a portion of the electromagnetic spectrum that is entirely untapped, free, safe, and provides a high potential bandwidth for wireless data transmission with rejecting the present RF interference [16]. Hence, VLC is a communication technology that uses LEDs as transmitters to emit both the light and information signals to the users. We should note that the power of the information signal must meet the illumination requirements, as well as being within the range of the LED's physical limits [17]. However, the non-linearity of LEDs in electrical-to-optical transfer can be efficiently avoided using pre-distortion mechanisms [18]. The VLC receiver contains a photo-detector (PD) component that has the ability to convert the received light intensity to a current signal. Data are transmitted using an intensity modulation (IM) technique at the transmitter, and received using a direct detection (DD) technique at the receiver (IM/DD) [19]. This means that the modulating signal must be real non-negative, and the existing modulation techniques in the RF networks adjusted to fit this property. Compared to RF networks, VLC networks provide higher data rates, larger EEs, lower battery consumption, and smaller latency. In addition, VLC can be

safely used in sensitive environments such as chemical plants, aircraft, and hospitals [20]. Because of the small coverage of the transmitters in VLC systems, an exhaustive reuse of frequency can be implemented. VLC is also power-saving since the consumed power for communication is already used for illumination and may also be used for energy harvesting. Because the light can be blocked by opaque objects, VLC functions properly only in line-of-sight (LoS) communications, which own a robust security since the unauthorized users who are out of sight cannot receive an information signal of good quality.

Despite all the aforementioned VLC advantages, VLC faces many technical challenges that must be resolved in the near future to achieve its full standardization and integration with future wireless systems. Some of these challenges in VLC networks are: channel estimation and shadowing effects, backhauling VLC traffic into large-scale networks, the rapid decrease in light intensity with distance, and the noise or interference that may be generated by nearby lighting systems. One common solution to partially overcome these challenges is to optimize the parameters of VLC networks. Another common solution is to supplement the VLC networks by RF networks. Hence, this thesis optimizes different types of VLC networks to improve the performance in terms of sum-rate, fairness, energy efficiency, and harvested energy. Different optimization techniques are proposed to allocate the transmit power, allocate the DC-bias, form the cells, distribute the users to APs, and select the links.

This chapter introduces the VLC fundamentals, defines VLC objectives and constraints, discusses the theoretical backgrounds needed to understand the subsequent chapters, and provides a summary for the contributions conduced in this thesis.

1.2 Background

1.2.1 Fundamentals of VLC systems

Because of its unique properties, a VLC channel is different from a RF or any other communication technology; its optical signal is modulated via the intensity of the signal, without carrying any information in phase or in frequency; the transmitted signal is positive and real, the optical power is proportional to input current signal (not to the mean square of the signal amplitude); the transmitted peak power is constrained by the LED's dynamic range and the illumination requirements.

VLC Transmitter

The LED lamp is the most appropriate transmitter used for both illumination and communication purposes. Each lamp usually consists of one or multiple LEDs driven by a circuit that controls the intensity of the brightness, using the the 'flowing-in' current. The function of the driver circuit is to transmit the data by modifying the flowing-in current, which, in turn, modifies the light intensity. The flowing-in current must be within the LED's dynamic range in order for the output (light intensity) to be linearly proportional to the input current. Because it shows the objects as they are without changing their real colors, the white color is commonly used for illumination and communication. Two common schemes are generally used in design white LEDs. One uses a blue LED with a yellow Phosphor layer [21], the other uses a combination of three LEDs (red, green, and blue) [22].

Because of its low cost and simplicity of implementation, the first type of LEDs

(the blue LED with a yellow phosphor layer) is more popular than the RGB type for designing white LEDs. However, it has a limited bandwidth, compared to RGB, because of the slow absorption and emission of the coating phosphor layer. Khalid *et al.* [21] showed that a 1 Gbps data rate could be achieved, using this type of LEDs. The RGB technique is better for communication as it uses the color shift keying modulation or color intensity modulation techniques that modulates the signal, using the three different LEDs. By doing so, data rates of 3.4 Gbps data can be achieved [22].

One important issue that should be considered, when designing the VLC, is the illumination requirements, which is the main purpose of the LED. In other words, the illumination range that is required should not be violated by the VLC system. This means that the performance of the VLC system is related to the illumination design requirements (more details are given in Section 1.2.1).

VLC Receiver

There are three types of devices that can be used as VLC receivers of the optical signal coming from the LED transmitter: 1) photo-detector (e.g. positive-intrinsic-negative and avalanche PD), 2) an imaging or camera sensor, 3) and a solar panel.

The PD is a diode device sensitive to the light intensity that can convert the received light to a current modulated by the intensity of the light received. The PDs that are commercially available can easily take samples of the received visible light at a rate of tens of MHz [23].

One of the advantages of a camera sensor is its availability on most mobile devices

such as smart-phones used to capture videos and images. The main advantage of a solar panel is that it can directly convert the received light to an electrical signal without the need for an external power supply [24].

Channel Model

The receiver receives the LoS optical signal and many copies of non-LoS, coming from reflections. According to [25], the optical power received from signals reflected more than once is negligible. Fig 1.1 shows a channel model of VLC links, containing the LoS and first reflected links. The LoS VLC link between the AP i and the user j can be expressed as follows [14], [26]:

$$h_{j,i} = \frac{A_p(m+1)}{2\pi d_{j,i}^2} \cos^m(\phi) g_{of} \cos(\theta) f(\theta), \tag{1.1}$$

where A_p is the physical area of the receiver PD, m is the Lambertian index given by $m = \frac{-1}{\log_2(\cos(\theta_{1/2}))}$, with $\theta_{1/2}$ the half-intensity radiation angle, $d_{j,i}$ the distance between AP i and user j, g_{of} the gain of the optical filter, ϕ the angle of irradiance at the AP, θ the angle of incidence at the PD, and $f(\theta)$ the optical concentrator gain is given by

$$f(\theta) = \begin{cases} \frac{n^2}{\sin^2(\Theta)}, & 0 \le \theta \le \Theta; \\ 0, & \theta > \Theta, \end{cases} \tag{1.2}$$

where n is the refractive index and Θ is the semi-angle of the field-of-view (FoV) of PD. Komine and Nakagawa [25] showed that the DC attenuation of the channel, from the first reflected link is given by
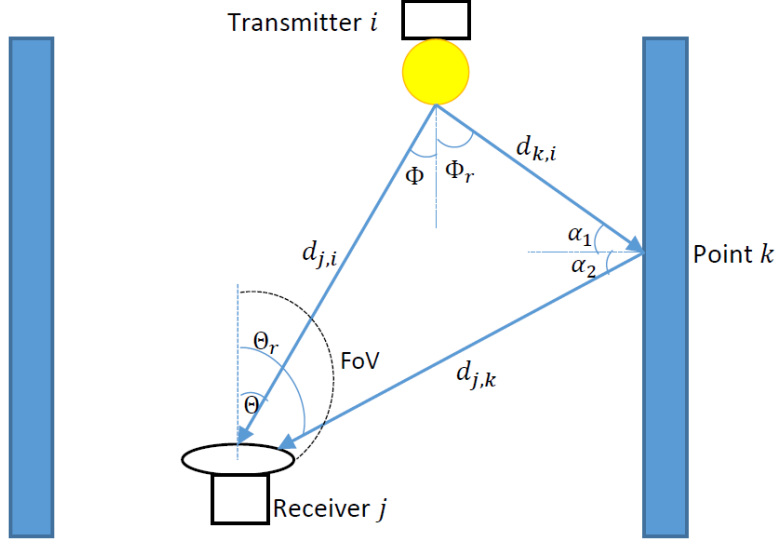
Figure 1.1: Channel model, including the LoS link and the first reflected link

$$dh_1 = \frac{(m+1)A_p}{2\pi d_{k,i}^2 d_{j,k}^2} \rho dA_s \cos^m(\phi_r) cos(\alpha_1) cos(\alpha_2) g_{of} \times f(\theta_r) \cos(\theta_r), \qquad (1.3)$$

where α_r and θ_r are the angels of the irradiance and incidence of the first reflection link, respectively, $d_{k,i}^2$ and $d_{j,k}^2$ are the distance from the AP i to the reflecting point k and the distance from the reflecting point k to the user j, respectively, ρ and dA_s are the reflection factor and the reflective area, respectively, α_1 and α_2 are the irradiance angles with respect to the reflected point and with respect to the receiver, respectively.

The above model is the general description of the VLC channel model. However, for an accurate representation for the VLC channel model, practical channel characteristics should be considered. For more information about channel models, we refer the interested reader to [27] and [28].

VLC Modulation Schemes

As mentioned previously, data cannot be transmitted by encoding the phase or frequency, and the modulation in VLC is implemented by varying the light intensity of the LED. On the other hand, the demodulation can be implemented by direct detection at the PD. Various IM/DD-based modulation techniques have been proposed and published in the literature. On-off keying was proposed for VLC, as a simple modulation scheme, where data are represented by two levels of light intensity [29], [30]. In order to obtain higher data rates, in comparison with what On-off keying offers, pulse width modulation and pulse position modulation schemes, in which data are represented by the pulse width and the pulse position, respectively, have been proposed. The data rate in pulse width modulation can be increased by combining it with the discrete multitone technique [31], while the data rate can be increased in pulse position modulation by using overlapping pulse position modulation [32], multi-pulse position modulation [33], or the overlapping multi-pulse position modulation [34].

Due to the non-linear VLC channel response, the aforementioned modulation schemes suffer from inter-symbol interference. To combat this impairment, the orthogonal frequency division multiplexing (OFDM) scheme, widely used in RF systems, should be modified to be compatible with the IM/DD technique. Because the light signal is a real non-negative signal, the complex bipolar signals generated by OFDM must be represented by real positive signals in VLC. The solution can be implemented by relaxing the Hermitian symmetry constraint and convert the bipolar signal to a unipolar signal. Two types of optical-OFDMs are widely used as VLC modulation

schemes: a DC-biased optical OFDM (DCO-OFDM) and an asymmetrically-clipped optical OFDM (ACO-OFDM). In DCO-OFDM [35], [36], a positive direct current is added to make sure that the signal is non-negative, and all the subcarriers are modulated to maximize the spectral efficiency. On the other hand, in ACO-OFDM, only odd subcarriers are used to modulate the data [37], resulting in a symmetric time domain signal.

Objectives and Constraints in VLC Networks

In this section, we present the established objectives for the design or optimization of the VLC networks and discuss the associated constraints that must be achieved. Certainly, some of the unique characteristics of VLC technology have generated new challenges, different from those in RF networks. As a result, the techniques used in traditional RF networks cannot directly be applied to VLC networks.

System Capacity: Several issues (that do not exist in the RF systems) must be considered, when deriving the VLC channel capacity. These are: 1) dimming requirements, 2) peak optical intensity constraint, 3) illumination requirements and the LED dynamic range, 4) and necessity for the input signal to be non-negative and real-valued. In addition, the channel gain for VLC is modeled almost as the Lambertian model [25], in which the channel gain for VLC is time-invariant but affected by geometrical parameters such as the locations of the transmitter and receiver. Because of the differences between RF and VLC systems, the capacity-achieving input distribution does not have to be Gaussian [38]. This means that the commonly derived Shannon channel capacity formula used for RF systems cannot be applied to

VLC ones. Consequently, many researchers have been investigating the VLC channel capacity under these constraints. In particular, the capacity of the scalar Gaussian channel constrained by amplitude power was proved to be achievable by a unique discrete random variable with a finite number of values [39].

Despite of all the studies which show that the optimal capacity-input distribution is discrete, a closed-form channel capacity is yet unknown. However, continuous input distributions provide a potential to have achievable rates that can be expressed in simple formulas, in contrast to discrete input distributions [40].

For the VLC channel capacity, Ahn and Kwon [41] proposed a numerical approach to determine the channel capacity for inverse source coding in VLC, without providing a closed-form expression for the VLC channel capacity, whereas Wang *et al.* derived closed-form expressions for the upper and lower bounds of the dimmable VLC channel capacity [42]. The lower bound was expressed as follows:

$$C \geq \frac{1}{2} \log_2 \left(1 + \frac{e}{2\pi} (\frac{\zeta P}{\sigma})^2 \right), \quad (1.4)$$

where ζ is the dimming target ranging from 0 to 1, P is the nominal optical intensity of LEDs, σ^2 is the Gaussian noise variance, and e is the Euler parameter. The channel gain (losses and opto-electronic transformation factors) is assumed to be equal to 1, in Equation 2.19. Expression (2.19) is the common expression used in the literature to estimate the system capacity.

Energy Efficiency: VLC networks are more energy-efficient than RF networks because LEDs, used as transmitters, are power-saving devices, and the same power is

used for both communication and illumination. Nevertheless, the transmitted power can be controlled within the given illumination limits to enhance the EE. The EE is required to be improved for 5G wireless technologies to reduce the consumed power that is expected tremendous number of devices that will be connected. The EE can be improved by efficient resources optimization, power allocation, energy transfer and harvesting, and hardware solutions [43].

The common approach to guarantee energy-efficient systems is to optimally allocate the resources to maximize the EE function subject to QoS and maximum transmit power constraints. The EE function can be defined as the system's benefit over the total consumed power. In other words, if the system's benefit is the sum rate, then the EE is

$$EE = \frac{R_T}{P_T},\tag{1.5}$$

where R_T is the sum rate and P_T is the total consumed power at the transmitters.

Another way for improving the EE is to formulate the optimization problem as minimizing the total amount of transmitted power, under a given set of QoS constraints. This type of optimization problems is easier to tackle than the problem of maximization of the EE function. This is because the EE function is not concave, in terms of allocating the transmit power. The common approach to tackle the EE maximization problem is to convert the non-convex problem into a sequence of convex optimization problems using the Dinkelbach's method. Another way to improve the EE in VLC networks is to harvest the energy by converting the received light intensity into a current that can be used for transmissions. This can be implemented by

equipping the receivers with solar panels.

Fairness: Fairness is an important issue in VLC networks for many reasons: 1) the dramatic decrease in the VLC channel value with the distance between the transmitter and receiver makes many users unable to switch from crowded cells to un-crowded ones; 2) the small coverage stimulates designers to fully re-use the frequency in the cells, resulting in severe interference with the signal received by some users.

Fairness is commonly measured using Jain's formula [44] for a single cell or for the whole cellular system. The fairness among users in the ith cell is given by

$$F_i = \frac{(\sum_{j=1}^{N_i} R_{j,i})^2}{N_i \sum_{j=1}^{N_i} R_{j,i}^2}, \tag{1.6}$$

while the fairness among users in N_{ap} cells is given by

$$F_s = \frac{(\sum_{i=1}^{N_{ap}} \sum_{j=1}^{N_i} R_{j,i})^2}{N_T \sum_{i=1}^{N_{ap}} \sum_{j=1}^{N_i} R_{j,i}^2}, \tag{1.7}$$

where N_i, N_{ap}, and N_T are the number of users associated with the cell i, the number of cells, and the total number of users in the system, respectively, and $R_{j,i}$ is the jth user data rate associated with the cell i.

Fairness can be achieved either by formulating the optimization problem to maximize the utility with a guarantee to achieve a proportional fairness [45], α-proportional fairness [46], or by adding the QoS constraints to the formulated optimization problem. The concept of the proportional fairness is to modify the objective function to imply both the system utility (e.g. sum-rate) and the fairness such as maximizing the

weighted sum-rate instead of the sum-rate itself, where the weights should be selected to achieve a proportional fairness as we do in Chapter 4.

Required Illumination Constraints: The two functions of LED, illumination and communication, are related to each other and must be studied and optimized jointly. In other words, the illumination requirements should be considered in designing the input current to the transmitter LED. This requirement implies that different constraints must be considered when optimizing the communication in VLC networks. The constraints are the peak optical power, dimming requirements, and flicker reduction.

For the peak power constraint, we should note that the input signal to the LED contains two components: the alternative signal (that contains the information), and the DC signal used to guarantee non-negative signal. The total energy emitted by the LED determines the transmitted optical power and the subsequent received signal strength, whereas the brightness is determined by the luminous intensity [25]. We denote Φ_{max}, Φ_{min}, and Φ_{avg}, as the predefined minimum illumination, maximum illumination, and the average illumination over the entire area, respectively. For the office work, an illuminance between 300 to 2500 lux is required [25].

The relation between the radiated optical power at LED and the luminous flux at the point i, which is distant from LED by d_i m with incidence and radiance angles θ and ψ, respectively, can be given by [47], [48]

$$h_i P_{opt} = \delta \Phi_i, \tag{1.8}$$

where δ is the optical to luminous flux conversion factor [48] which its value depends on the LED type; P_{opt} is the optical power, Φ_i is the luminous flux at point i, and h_i is given by:

$$h_i = \frac{m+1}{2\pi d_i^2} cos^m(\theta)cos(\psi), \tag{1.9}$$

where m is the Lambertian index given in Section 1.2.1.

One additional constraint for communication is that the input DC-biased current (DC and AC currents) to the LED must be within the dynamic range of the LED to have the radiated optical power linearly proportional to the input current [49]. For instance, the practical dynamic range of the LED Vishy TSHG8200 is within [5 mW, 50 mW].

To meet the illumination requirements at all points in the floor area, the upper and lower bounds of the optical power should be set accordingly. Considering both the bounds of the LED dynamic range and the illumination limits, the optical power at the transmitting LED must be confined by

$$\max(P_{min,ill}, P_{min,D}) \leq P_{opt} \leq \min(P_{max,ill}, P_{max,D}), \tag{1.10}$$

where $P_{min,ill}$ and $P_{max,ill}$ are the minimum and maximum optical power required for achieving the corresponding illumination requirements, respectively; $P_{min,D}$ and $P_{max,D}$ are the maximum and minimum power limits for the LED dynamic range, respectively.

The dimming control is a desirable process for the illumination purpose [50]. For

power saving, LEDs can be dimmed to desired levels, using appropriate modulation schemes [29], such as multi-pulse position modulation [51]; or variable on-off-keying [52].

Another purpose for the used modulation scheme is to mitigate the light intensity fluctuation to be unnoticeable by the human eyes. To guarantee the flickering is above the human eyes' fusion frequency, flickering frequency must be at least greater than 200 Hz [53]; this can be avoided by using the Run Length Limited codes that are used to reduce the long runs of 0s and 1s.

Coverage Probability

Since the LEDs in VLC can cover only a small area, and the coverage probability decreases dramatically as the distance increases, the coverage is an important issue in VLC networks and should be considered when designing the networks' parameters. The coverage probability can be defined as the probability that the received data rate for typical user is greater than or equal to a certain data rate threshold. All the geometrical parameters of the VLC channel affect the coverage probability, but we focus our discussion on those having major impacts such as the distance, optical power intensity, and the user's FoV. If we consider a system model consisting of multiple VLC APs and the considered user j is served only by one AP i, increasing the optical power would surely enhance the channel link from the AP i to the user j, but would increase the interference from all other APs significantly. The user's FoV plays a significant role in affecting the coverage probability, since decreasing the user's FoV leads to enhancing the VLC channel and decreasing the number of interfering APs, but we should also note that an extensive decrease in the user's FoV leads to
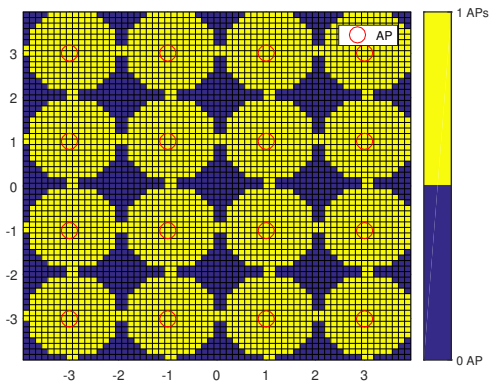
(a) FoV = 30°
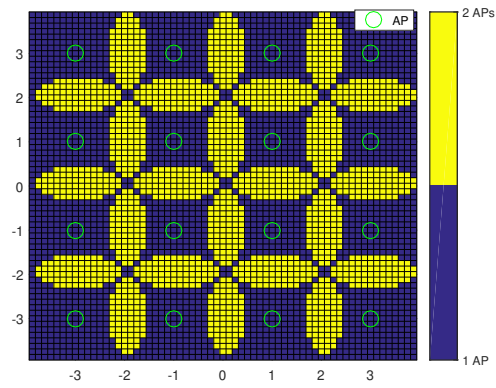
(b) FoV = 40°
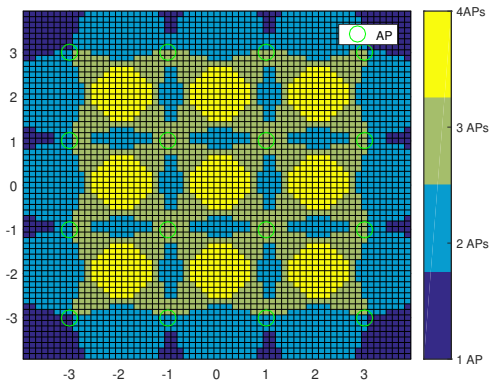
(c) FoV = 50°
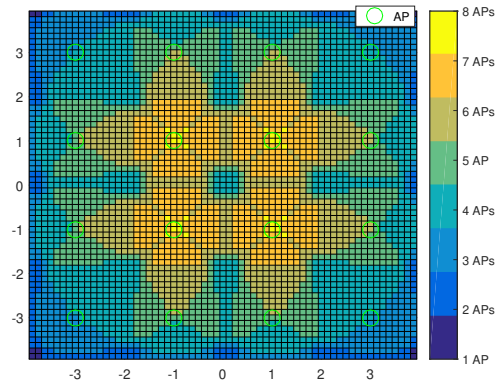
(d) FoV = 60°

Figure 1.2: Number of APs that can cover the area based on the user's FoV.

Table 1.1: Simulation Parameters

Name of the Parameter	Value of the Parameter
Maximum bandwidth of VLC AP, B	20 MHz
The physical area of a PD for information users, A_p	0.1 cm^2
The physical area of a PD for EH users, A_p	0.04 m^2
Half-intensity radiation angle, $\theta_{1/2}$	60°
FoV semi-angle of PD, Θ	30$^o - 60^o$
Gain of optical filter, g_{of}	1
Refractive index, n	1.5
Efficiency of converting optical to electric, ρ	0.53 [A/W]
Maximum input bias current, I_H	12 mA
Minimum input bias current, I_L	0 A
Fill factor, f	0.75
LEDs' power, P_{opt}	10 W/A
Thermal voltage, V_t	25 mV
Dark saturation current of the PD, I_0	10^{-10} A
Noise power spectral density of VLC, N_0	10^{-21} A^2/Hz
Room size,	8×8
Room height,	2.5 m
User height	0.85
Number of VLC APs,	4×4
Number of users,	5-35
Monte-Carlo for user distribution,	100 different user distributions
RF	
Number of RF APs	1
Location of RF AP	(0,0) in the ceiling
Transmit power	10 Watt
The distance of breakpoint	5 m
Central carrier frequency	2.4 GHz
Bandwidth	20 MHz
Angle of arrival/departure of LoS	45°
Standard deviation of shadow fading (before the breakpoint)	3 dB
Standard deviation of shadow fading (after the breakpoint)	5 dB
Noise power spectral density	-174 dBm/Hz

decrease of the coverage probability. On the other hand, for a given FoV, increasing

the height of the APs leads to an increase in the number of APs in the user's field of

view, meaning that the number of interfering APs would increase, and the path loss from the AP i to the user would also increase.

Fig. 1.2 represents the effect of a user's FoV on the coverage probability by showing the number of APs that can cover the area with different user's FoV. Consider an $8 \times 8 \times 3$ m³ room equipped with 4×4 VLC APs that are at ceiling level and serving users with height 0.85 m. In Fig. 1.2, we use the simulation parameters provided in Table 5.1 (for the information users) to find the LoS channel (1.1) form all APs to each point in the room with assuming that each point is a receiver with the given FoV. We adopt only the LoS link because it is dominating in VLC and the channel is degraded more than 90 percent if the LoS link is absent [54].

Fig. 1.2 shows that the coverage probability increases as the user's FoV increases. It shows the number of APs that can cover each spot in the room with the given FoV. On the other hand, Fig. 1.3 shows that the channel quality decreases as the user's FoV increases. In Fig. 1.3, we assume that we only have one AP fixed at the ceiling center and one receiver located directly under the AP with the given distance and given FoV. We also use Table 5.1 to find the LoS channel (1.1). Figs. 1.2 and 1.3 show that the user's FoV has a great impact on the channel quality and the coverage probability, meaning that optimizing the FoV would have a significant impact on the VLC systems.

The Harvested Energy: An additional function to LEDs, besides the illumination and communication, is the transfer of power, using the light intensity. When the VLC network consists of users that need to harvest the energy, the parameters should be designed to find a compromise between the three functions. The receiver
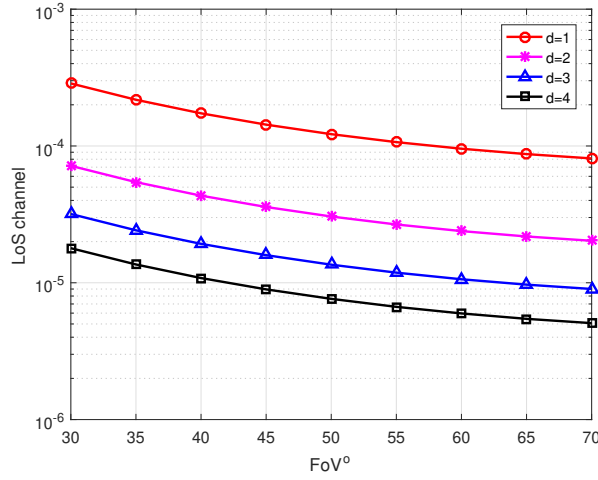
Figure 1.3: The effect of user's FoV on the channel quality with different transmitter-receiver distance, when the angels of radiance and incidence are zero.

can harvest the energy by equipping it with a solar panel that can convert the received modulated light signal into an electrical signal without an external power supply. Because the received current signal at the receiver contains both DC and AC currents, the DC current can be blocked and forwarded to the energy harvesting circuit. Li *et al.*, in [55], derived the energy that can be harvested by a user from one LED as:

$$E = f I_{DC} V_{oc}, \tag{1.11}$$

where f is a fill factor of approximately 0.75, I_{DC} the received DC current, and

$$V_{oc} = V_t \ln(1 + \frac{I_{DC}}{I_0}), \tag{1.12}$$

where V_t is the thermal voltage, and I_0 the dark saturation current of the PD. If we denote the transmitted DC current by b, the received DC current can be expressed as by $I_{DC} = \rho h P_{opt}$. Hence, if we have multiple LEDs, the harvested energy at the user

j is given by:

$$E_j = f\rho P_{opt} V_t \mathbf{h}_j^T \mathbf{b} \ln(1 + \frac{\rho \mathbf{h}_j^T P_{opt} \mathbf{b}}{I_0}), \tag{1.13}$$

where $\mathbf{h}_j$ is the channel vector between the LEDs and the user j, and $\mathbf{b}$ is the DC Bias current vector at LEDs.

1.2.2 Convex Optimization

In general, every optimization problem can be expressed as minimizing an objective function under cerain group of constraints. The regular form of an optimization problem is given by [56]

$$\min_{\mathbf{x}} \quad f_0(\mathbf{x}) \tag{1.14a}$$

$$s.t \quad f_i(\mathbf{x}) \leq 0, \quad i = 1, 2, \,.,n \tag{1.14b}$$

$$h_j(\mathbf{x}) = 0, \quad j = 1, 2, \,\,.,m \tag{1.14c}$$

where $\mathbf{x}$ is the vector of optimization variables, which can be also a scalar or a matrix, f_0 is the objective function, $f_i, i = 1, .., n$, are the inequality constraint, and $h_j, j = 1, \,.,m$, are the equality constraints. The optimization problem is defined as a feasible, if there is at least one vector $\mathbf{x}$ that achieves all the constraints; if not, it is defined as an in-feasible optimization problem. The vector $\mathbf{x}$ that minimizes the cost function among all vectors that satisfy the constraints is called the optimal solution of Problem (1.14), and it is denoted by $\mathbf{x}^*$. Problem (1.14) is defined as a linear programming if the cost function and all the constraint functions are affine, where any function is

affine or linear if it satisfies the following condition

$$f(\alpha x_1 + \beta x_2) = \alpha f(x_1) + \beta f(x_2) \tag{1.15}$$

for all $x_1, x_2 \in R^n$ and $\alpha, \beta \in R$. To define the convexity of any optimization problem, the cost function and all constraint functions must be convex. The function f is called convex if it achieves the following condition

$$f(\phi x_1 + (1 - \phi)x_2) \leq \phi f(x_1) + (1 - \phi)f(x_2), \tag{1.16}$$

where $0 \leq \phi \leq 1$. In the same way, the function f is called concave if it achieves the following condition

$$f(\phi x_1 + (1 - \phi)x_2) \geq \phi f(x_1) + (1 - \phi)f(x_2), \tag{1.17}$$

where $\phi \in [0, 1]$. From (1.15) and (1.16), it is easy to show that any linear function is a convex while a convex function is not necessarily a linear. Hence, convexity is more general then linearity [56]. Another way to know whether the function is convex or not is by checking the first and second order conditions with having the condition that the function f is differentiable achieved, the function f is called convex if and only if its domain is convex and $f(w) \geq f(v) + \nabla f(v)^T(w - v), \quad \forall v, w \in dom(f)$. The second order condition for f to be convex if and only if its domain is convex and the Hessian matrix $\nabla^2 f$ is positive semidefinit $\forall \; x \in dom(f)$. To handle any optimization problem, it should be first proved to be convex or not. Once it is demonstrated as a

21

convex optimization problem, many standard algorithms can be used for such kind of convex optimization problems or it can be solved by one of the available solvers such as [57].

1.2.3 Non-Orthogonal Multiple Access (NOMA) Scheme

In this section, we introduce NOMA, a new technology nominated for the fifth generation (5G) wireless networks aimed at increase the throughput, decrease the latency, and improve the fairness and connectivity. The rational behind NOMA is the use of a single resource component by multiple users, whether this component is a subcarrier, a time slot, or a spreading code. With this basic concept, different types of NOMAs, such as the power domain NOMA (PD-NOMA), pattern division multiple access (PDMA), sparse code multiple access (SCMA), were presented as good candidates for the 5G multiple access technique. More details on NOMA in traditional RF networks are provided in [58], [59].

In VLC networks, researchers are interested only in power domain NOMA (PD-NOMA). The goal of PD-NOMA is to set different power levels for different users. For instance, for two users served by the same base station (BS), and using the same OFDM subcarriers, the BS assigns a high power to the user with poor channel and a low power for the user with a better channel. In other words, assuming that $h_1 > h_2$, where h_i is the channel of the ith user, the BS transmits the signal of User 2 with higher power. User 2 decodes the received signal and treats User 1's signal as noise, whereas User 1 first decodes the signal of User 2, and then removes it from the received signal, after that it decodes its own signal. To generalize this idea, we assume that we
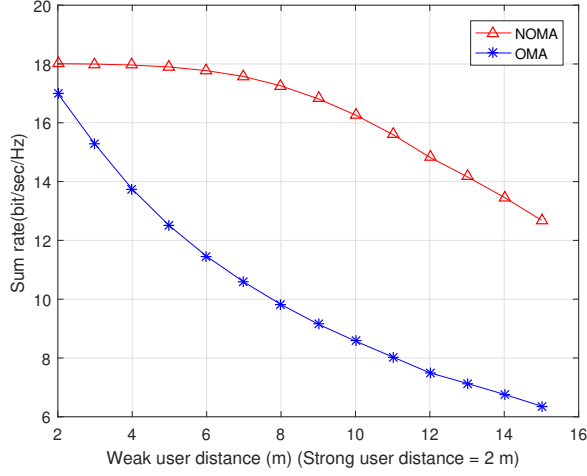
Figure 1.4: The impact of increasing the distance of the weak user with achieving the fairness constraint that both users receive equal data rate, when FoV $= 40$, incidence angle $= 0$, and irradiance angle $= 0$.

have N users served by the same BS, and first categorize them based on their channel gains as $h_1 \leq h_2 \leq .... \leq h_N$. When using the NOMA technique, the BS transmits the signal of all users using same carrier, and the received signal, at the kth user, can be expressed as follows:

$$y_k = h_k \sum_{j=1}^{N} \alpha_j \sqrt{P} s_j + n_k, \tag{1.18}$$

where α_j is the power coefficient of the user j, s_j is the information signal of the user j, and n_k is the additive white Gaussian noise. According to NOMA, users with a lower channel gain will have a higher power, meaning that $\alpha_1 \geq \alpha_2 \geq .... \geq \alpha_N$. Then, the successive interference cancellation is implemented to decode the signals received by the users. In other words, User N must decode all the signals of all users to have its own signal, and User $N - i$ has to decode $N - i$ signals to obtain its intended signal. It is clear that, as the number of users increases, the complexity of decoding

23
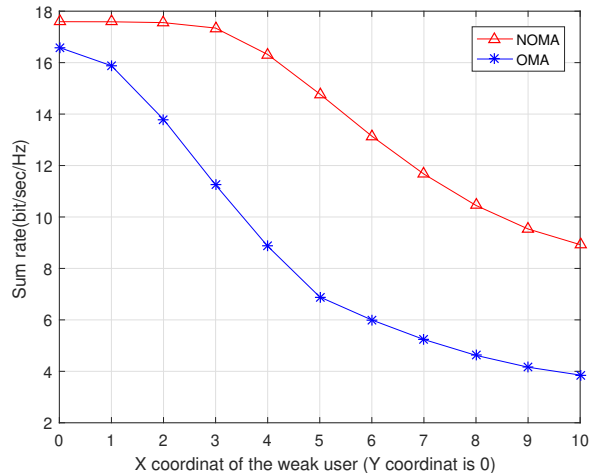
Figure 1.5: Shifting the weak user in the X coordinate where the incidence and irradiance angles changes accordingly, the strong user located at (0,0) coordinate, FoV = 40.

the signal is increased. In addition, the residual interference coming from inaccurate channel estimation increases with the number of users.

Implementing the NOMA in VLC networks requires considering the unique properties of VLC networks such as the limited bandwidth of LEDs, the maximum transmit power that is restricted by the illumination requirements, the blockages that make the channel between the transmitter and receiver close to zero, and the dramatic deterioration in the channel, as the distance increases. In addition, the channel value can be controlled by changing the FoV of the receivers or the semi-angles of the transmitters (if they are tunable), and these two factors can be selected to improve the performance of NOMA-VLC networks. Because the PD-NOMA scheme is based on successive interference cancellation (SIC), NOMA-VLC networks require all users' CSIs to be available, which is the case in VLC. It was also shown that the NOMA scheme performance is enhanced as the SNR increases [60], which is the case of VLC link. These features offered by NOMA-VLC networks led many researchers to investi-

24

gate these networks and find out how the NOMA outperforms OMA schemes in VLC systems.

In Figs. 1.4 and 1.5, we consider a system model consisting of one VLC AP fixed in the ceiling and two users in the floor. We assume that one user is located directly under the VLC AP with 2 m distance which is considered the strong user. Figs. 1.4 and 1.5 present simulation of how the NOMA outperforms OMA in VLC networks, when only the distance of the weak user increases (Fig. 1.4) and when the distance, incidence, and irradiance angles change (Fig. 1.5). 'Strong' and 'weak' users mean the user with the best channel and the user with the worst channel, respectively.

1.3   Dissertation Contributions and Outline

In this section, we summarize the contributions achieved in this thesis for the different considered system models. Specifically,

- Chapter 2 optimizes a hybrid VLC/RF network for maximizing the system capacity and balance the load. In particular, we propose a new joint load balancing (LB) and power allocation scheme for a system consisting of one RF AP and multiple VLC APs. An iterative algorithm is proposed to distribute the users on the APs and distribute the powers of the APs on their users. In PA subproblem, an optimization problem is formulated to allocate the power of each AP to the connected users for the total achievable data rate maximization. A new efficient algorithm that finds the optimal dual variables after formulating them in terms of each other is proposed. This new algorithm provides faster

convergence and better performance than the traditional subgradient method. After the power is allocated, the users of the minimum data rate start seeking for other AP that offers a higher data rate. Users with lower data rates continue re-connecting from AP to other to balance the load only if this travel increases the summation of the achievable data rates and enhances the system fairness. Two approaches are proposed to have the joint PA and LB performed: a main approach that considers the exact interference information for all users, and a suboptimal approach that aims to decrease the complexity of the first approach by considering only the approximate interference information of users. The numerical results demonstrate that the proposed algorithms improve the system capacity and system fairness with fast convergence.

- Chapter 3 studies a standalone VLC network where the number of APs is much more than the number of users. The goal is to form the cells and allocate the power to maximize the system EE. Based on the UC design, we first show that the cell formation and power allocation are interlinked problems and should be treated jointly. We start by proposing a new algorithm for users' clustering and then associating all the APs to the clustered users based on a proposed metric. We then propose two algorithms that jointly allocate the power, under QoS constraints, and decide which APs must be prevented from participating in communication. The first algorithm is designed to maximize the EE, while the other algorithm is designed to reduce the complexity of the first algorithm with acceptable degradation in the EE. In addition, different from the related

literature that allocated the power with the worst case interference information, we propose an iterative algorithm that allocates the power based on exact interference information, which significantly improves the EE. The numerical results demonstrate that the proposed algorithms significantly improve the EE compared to the existing work.

- In Chapter 4, a new users cooperation scheme is introduced based on the cooperative NOMA principle to balance the VLC networks. This transmission scheme provides two options for the weak users, either to be served by the direct VLC link or by the relayed hybrid VLC/RF link that is relayed through a strong user. Such scheme extends the system coverage, mitigates the blockages effect, and improves the system sum-rate and fairness. For a system model consisting of one VLC AP and multiple users, Chapter 4 formulates an optimization problem that jointly pairs the users, selects the optimal link for each weak user, and allocates the messages' power to maximize the weighted sum-rate function. We provide an optimal and suboptimal solutions for such mixed-integer non-covex optimization problem and compare the solutions to a proposed baseline simple approach and the optimal NOMA scheme. Simulation results show that the proposed scheme significantly improves the VLC network performance in terms of sum-rate and fairness compared to NOMA.

- Chapter 5 considers a VLC network, where multiple APs serve both EHUs, i.e., users which harvest energy from light intensity, and IUs, i.e., users which gather data information. In order to jointly balance the achievable sum-rate

at the IUs and the energy harvested by the EHUs, we consider maximizing a network-wide utility, which consists of a weighted-sum of the IUs sum-rate and the EHUs harvested-energy, subject to individual IU rate constraint, individual EHU harvested-energy constraint, and AP power constraints, so as to jointly determine the DC-bias value at each AP, and the users' powers. The chapter solves such a difficult non-convex optimization problem using an iterative approach which relies on inner convex approximations, and compensates for the used approximations using proper outer-loop updates. The chapter further considers solving the special cases of the problem, i.e., maximizing the sum-rate, and maximizing the total harvested-energy, both subject to the same constraints. Numerical results highlight the significant performance improvement of the proposed algorithms, and illustrate the impacts of the network parameters on the performance trade-off between the sum-rate and harvested-energy.

- Chapter 6 concludes the thesis and presents several open research problems that are appropriate as a future work. We also discuss what are the important issues that should be considered to extend the proposed techniques to be applicable in outdoor VLC networks.

JOINT OPTIMIZATION OF POWER ALLOCATION AND LOAD BALANCING IN HYBRID VLC/RF NETWORKS

2.1   Introduction

Despite all the advantages of VLC systems mentioned in the first chapter, they suffer from several limitations that contribute to the degradation of the system's performance such as a small coverage area, non-LoS failure transmission, frequent handover, and inter-cell interference. This leads to unbalanced systems, with some users receiving a poor service, while others may receive a high QoS. In particular, the objects existed in rooms might block the LoS link of some intended receivers, leading to a degradation

of the channel by up to 90 percent of the LoS channel [54], and, as a consequence, a significant deterioration of the data rates for the intended users. However, these opaque objects can block the inter-cell interference coming from the adjacent VLC APs for other users. This means that the fluctuation of the received QoS at users is high and that the blockages significantly affect the system fairness and the balance of the systems. Another cause for unbalanced VLC systems is the handover. For the reason that the coverage area of LEDs is small, the mobile users would suffer from wasting resources by sending and transmitting the overhead of the required handover. The small coverage area of the LEDs in VLC networks leads to a decrease in the throughput of both the system and the mobile users due to the overhead generated by such handovers [61], [62], [63]. However, by dividing the time into sufficiently short periods, we can have quasi-static periods known as 'states'. The handover consumes time, on average from 30 ms to 300 ms [64]. Another issue due to the small coverage area is the fact that the crowded static users cannot be distributed to the deployed cells, resulting all or most of them will be connected to one cell. This causes some APs to be overloaded, and consequently leads to a poor service for the connected users, while the other APs are unloaded or have a lower number of users. The bright side of the VLC's small coverage area is the fact that the whole bandwidth can be fully re-used in all cells, which improves the spectral efficiency of the overall system [65]. However, re-using the full frequency in cells generates inter-cell interference, to some extent. Inter-cell interference can be accepted for the sake of improving the system's spectral efficiency. On the other hand, the services received by the users located at the edges of the cells would be affected by this inter-cell interference. To summarize,

because of these issues, the users located at the edges of cells, blocked by objects, in motion, or connected to overloaded APs can not receive a good QoS like the other users. This significantly deteriorates both the performance and fairness of the VLC systems. One of the most common solutions to the aforementioned VLC issues is to supplement the standalone VLC networks with RF networks. Compared to VLC networks, RF networks are known for their ubiquitous presence (high coverage area) and proper operation in non-LoS environments. In addition, the devices connected to RF networks do not suffer from VLC interference and vice-versa [66]. Therefore, adding one or more RF APs to VLC networks mitigates the SNR fluctuation, balance the load of cells, mitigates the LoS blockages, and reduces inter-cell interference. This chapter examines the benefits of adding one RF AP to multi-cell VLC system in terms of system capacity and fairness.

2.2   Literature Review

Several techniques have been proposed to balance the load and tackle these issues by an efficient user distribution among VLC/RF APs [67], [68], [63], [69], [61], [70], [71], [72], [73], [74], [75], [76], [77], [78], [62], [79], [80]. LB consists of two missions: the APs' assignment (APA) and allocating the resources, whether this resource is a time slot in TDMA schemes or a sub-carrier in OFDMA schemes. Specifically, Stefan and Haas [67] started to study the APA by distributing the users between one RF AP and one VLC AP. Some of the users were associated to the VLC AP to alleviate the load of the RF AP, and the infeasible VLC connections were transferred to the RF AP. In [68], by

having multiple VLC and RF APs, the advantages of combining RF and VLC networks were investigated, and it has been proposed that users can be distributed dynamically, on both the VLC and RF networks, based on the users' channel condition. Users can then migrate to the AP offering higher data rates. The APA was implemented in [68] under the assumption that the resources are allocated fairly among users. It was concluded that the hybrid VLC/RF networks improved the performance significantly, compared to the VLC or RF standalone networks. Authors of [63] proposed to first associate the users to the VLC network, and then, to re-allocate the users receiving a lower data rate than a predefined threshold to RF APs. In [69], authors formulated a centralized and distributed optimization problem for user association to the APs (whether this AP is VLC or RF AP) with allocating the resources jointly among users. The centralized optimization problem, with considering the proportional fairness [81], was formulated as a mixed-integer non-linear programming (MINLP), which is highly complex. Hence, a distributed algorithm was also proposed with lower complexity compared to the centralized algorithm.

Wu and Haas [72] considered the LoS VLC channel blockages in the formulated optimization problem. They modified the formulated optimization problem to accommodate the LoS VLC channel blockages. The main idea is that, the users that suffer from a high occurrence rate of channel blockages should travel to the RF networks, whereas the users that do not suffer from blockages, or the ones that suffer from a low rate of blockages (to avoid the effect of handover overhead), should stay in the light-fidelity (LiFi) networks.

To avoid the complexity of solving these optimization problems, fuzzy logic-based

approaches were proposed for balancing the load in VLC networks [73], [74], and [75]. Authors of [73] and [74] proposed two-stage assignment process for the users in one RF AP and multiple VLC APs. They first decided which users should be connected to the RF AP, then they distributed the remaining users to the VLC APs, regardless of the presence of the RF AP and its connected users. In the fuzzy logic approach, the user j scores the APs, based on its offered throughput, SNR, inter-cell interference from the adjacent APs, and activity of the adjacent VLC APs, then decides whether to connect to the RF AP or to the VLC network, based on the resulting score. Similarly, authors of [75] used this approach to handle the handover in a dynamic hybrid VLC/RF system model. In their scheme, they considered several parameters as an input to the fuzzy logic approach: the instantaneous and average channel state information (CSI), user speed, and the minimum required data rate at users.

In [76], authors used another approach called the 'evolutionary game theory, to solve the joint LB and resource allocation problem. Some practical issues were considered in their study, including the receiver's orientation angle, LoS blockage in RF and VLC APs, and the diversity in the users' data requirements. In addition, the channel of LiFi was characterized with considering these practical factors. Authors in [77] studied and compared the common approaches used for balancing the load in the hybrid VLC/RF networks which are: 1) optimization based algorithms, 2) evolutional game theory, 3) fuzzy logic based algorithms. They showed that, for the dynamic systems when the handover is considered besides the AP assignment and the resource allocation, the fuzzy-logic-based algorithms outperformed the other approaches, whereas for the static systems, the optimization-based algorithms are the

best, with a slight improvement over the simpler EGT approach.

Some of the above work focused only on assigning the APs (which AP should serve which user) and the others focused on solving the problem of joint APs assignment and time or resource allocation without considering the power allocation problem. In other words, the joint LB and power allocation for a hybrid VLC/RF network has not been studied before.

2.3   Contributions

In this chapter, different from the above literature mentioned, we study the two problems of power allocation and LB in a hybrid VLC/RF network for the sake of data rate maximization and system fairness improvement. The network consists of multiple VLC APs and one RF AP. First, each user is connected to its closest AP. Then, each AP performs its optimization problem (allocates the power for the associated users) in order to maximize the summation of the achievable data rates per AP. After that, the users with the lower data rates start reconnecting from AP to other to balance the load only in case this transfer increases the summation of the achievable data rates. This transfer of users continues until no improvement in the summation of data rates is achieved. We prove the convergence of the proposed algorithm analytically and numerically. The inter-cell interference makes the joint power allocation and LB problem very difficult. Therefore, two approaches are proposed to have the joint power allocation and LB implemented: 1) the approach that considers the instantaneous (exact) interference information for all users, 2) and a suboptimal approach

that aims to decrease the complexity of the first approach by considering only the approximate interference information of users. We propose a suboptimal approach to decrease the complexity of the procedures significantly with a negligible loss in the performance. The procedures are simplified in such a way when a user connection is transferred, only two APs perform the power allocation problem and not all the APs. In the power allocation optimization subproblem, in the VLC and RF APs, we formulate the problem for maximizing the summation of the achievable users data rates under certain QoS constraints. These QoS constraints are formulated to control the tradeoff between the system capacity and system fairness. For a given interference information, the power allocation problem is proved to be concave but not easy to tackle. Similar power allocation problems were studied before such as [82], [83], [84]. In finding the dual variables, the authors of these references used the subgradient method, which is very sensitive to step size selection and needs a large number of iterations for convergence. Here, we derive a new efficient algorithm that finds the optimal dual variables after formulating them in terms of each other without requiring to optimize the step size or selecting the initial values carefully. This new algorithm provides faster convergence and better performance than the traditional subgradient method.

The rest of this chapter is organized as follows. The system and channel models are introduced in Section 2.4. In Section 2.5, we present the problem formulation and proposed algorithms. Some simulation results are presented and discussed in Section 2.6. Finally, the chapter is concluded in Section 2.7.

2.4 System and channel Models

The system under consideration consists of N_{ap} VLC APs, one RF AP, and N_u users as shown in Fig. 2.1. The users are distributed uniformly in the room and the APs are fixed in the ceiling of the room. Each VLC AP is equipped with multiple LEDs that use IM to transmit the light signal to the users, which receive the light by a PD. The RF AP is assumed to cover all the room area. Also, the location of users are assumed to be unchanged during a short period of interest T. Thus, the VLC and RF CSI of both the VLC and RF links is considered to be constant during this period. We assume that the maximum available bandwidth at the AP i is divided fairly among all the users connected to that AP.
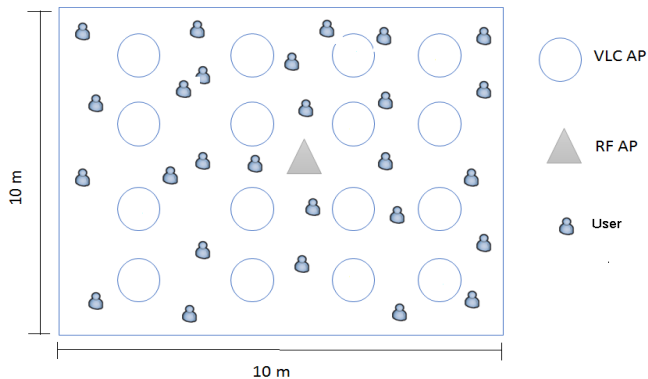
Figure 2.1: System model.

The VLC channel between the ith LED and the jth user is denoted by $h_{i,j}^{(v)}$ and can be modeled as given in (1.1)

In a VLC network, the LED has to operate in the linear region so that the optical power at its output is a linear function of the input voltage. In VLC networks, the signal is deteriorated significantly in the non-LoS VLC transmissions that might lead

36

to unsuccessful data transmission [82], [85], [69], so, in this chapter, we work only on LoS paths. This assumption does not affect the proposed algorithm since it does not depend on a specific channel model. In other words, whatever the channel model is, the proposed algorithm for the power allocation will give us the optimal solution as will be shown. Therefore, when the LoS path is available, $h_{j,i}^{(v)}$ is given by (1.1); otherwise, $h_{j,i}^{(v)} = 0$. The probability of the availability of the LoS from an AP to a user is denoted by α and it is assumed to be uniformly distributed. It was shown in [82] that the average electrical power of the received signal at user j from the VLC AP i is calculated as follows

$$P_{elec,j,i} = (\rho\sqrt{P_{j,i}^{(v)}}h_{j,i}^{(v)})^2, \tag{2.1}$$

where ρ is the optical-to-electric conversion efficiency, $P_{j,i}^{(v)}$ is the allocated power for user j from the AP i, where $P_{i,max}^{(v)}$ is the maximum transmitted optical power of the AP i. The received SNR at user j from the VLC AP i can be expressed as

$$\Gamma_{j,i}^{(v)} = \frac{(\rho\sqrt{P_{j,i}^{(v)}}h_{j,i}^{(v)})^2}{(B_{i,max}^{(v)}/N_i)N_0^{(v)} + \rho^2 \sum_{l=1,l\neq i}^{N_p} P_{B_{j,l}}^{(v)} h_{j,l}^{(v)2}}, \tag{2.2}$$

where $B_{i,max}^{(v)}$ is the maximum available bandwidth at the AP i, N_i is the number of users connected to the AP i, $N_0^{(v)}$ is the noise power spectral density, and $P_{B_{j,l}}^{(v)}$ is the interference power at user j caused by the AP l. It is worth to note that $P_{B_{j,l}}^{(v)}$ must be calculated carefully since it represents the power allocated from the AP l to the same frequency spectrum that is allocated for user j. For instance, if the AP l is associated

37

with 4 users, and user j along with another user are connected to AP i, $P_{B_j,l}^{(v)}$ should be calculated as the summation of the powers of 2 users out of the 4 users that are connected to the AP l and use the same spectrum frequency used by user j.

According to [82], [69], the maximum data rate that can be achieved at user j from the VLC AP i can be approximated by

$$R_{j.i}^{(v)} = (B_{i,max}^{(v)}/N_i) \log_2 \left(1 + \Gamma_{j,i}^{(v)}\right). \tag{2.3}$$

For RF transmission, as mentioned before, the RF cell is assumed to cover all the room area and the channel is considered to be flat fading and can be partitioned into non-overlapping channels of unequal bandwidths. We adopted the RF channel that is modeled in [63] and the RF channel between user j and the RF AP is denoted by $h_j^{(r)}$. The data rate achieved by the RF link between user j and the RF AP can be expressed as

$$\Gamma_j^{(r)} = \frac{P_j^{(r)}|h_j^{(r)}|^2}{(B_{max}^{(r)}/N_r)N_0^{(r)}}, \tag{2.4}$$

where $B_{max}^{(r)}$ is the maximum available bandwidth at the RF AP and N_r is the number of users connected to the RF AP. The achievable data rate that can be achieved by user j from the RF AP is given by

$$R_j^{(r)} = (B_{max}^{(r)}/N_r) \log_2 \left(1 + \Gamma_j^{(r)}\right). \tag{2.5}$$

2.5   Problem Formulation

The problem here is how to assign all the users to the APs and how to allocate the APs powers for the assigned users aiming to maximize the system capacity with keeping the fairness between the users at an acceptable level. Therefore, we start by assigning the users based on their distance from the APs, where each user selects the closest AP to it. Then, each AP performs its own power allocation problem for its associated users.

The achievable data rate of user j is expressed as

$$R_{j,i} = \begin{cases} R_{j,i}^{(v)}, & i \in \mathcal{C}_v; \\ \\ R_{j,i}^{(r)}, & i \in \mathcal{C}_r, \end{cases} \tag{2.6}$$

where $\mathcal{C}_v$ denotes the set of the VLC APs and $\mathcal{C}_r$ denotes the RF AP.

2.5.1   Power Allocation in VLC and RF Access Points

In this section, we aim to allocate the power for the N_i users that are connected to the AP i. The objective function here is to maximize the summation of the users data rates under certain QoS constraints. These constraints are formulated to guarantee some fairness for users per APs. We formulate the optimization problem as a general form for the VLC APs or the RF AP. Hence, $[P_{j,i} \quad B_{j,i} \quad h_{j,i} \quad N_0] = [P_{j,i}^{(v)} \quad (B_{i,max}^{(v)}/N_i) \quad \rho h_{j,i}^{(v)} \quad N_0^{(v)}]$, if the AP i is a VLC AP, and if the AP i is a RF AP, so $[P_{j,i} \quad B_{j,i} \quad h_{j,i} \quad N_0] = [P_j^{(r)} \quad (B_{max}^{(r)}/N_r) \quad h_j^{(r)} \quad N_0^{(r)}]$. Therefore, the

optimization problem of the AP i can be expressed as

$$\max_{P_{1,i},...,P_{N_i,i}} \sum_{j=1}^{N_i} R_{j,i} \tag{2.7a}$$

$$s.t. \quad R_{j,i} \geq \gamma_{j,i}, \ j = 1,..,N_i \tag{2.7b}$$

$$\sum_{j=1}^{N_i} P_{j,i} \leq P_{i,max}, \tag{2.7c}$$

$$P_{j,i} \geq 0 \quad \forall j, \tag{2.7d}$$

where N_i is the number of users associated with the AP i, and $\gamma_{j,i}$ is the minimum data rate that can be achieved at user j from the AP i, which is given by

$$\gamma_{j,i} = \beta \frac{B_{i,max}}{N_i} \log\left(1 + \frac{(P_{i,max}/N_i)|h_{j,i}|^2}{(B_{i,max}/N_i)N_0 + X_{j,i}}\right), \tag{2.8}$$

where $X_{j,i}$ is the interference term of user j and is equal to $\rho^2 \sum_{l=1,l\neq i}^{N_p} P_{B_{j,l}}^{(v)} h_{j,l}^{(v)2}$ if the AP i is VLC, and in the case of RF AP, $X_{j,i} = 0$, and β is a value in the interval $[0,1]$. If we select $\beta = 1$, this means that the AP will distribute its resources fairly (regardless of users channels), where each user gains the same power $P_{i,max}/N_i$ and same bandwidth $B_{i,max}/N_i$. On the other hand, if β is close to zero, this means that the objective function is released from the first constraint, which leads to increase the AP capacity.

Jain's fairness index is used to measure the AP fairness and the whole system fairness. Therefore, the fairness of the AP i is given by

$$F_i = \frac{(\sum_{j=1}^{N_i} R_{j,i})^2}{N_i \sum_{j=1}^{N_i} R_{j,i}^2}, \tag{2.9}$$

and the fairness of the system is given by

$$F_s = \frac{(\sum_{i=1}^{N_{ap}} \sum_{j=1}^{N_i} R_{j,i})^2}{N_{ap} \sum_{i=1}^{N_{ap}} \sum_{j=1}^{N_i} R_{j,i}^2}. \tag{2.10}$$

The Problem in (2.7) is not easy to tackle since in the case where the AP i is a VLC AP, the interference term in the objective function makes the problem difficult. On the other hand, if the interference terms are given, the Problem in (2.7) becomes a concave problem and can be solved by using the Lagrangian dual problem. First, we solve this problem under the assumption that the interference terms are given then we provide an iterative algorithm that achieves the optimal power allocation. Obviously, the Constraints in (2.7c) and (2.7d) are linear functions, while the objective function and the Constraint in (2.7b) are well known as concave functions as shown in [82] and [84]. Therefore, the optimization Problem in (2.7) is a concave problem with one global optimum solution. Hence, we can use the dual problem to achieve the optimal solution, where the strong duality holds in the concave problems. The dual optimization problem of the Problem in (2.7) can be expressed as follows

$$\zeta = -\sum_{j=1}^{N_i} R_{j,i} - \sum_{j=1}^{N_i} \mu_{j,i}(R_{j,i} - \gamma_{j,i}) + v_i \left(\sum_{j=1}^{N_i} P_{j,i} - P_{i,max} \right), \tag{2.11}$$

where μ_j is the Lagrangian multiplier for the data rate constraint of the jth user and v_i is the Lagrangian multiplier for the total power constraint.

In the following, an efficient algorithm is proposed to solve the Problem in (2.7) by minimizing the dual problem in (5.30). From the Karush-Kuhn-Tucker (KKT)

conditions [56], we have

$$\frac{\partial \zeta}{\partial P_{j,i}} = 0, \tag{2.12}$$

where

$$P_{j,i} = \frac{(1 + \mu_{j,i})B_{j,i}}{v_i \ln(2)} - \frac{N_0 B_{j,i} + X_{j,i}}{|h_{j,i}|^2}, \tag{2.13}$$

where the variable $\mu_{j,i}$ must guarantee that the Constraint in (2.7b) is feasible and v_i must guarantee that the Constraint in (2.7c) is feasible too. Now, these dual variables must be found to obtain $P_{j,i} \ \forall \ j$. In several papers such as [82], [83], [84], the authors found such dual variables by using the gradient decent method, which is an iterative algorithm that needs a large number of iterations to converge, a very careful selection of the step size, and a careful initial values selection for the dual variables. Proposing another approach that get red off these requirements (optimizing step size and the careful selection of the initial values) significantly simplifies the problem and provides a better performance. Here, we find a closed-form expression for v_i in terms of $\mu_{j,i}$ and vise versa. Then, we solve them alternatively until they converge. First, it is trivial showing that the Constraints in (2.7c) must hold with equality at optimality. Otherwise, we can increase one of the power variables until the constraints hold with equality, which leads to increasing the objective function, and hence, contradicting the optimality. By substituting (5.29) in (2.7c), we have

$$v_i = \frac{\sum_{j=1}^{N_i} B_{j,i}(1 + \mu_{j,i})}{\ln(2)\left(P_{i,max} + \sum_{j=1}^{N_i} \frac{B_{j,i}N_0 + X_{j,i}}{|h_{j,i}|^2}\right)}. \tag{2.14}$$

Similarly, by substituting (5.29) in (2.7b), $\mu_{j,i}$ must be

$$\mu_{j,i} \geq \frac{v_i \ln(2) P_{j,i}^{min}}{B_{j,i}} + \frac{v_i \ln(2)(B_{j,i} N_0 + X_{j,i})}{B_{j,i}|h_{j,i}|^2} - 1, \tag{2.15}$$

where $P_{j,i}^{min}$ is given by

$$P_{j,i}^{min} = \frac{(2^{(\gamma_{j,i}/B_{j,i})} - 1)(B_{j,i} N_0 + X_{j,i})}{|h_{j,i}|^2}, \ j = 1, .., N_i, \tag{2.16}$$

which is the minimum required power to achieve Constraints (2.7b). Hence, (2.14) and (2.15) depend on each other and can be solved alternatively starting from an initial value of one of them until they converge. After that, (5.29) is used to find the optimal power allocation. Algorithm 1 is proposed to solve the optimization problem in (2.7) with a given interference information. Condition 5 in Algorithm 1 examines

---
Algorithm 1 Power allocation for the AP i.
---

1. Input $B_{j,i}$, $\mu_{j,i}(0)$ $\forall j$.

2. for $q = 1 : M$

3. Find $v_i(q)$ from (2.14) and $\forall j$, calculate $P_{j,i}$.

4. For all j, check if the calculated $P_{j,i} \geq P_{j,i}^{min}$. If so, $\mu_{j,i}(q) = \mu_{j,i}(q-1)$; otherwise, calculate $\mu_{j,i}(q)$ from (2.15) by equating both sides, then update $P_{j,i}$.

5. If $|v_i(q) - v_i(q-1)| \leq \epsilon$, break;

6. end for

7. Find $P_{j,i}$ $\forall j$ using (5.29).

---

the convergence of all dual variables v_i and $\mu_{j,i}, j = 1, 2, .., N_i$.

Convergence analysis

Here, we analyze Algorithm 1 in terms of convergence. Before we start analyzing the convergence, we should note that the values of $P_{j,i}$ $\forall j$ after Step 3 are different from the values of $P_{j,i}$ $\forall j$ after step 4 (i.e., the values of $P_{j,i}$ $\forall j$ change twice in the same iteration). Specifically, in Step 3, the power values are changed because of updating the value of v_i, while in Step 4, the power values are changed because of updating the values of $\mu's$. To avoid this confusion, we denote the values of $P_{j,i}$ $\forall j$ after Step 3 by $P_{j,i}^{(3)}$ and denote the values of $P_{j,i}$ $\forall j$ after Step 4 by $P_{j,i}^{(4)}$.

At any q^{th} iteration, it can be shown that in Step 3, the variable $v_i(q)$ steers the summation of powers to be equal to $P_{i,max}$ (i.e., to achieve Constraint (2.7c) with equality). In other words, if we find $v_i(q)$ at Step 3 and substitute it in (5.29) $\forall j$, we find that $\sum_{j=1}^{N_i} P_{j,i}^{(3)}(q) = P_{i,max}$. On the other hand, Step 4 implies that each $P_{j,i}^{(3)}$ that is less than the corresponding $P_{j,i}^{min}$ (i.e. each $P_{j,i}^{(3)}$ that does not satisfy the corresponding constraint in (2.7b)) is increased by increasing the associated $\mu_{j,i}$ to achieve that $P_{j,i}^{(4)}(q) = P_{j,i}^{min}$. This increase in power yields violating Constraint (2.7c) to be as $\sum_{j=1}^{N_i} P_{j,i}^{(4)}(q) \geq P_{i,max}$. Hence, in the $(q+1)^{th}$ iteration, $v_i(q+1)$ will be greater than $v_i(q)$ to have that $\sum_{j=1}^{N_i} P_{j,i}^{(3)}(q+1) = P_{i,max}$ again.

Without loss of generality, we assume that in the qth iteration, $P_{j,i}(q) < P_{j,i}^{min}$ for $j = 1, .., k-1$ and $P_{j,i}(q) \geq P_{j,i}^{min}$ for $j = k, .., N_i$. From (5.29), we note that the increase in v_i leads to decreasing each $P_{j,i}^{(3)}$ $\forall j$ with keeping the constraint $\sum_{j=1}^{N_i} P_{j,i}^{(3)}(q+1) = P_{i,max}$ satisfied. Hence, we have that $P_{j,i}^{(3)}(q+1) < P_{j,i}^{(3)}(q)$, $j = K, ..., N_i$ (because Step 4 causes no change in these powers in the iteration q), and $P_{j,i}^{(3)}(q+1) >$

$P_{j,i}^{(3)}(q)$, $j = 1, ..., k - 1$ to keep the constraint $\sum_{j=1}^{N_i} P_{j,i}^{(3)}(q + 1) = P_{i,max}$ satisfied. This means that $\mu_{j,i}(q + 1)$ must be increased to achieve the constraint $P_{j,i}^{(4)}(q + 1) = P_{j,i}^{min}$, $j = 1, .., k - 1$ but with less amount than what was required in $\mu_{j,i}(q)$. Consequently, with implementing one iteration more, we have

$$\mu_{j,i}(q + 2) - \mu_{j,i}(q + 1) < \mu_{j,i}(q + 1) - \mu_{j,i}(q), \; j = 1, .., k - 1. \qquad (2.17)$$

Similarly,

$$v_i(q + 2) - v_i(q + 1) < v_i(q + 1) - v_i(q), \qquad (2.18)$$

Therefore, as the number of iterations increases, the amount of change in v_i and all $\mu_{j,i} \forall j$ approaches zero. Thus, Algorithm 1 is convergent.

It is also important to note that in Equation (2.15), v_i is a factor of the expression $1 + \mu_{j,i}$, which means that starting with any initial values for $\mu_{j,i}$ will be compensated by v_i to have the same value of $P_{j,i}$ as Equation (5.29) shows. Hence, Algorithm 1 does not depend on the initial values.

Finding the exact interference information

Now, in the VLC APs, the problem is how to find the instantaneous interference $(X_{j,i})$ of each user, which is difficult to be found because the term $X_{j,i}$ of user j depends on all powers of the APs that are allocated for the jth user frequency spectrum. Therefore, we provide an iterative algorithm that solves the power allocation problem of all the VLC APs with finding the instantaneous interference of each user. Algorithm 2 provides

45

Algorithm 2 Power allocation for all the VLC APs with a given distributed users.

1. Each AP allocates the power for the users equally.

2. for $q = 1 : M$

3. Calculate $X_{j,i}^{(q)}$ for all users in the system.

4. Perform Algorithm 1 for all APs.

5. if $\sum_{i=1}^{N_p} \sum_{j=1}^{N_i} (X_{j,i}^{(q)} - X_{j,i}^{(q-1)})^2 \leq \epsilon$; break;

6. End for

---

the optimal power allocation for a given distributed users. It is worth stating that the RF AP performs its power allocation using Algorithm 1 and it is not included in Algorithm 2. This is because the interference of the users connected to the RF AP is zero. In Algorithm 2, the only step that needs to exchange the information between APs is Step 3 (Calculating the interference). To calculate the interference $X_{(j,i)}$, the AP i must know the power allocated from the other APs for the BW used by User j. Therefore, the APs must exchange their power information to have the interference information at each user.

2.5.2 Load Balancing

As stated earlier, initially, each user is connected to its closest AP. Then, each AP performs its own power allocation problem as shown in the previous section. However, some APs will be overloaded, which may cause some users connected to these APs to receive a poor QoS. Therefore, after the power allocation optimization problem (Algorithm 2) is performed, the user with the poorest QoS is reconnected to either the RF AP or another adjacent VLC AP if the later can provide a better service and

increase the system capacity. The users connected to the RF AP do not receive any interference so that the strongest candidate AP for the user (which needs to reconnect to another AP) to travel to is the RF AP. The approach here is to arrange the users as a queue starting from the user with the lowest QoS up to the highest quality serviced user. Then, each user in its turn tests if the RF AP can provide a better achievable data rate for it or not. If so, the user migrates to the RF AP; otherwise, the user transfers to another adjacent AP if that AP can provide a better achievable data rate for him. These procedures continue until no improvement in the system capacity can be achieved. From the power allocation problem in (2.7), each VLC AP offers for each user its QoS denoted by $\gamma_{j,i}$, which is a function of the number of users connected to that AP as shown in (2.8). Hence, the maximum offered achievable data rate for user j that is connected to the AP i is given by

$$\bar{R}_{j,k} = \max_{k \in \chi_i} (\gamma_{j,k}), \qquad (2.19)$$

where χ_i is the set of the APs that are very close to the AP i and $N_k < N_i - 1 \; \forall \, k$. Since $\gamma_{j,k}$ depends on the value of β, if $N_k = 0$, that means the AP k offers all its resources for the coming user, and hence, $\beta = 1$ in (2.19). Otherwise; if $N_k \geq 1$, β is determined by the AP k. It is important to state that the transfer of a user connection changes the interference information, which enforces the system to re-implement Algorithm 2 with each transfer. This process of transfer continues only if there is an improvement in the system capacity. To prove the convergence of this approach, first, we should note that the step of sorting users is conducted at the beginning of every round of testing

all users not with each user transfer. In addition, we cancel each user transfer from one AP to another that produces a degradation in the system capacity. Consequently, with each user transfer the system capacity increases, and as we know the capacity has a limit, which means that the convergence is occurred when we approach that capacity limit.

2.5.3 Suboptimal Approach: Averaging the Interference

The disadvantage of the above approach is its high complexity since with each user connection transfer, all the APs must perform the power allocation problem, which is highly complex. The reason behind that is the need for exact interference information to implement both the power allocation and LB together. In this section, we aim to simplify the problem solution by relaxing this demand. User j experiences interference from each AP with a power that might be less or greater than the average power. This average power is calculated under the assumption that each AP distributes its power equally for its associated users. Therefore, the essence of the approach here is that instead of obtaining the instantaneous interference, we obtain the average interference that is calculated by averaging the power of the interference coming from all the APs. Therefore, the approximate inter-cell interference at user j that is connected to the AP i is given by

$$X_{j,i} = \sum_{l=1,l\neq i}^{N_p} \frac{P_{l,max}}{N_i} h_{j,l}^2.$$

(2.20)

The above assumption significantly simplifies the problem as there is no need to implement the power allocation optimization at all the APs at each user connection

Table 2.1: Simulation Parameters

Name of the Parameters	Value of the Parameters
Room hight	3 m
Maximum bandwidth of VLC AP, $B_{max}^{(v)}$	30 MHz
Maximum bandwidth of RF AP, $B_{max}^{(r)}$	30 MHz
The physical area of a PD, A_p	$0.1cm^2$
Half-intensity radiation angle, $\theta_{1/2}$	60°
FoV semi-angle of PD,Θ	90°
Gain of optical filter, g_{of}	1
Refractive index, n	1.5
Optical to electric conversion efficiency, ρ	1
Transmitted power of the VLC AP, $P_{max}^{(v)}$	4 watt
Transmitted power of the RF AP, $P_{max}^{(r)}$	2 watt
Noise power spectral density of LiFi, $N_0^{(v)}$	10^{-21} $A^2/$Hz
Variance of AWGN in RF AP, $N_0^{(r)}$	10^{-19} $A^2/$Hz

transfer. In other words, we only need to perform the power allocation optimization

problem (Algorithm 1) at only two APs (the departed from and the arrived to APs).
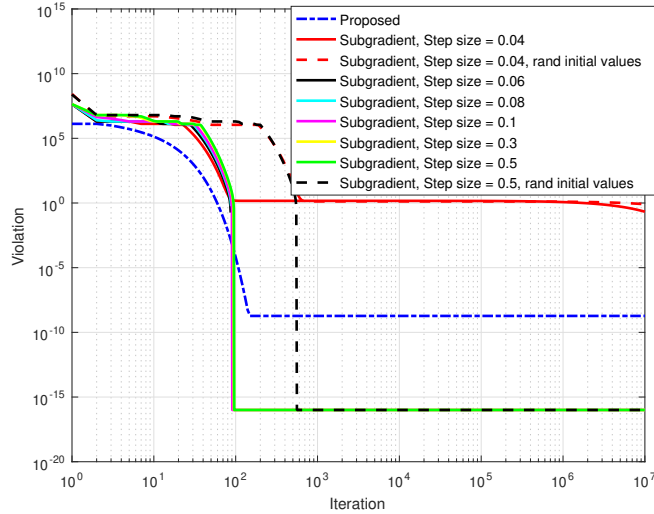
Figure 2.2: Comparison between the proposed Algorithm 1 and the subgradient method with different step sizes by plotting the violation of the constraints versus number of iterations for AP i, $P_{i,max} = 10$ Watt.
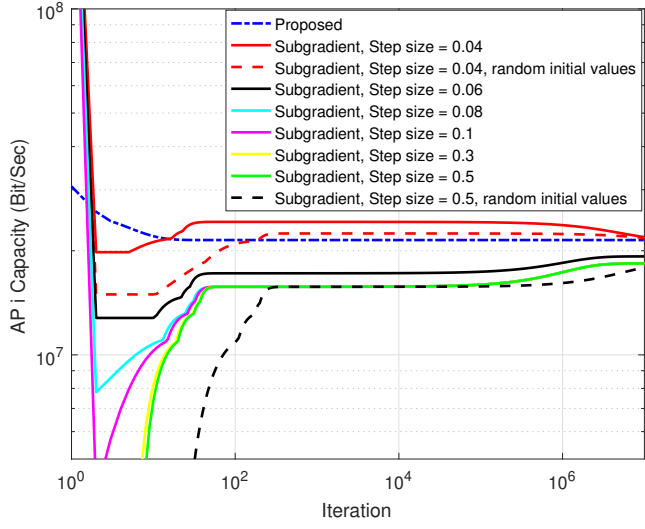
Figure 2.3: Comparison between the proposed Algorithm 1 and the sub-gradient method with different step sizes by plotting the system capacity versus number of iterations, $P_{i,max} = 10$ Watt.

2.6   Simulation Results
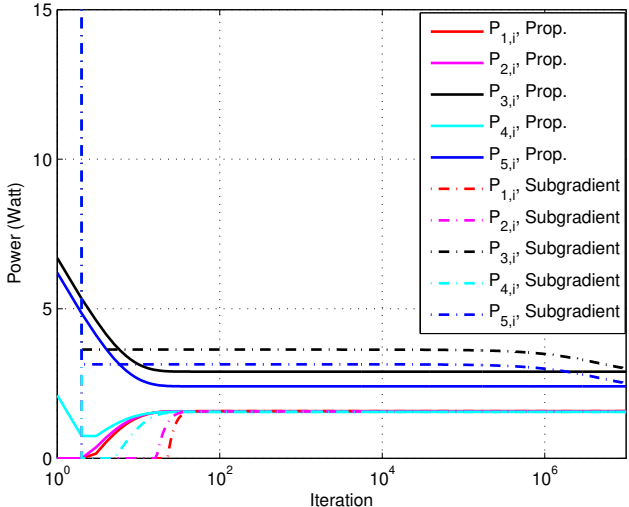
Figure 2.4: Convergence of the proposed Algorithm 1 of the users powers connected to AP i and compare it with the subgradient method, step size $= 0.04$, $P_{i,max} = 10$ Watt.

In this section, we verify the capability of the proposed algorithms for enhancing

the performance of the hybrid VLC/RF network. We show the convergence of the
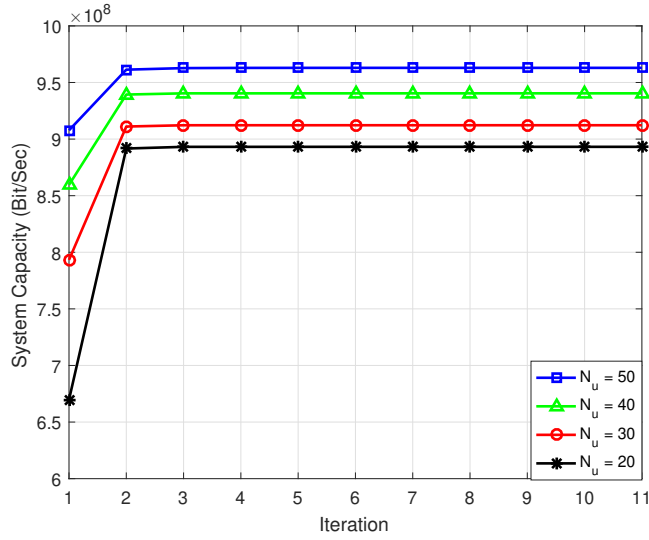
Figure 2.5: System capacity versus number of iterations for Algorithm 2 with different numbers of system users.
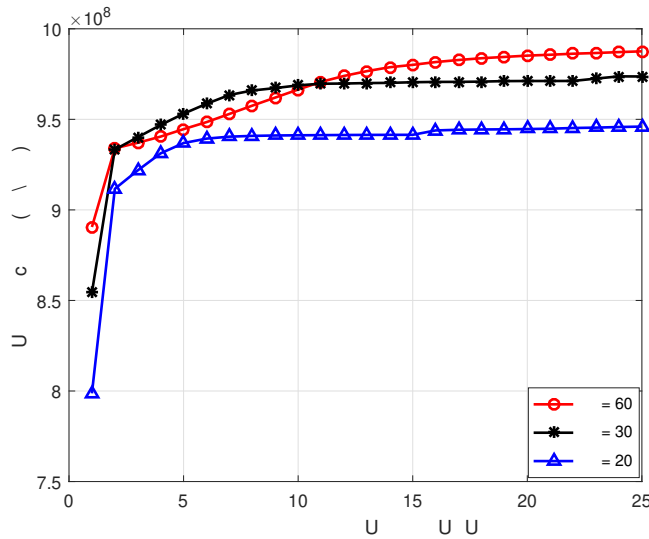
Figure 2.6: System capacity versus number of transferred users for different numbers of system users.

proposed algorithms and how they increase the system capacity. A 10×10 room area is assumed with 16 VLC APs and 1 RF AP fixed in the ceiling. The values of all parameters in the considered VLC/RF system are given in Table 2.1. Monte-Carlo simulation is used to asses the performance of the proposed algorithms where in each

simulation iteration, a uniform random number is generated between 0 and 1. If that number is less than α (the probability of the availability of the LoS), the LoS component is available; otherwise, LoS component is not available.

In Fig. 2.2 and Fig. 2.3, we show the performance and convergence of the proposed Algorithm 1 implemented at AP i and compare it with the subgradient method. Both figures should be analyzed together because Fig. 2.2 shows the maximum constraint violation of the approaches (i.e., how much the approaches are close from achieving the constraints versus the number of iterations), while Fig. 2.3 shows the value of the objective function for the different approaches versus the number of iterations. It is observed that the subgradient method with large step size, such as step size $=$ 0.5, achieves the constraints slightly faster than the proposed approach as shown in Fig. 2.2, but it can not achieve the same system capacity as the proposed approach can achieve as shown in Fig. 2.3. In other words, if we assume that the violation tolerance is 10^{-4}, both approaches, the proposed and the subgradient with large step size, almost satisfy the constraints after 100 iterations, while the proposed approach provides higher AP capacity than the subgradient method as shown in Fig 2.3. On the other hand, the subgradient method with small step size, such as step size $= 0.04$, starts to satisfy the constraints after more than 10^7 iterations as shown in Fig. 2.2, and after that huge number of iterations, it starts approaching the capacity achieved by the proposed approach as shown in Fig 2.3. In addition, we implement the subgradient method with random initial values of the dual variables to show that the subgradient methods depends highly on the selected initial values, while the proposed algorithm does not. It is important to note that the disadvantages of the subgradient method

52

is that the step size must be optimized to have the best performance, which is an additional problem that complicate the already subgradient method. Besides, the initial values for the dual variables must be selected carefully. It is known that in the subgradient method, the smaller step size, the closer optimal values we obtain as the number of iterations goes to infinity. Hence, as shown in Fig. 2.4, the proposed approach provides the same power values of the subgradient method (step size = 0.04) in less than 100 iterations, while the subgradient method achieves some of those values after 10^7 iterations. Fig. 2.4 also shows that the subgradient method violates the maximum power constraints over a wide range of iterations and it starts satisfying that constraint after huge number of iterations (10 million iterations).

Fig. 2.5 shows the convergence of Algorithm 2. It is clear that Algorithms 2 needs at most three iterations to converge. Furthermore, the number of iterations needed to converge does not depend on the number of users in the system, which means that the number of users does not affect the convergence of Algorithm 2. This indicates that Algorithm 2 rapidly converges to the optimal solution. In addition, it can be seen from Fig 2.5 that the value of the system capacity at iteration 1 is the resultant of allocating the power equally between users (Step 1 in Algorithm 2), and the value of the system capacity at iteration 2 is the result of solving the optimization problem, where the interference information is calculated from the power allocated in the first iteration which is the equal power allocation, and so on. Therefore, Fig. 2.5 highlights the significant contribution of the proposed allocation power algorithm over allocating the power equally among users.

In Fig. 2.6, the relation between the system capacity and number of reconnected

users is shown with different numbers of total users. The number of transferred users means how many users transferred their connections form one AP to another. It can be seen that the more the users transfers, the better the system capacity till the system saturates. Also, it is obvious that more users transfers are needed for the system to reach the saturation point as the number of users increases, as expected. In other words, the rate of increasing the system capacity with 60 users is less than the rate of increasing the system capacity with 20 or 40 users.
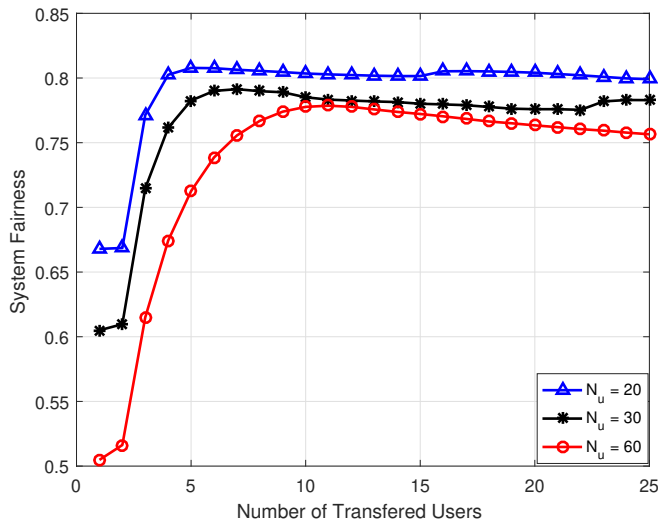
Figure 2.7: System fairness versus number of transferred users for different number of system users.

The impact of total number of users on the system fairness is studied in Fig. 2.7. It is clear from this figure that as the number of transferred users increases, the system fairness is more enhanced with the best results achieved at the minimum number of total users. Enhancing the system fairness and capacity together with each user transfer comes from the fact that the users with poor services travel from the overloaded APs to have better services from other less overloaded APs. This helps

in decreasing the variance of the received data rate among users and provides a more efficient utilization of APs resources.
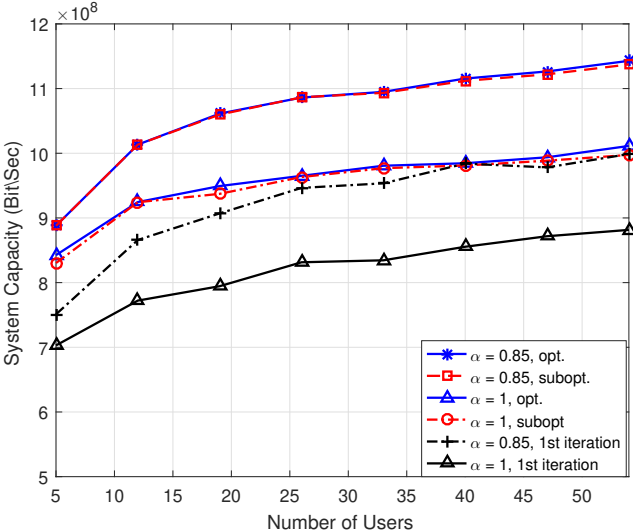
Figure 2.8: Comparison between Algorithm 2 and the suboptimal approach in terms of system capacity for different values of α.
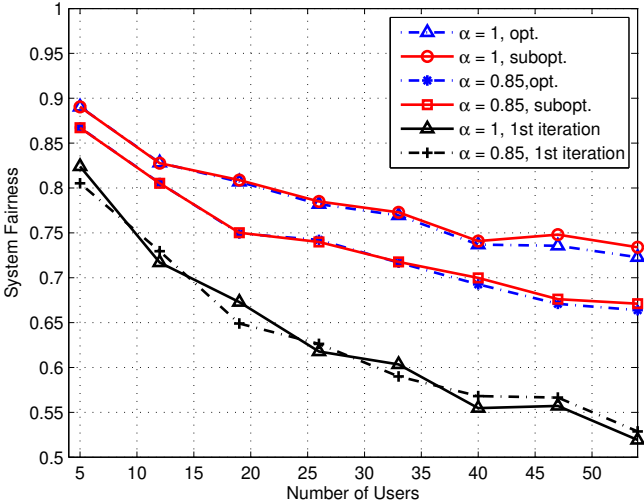
Figure 2.9: Comparison between Algorithm 2 and the suboptimal approach in terms of system fairness for different values of α.

Fig. 2.8 shows the relation between the number of users and the total system capacity for different values of α. Here, $\alpha = 1$ means no blockages is happened, while

$\alpha = 0.85$ means that the probability of having an objects between APs and users is 0.15. It is shown that the difference between the performance of Algorithm 2 and the suboptimal solution (averaging the interference) is negligible. We also investigate the effect of number of users on the system fairness in Fig. 2.9. The approach that considers the approximate interference information slightly performs better than the approach that considers the exact interference in terms of the system fairness. This is due to the fact that the former depends on calculating interference matrix based on the assumption that the power at the APs is distributed fairly among users, which leads to a more fair power allocation among users than the later. As can be seen from Fig. 2.8 and Fig. 2.9, as the probability of the LoS availability decreases, the system capacity increases while the fairness decreases. This is because increasing the blockages rate in the hybrid VLC/RF networks can enhance the system capacity rather than compromising it. In other words, the blockages are more likely to prevent the users from receiving the optical interference than blocking the intended signals. On the other hand, blocking some users from some VLC APs increases the variance of the received data rates among users which leads to decrease the system fairness. The figures show also how the proposed joint LB and power allocation algorithms significant improve the system capacity and fairness compared to the case where one iteration is implemented only (each user is assigned to its closest AP and each AP implements the power allocation only once).

2.7 Conclusion

In this chapter, a joint LB and power allocation algorithms for hybrid RF/VLC network were proposed. An iterative algorithm was proposed to maximize the total system capacity and enhance the system fairness. Two approaches were implemented: 1) the approach that is based on the exact interference information for all users, which provided better performance, 2) and a suboptimal approach that is based on the approximate interference information, which had a less complexity compared to the first approach. In the power allocation subproblem, we derived a new efficient algorithm that finds the optimal dual variables after formulating them in terms of each other. This new algorithm provided a faster convergence and a better performance than the traditional subgradient method. As a future work, we recommend to implement the joint power and bandwidth allocation with load balancing in mobile users.

ALGORITHMS FOR ENERGY-EFFICIENT VLC NETWORKS WITH USER-CENTRIC CELL FORMATION

3.1 Introduction

In Chapter 2, we show that VLC networks can be supported by RF AP to improve both the system capacity and fairness. Another approach to improve the VLC systems' performance is by having the VLC APs cooperating and coordinating their transmission. This approach removes or mitigates interference, improves the space diversity

gain, increases coverage, decreases the handover overhead, and decreases the received SNR fluctuations. A coordinated multi-point (CoMP) transmission technique can be implemented by connecting multiple APs through backbone networks so that they can cooperate to design their transmitted signals. Therefore, the joint transmission (JT) can be implemented between the coordinated transmitters to form one cell.

One advantage of VLC networks is that they can be considered as highly dens networks, where the lamps fixed in the ceiling are most probable to be much more than the number of receivers in indoor environments. In highly dense networks, it is important to consider the consumed power that used for communication. Hence, this chapter considers maximizing the EE in highly dense VLC networks. VLC networks has been considered as an energy-efficient technology [43], as the LEDs, which are used as transmitters, are energy-efficient devices [15], and because the consumed power used for communication is also used for illumination. However, the acceptable illumination is ranging between maximum and minimum requirements, which means that the consumed power can be controlled within these limits to maximize the EE. In other words, the extra power consumed for communication should be minimized with keeping the required QoS achieved to improve the system's EE.

Aiming to maximize the EE in VLC, several factors can be employed such as cell formation based on the UC design and power allocation. Because the inter-cell interference is a major reason behind the QoS and EE degradation, the cell formation has been proposed to mitigate this problem by grouping multiple APs to be in a one cell. Efficient cell formation design is a crucial step that has a great impact on the EE of the system.

3.2 Literature Review

Extensive work has been done for throughput and system capacity maximization in VLC networks using different modulation schemes [86], [87], power allocation and load balancing [69], [80], [63], [88], [79], [89], and using MISO [90] and MIMO schemes [91]. Cooperation between APs has also been proposed to enhance the VLC system performance by mitigating the interference [92], [93], and decreasing the handover with mitigating the blockages effect [94].

For managing interference in the N APs and N users system model, the APs in the proposed system in [93], were designed to organize themselves into a cooperative coalition based on the game theory coalition formation. In [92], authors adopted the joint transmission scheme to alleviate the effect of the co-channel interference and to improve the system throughput and the quality of the received signal. In addition to the co-channel interference, the impact of blockages on users can be mitigated using the CoMP joint transmission scheme [94]. Authors of [94] proposed an approach that assigns multiple transmitters to each user, with proportional fairness. Serving a user by multiple LEDs transmitters significantly mitigates the rate of blockages and the handover overhead.

In [95], Zhang *et al.* investigated the UC design for VLC, for which the cells' structures are not with regular shape. First, the users were clustered to multiple clusters, then the APs were distributed to the clustered users. In [96], Li *et al.* used the UC design to improve the system fairness by proposing algorithms aimed at scheduling users and maximizing the sum utility of the system. In [47], in addition to

forming the cells and associating the APs, the powers were allocated to the clustered users to maximize the EE. In [1], authors used these techniques of cell formation and power allocation to design energy-efficient scalable video streaming with considering an adaptive modulation mode assignment. The common clustering approach used in [96], [47], [1] is the edge distance clustering.

3.3 Contributions

in this chapter, we design an energy-efficient VLC network by proposing new efficient algorithms that jointly form the cells, allocate the power for the users, and select the appropriate APs. More specifically,

- We propose a new user clustering algorithm that aims at minimizing the distance of the clustered users to their centers and maximizing the distance between the different centers in order to mitigate the inter-cell interference.

- We establish a metric for each AP in order to select the appropriate users' cluster to work on.

- We show that the power allocation and APs association problems are not independent as tackled in the previous works. Therefore, we develop a new algorithm that finds a solution for joint power allocation and AP selection, resulting in a significant improvement in the EE.

- We propose a low-complexity solution for the joint problem of power allocation and APs selection aimed at decreasing the complexity with an acceptable

degradation in the EE compared to the first proposed algorithm.

- In the power allocation subproblem, in the previous works [47], [1], [96], authors allocated the power based on the worst case of inter-cell interference which is a fake interference information. Here, we propose an iterative algorithm that approaches to having the exact interference information and improves the EE as the number of iterations increases. In addition, for solving the power allocation problem, we modify the traditional subgradient method by introducing closed-form expression for some dual variables, resulting in speeding up the convergence.

The rest of this chapter is organized as follows. The system and channel models are introduced in Section 3.4. In Section 3.5, we present the problem formulation and the proposed solutions. Some simulation results are presented and discussed in Section 3.6. Finally, the chapter is concluded in Section 3.7.

3.4 System and Channel Models

The system under consideration consists of N_A VLC APs and N_u users, as shown in Fig. 3.1. The users are distributed uniformly in the area and the APs are fixed in the ceiling of the room. Each AP is equipped with multiple LEDs that use IM to transmit the light signal to the users that can receive and convert the light to current, using PDs. Also, the locations of users are assumed to be unchanged during a short time duration T. This assumption can be justified by assuming that all the mobile users are better to be served by WiFi APs to avoid the numerous handover usually occurs in
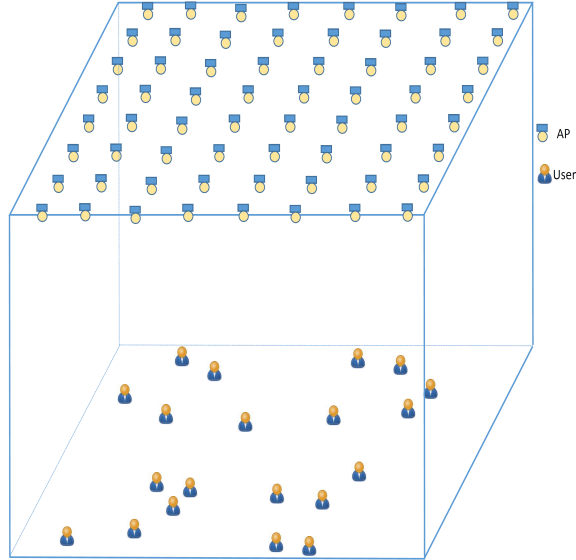
Figure 3.1: System model (an example of distributing the users uniformly in the area).

VLC networks [61], [63]. Thus, the CSI of the VLC links is considered to be constant during T period. Several indoor environments can prove that the number of lamps fixed in the ceiling are more than the number of users inside the considered room such as labs, houses, offices, companies, etc. This motivates us to assume that the number of users is less than the number of APs. However, the proposed algorithms in this chapter can be implemented even if the number of users are more than the number of APs. For instance, if the number of users are twice the number of APs, a user scheduling algorithm can be implemented where half of the users served by the first time slot while the others served in the second time slot, and the proposed procedures can be implemented within each time slot. The VLC channel model is given in (1.1) in chapter 1.

3.4.1 Transmission Technique

For white LED transmission, we use the single blue LED chip with a phosphor layer, which is commonly used, where the modulation bandwidth B is normally around 20 MHz, however this measured bandwidth is related to the specific LED product employed. The energy-efficient ACO-OFDM is used as a modulation scheme in the proposed system model. In each formed cth cell, we have $N_{A,c}$ APs transmitting the signal vector $\mathbf{Y}_{t,c} \in \mathbb{R}^{N_{A,c} \times 1}$ to $N_{u,c}$ users. The equivalent channel can be modeled as a multi-users MISO system and the vectored transmission (VT) zero-forcing based is used to eliminate the intra-cell interference. Hence, we can express the received signal vector of a particular sub-channel in the cluster c by

$$\mathbf{Y}_{r,c} = \rho \mathbf{H}_c \mathbf{G}_c \bar{\mathbf{P}}_c \mathbf{Y}_{t,c} + \mathbf{n_c}, \tag{3.1}$$

where $\mathbf{H}_c \in \mathbb{R}^{N_{u,c} \times N_{A,c}}$ is the channel attenuation matrix between the end users and the APs in the cluster c, $\bar{\mathbf{P}}_c = \mathrm{diag}(\mathbf{P}_c)$, where $\mathbf{P}_c$ is the electronic power vector assigned to the users belong to the cluster c, $\mathbf{n_c}$ is the noise plus the inter-cell interference, and $\mathbf{G}_c$ is the pre-coding matrix that is designed to diagonalize the channel matrix by setting $\mathbf{G}_c = \mathbf{H_c}^H (\mathbf{H_c H_c}^H)^{-1}$. This process (diagonalizing the channel or eliminating the intra-cell interference) needs the accurate knowledge of the users' channels. Since the VLC channels are pre-dominantly static, the user's channel can be attained using a single attenuation factor. It can be estimated at the user side and then fed back to the AP side at the cost of modest overhead [47]. It is important to note that the amount of the exchanged information depends on the cluster size or the number of

cells in the VLC systems. A low number of cells (large cells' size in average) leads to a less inter-cell interference and a large amount of exchanged information, while a high number of cells (small cells' size in average) leads to a high inter-cell interference and a small amount of exchanged information. Hence, the number of cells must be selected carefully based on the needed applications. The achievable data rate at the user j in cluster c is given by

$$R_{j,c} = \beta \log \left(1 + \frac{(\rho^2/2)P_{j,c}}{BN_0 + X_{c,j}} \right), \tag{3.2}$$

where $P_{j,c}$ is the assigned power for the user j in the cell c, $X_{c,j}$ is the interference received at the user j in the cell c, N_0 is the noise power spectral density, and β is a value which depends on the applied modulation scheme. Because of the assumption that the ACO-OFDM modulation scheme is applied, the value of $\beta = B/4$, where B is the modulation bandwidth. The transmit power at AP i in the cluster c, which is the power consumed for communication, is given by

$$p_{i,c} = \sum_{j=1}^{N_{u,c}} g_{i,j}^2 P_{j,c}, \tag{3.3}$$

where $g_{i,j}$ is the element located in the ith row and j^{th} column in matrix $\mathbf{G}_c$.

3.5 Problem Formulation

In this section, we present algorithms and steps to efficiently form the cells and allocate the powers to maximize the EE. The general procedures are represented in Fig.

(a) Traditional procedures.   (b) Proposed procedures.
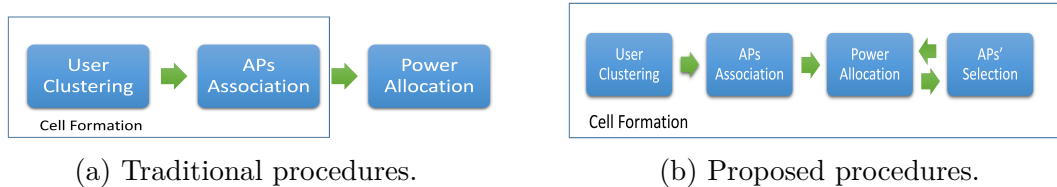
Figure 3.2: Comparison between the proposed and the traditional procedures for EE maximization.

3.2, where the difference between the proposed and the traditional procedures [96], [47], [1] is shown. We start by proposing a users' clustering algorithm, establishing metrics for associating all APs to the clustered users, formulating the power allocation optimization problem with providing an efficient solution, and proposing two different iterative algorithm (one for seeking the optimality and the other for seeking the simplicity) to jointly allocate the power and select the participating APs in communication. These individual procedures are followed by a flowchart that shows how the proposed algorithms and steps are arranged and implemented, in general, to maximize the EE.

3.5.1 Cell Formation

Here, we provide a new UC clustering algorithm under a given number of clusters, we then provide a new procedures for APs association to the formed users' clusters. Our targets in users' clustering are to cluster the users based on their distances to each others and to maximize the separation between the clusters. The main contribution of our clustering approach is the initial steps that have a significant impact on the final results in terms of EE.

66

User-Centric Clustering

In this section, we aim to group the users in a predefined K clusters aiming to maximize the EE of the whole network. Clustering the users based on their geographical positions, to have the summation of the distances of all users in a cluster to their centers as small as possible, definitely helps in improving the EE of the system. Due to its simplicity and speed, The traditional K-means clustering method has been widely used in clustering. It is designed to minimize the following objective function

$$U = \sum_{k \in K} \sum_{j \in c} \|\mathbf{x}_{j,k} - \mathbf{c}_k\|^2, \tag{3.4}$$

where $\mathbf{x}_{j,k}$, $\mathbf{c}_k \in \mathcal{R}^2$ are the position of the user j in the cluster k and the center position of the cluster k, respectively. There are multiple improved versions of the K-means method in the literature. Here, we pick the improved version of the K-means method proposed in [97], which is called K-means++, to build on. Briefly, the K-means++ augmented the K-means method with a randomized seeding technique which helps in improving the speed and the accuracy. More details on the K-mean++ clustering method are provided in [97].

If a different clustering schemes are given, it is highly complex to implement both the APs association and power allocation to specify the best clustering scheme that provides the highest EE. To simplify the problem, first several clustering design are offered, then the best clustering design that helps in mitigating the inter-cell interference is estimated. The main disadvantage in the K-means++ method is that the selection of the initial centers may lead to a poor EE. This is because it is based on a probabilis-

tic initial selection and it is not built for the special structure of the VLC networks that is highly affected by the inter-cell interference. Therefore, beside the objective of the K-means++ algorithm, we augment another objective that helps in decreasing the inter-cell interference. This objective is to maximize the average distance between the users in the different clusters. This means having the distances between the cluster centers as far as possible. To achieve such objective, it is important to note that if K points are given and the distances between them $d_{i,j}, \ i = 1, \ldots, K, \ j = i + 1, \ldots, K,$ under the constraint that the summation of them is less than or equal D, the solution of the following optimization problem

$$\max_{d_{i,j}} \prod_{i=1, \ j=i+1}^{K} d_{i,j}, \quad s.t. \quad \sum_{i=1, \ j=i+1}^{K} d_{i,j} \leq D, \tag{3.5}$$

is $d_{i,j} = \frac{D}{K}, \ i = 1, \ldots, K, \ j = i + 1, \ldots, K$. This means that if we have MK centers, the K centers out of MK, which have maximum distance between them, can be found by finding the product of the distances of all possible K centers and picking up the maximum result, where M is an integer value and greater than or equal 1.

The main idea of the proposed algorithm is to start with a number of initial centers that is much more than K, then select the centers that have the maximum distance between them. Therefore, the following Algorithm 3 is the proposed clustering algorithm.

Increasing M would enhance the performance and increase the complexity, and decreasing it would decrease the complexity and degrade the performance. The complexity of Algorithm 3 is at most M times the complexity of the K-means++ algo-

Algorithm 3 User clustering algorithm.

---

1. Select a user randomly to be the first center c_1.

2. For each user find the the shortest distance $D(x)$ from the considered user to the closest center.

3. Take a new center c_k, selecting $x \in X$ with probability $\frac{D(x)^2}{\sum_{x \in X} D(x)^2}$, and repeat that until we have K centers.

4. For each $k \in 1, ..., K$, set the cluster C_k to be the set of points in X that are closer to c_k than they are to c_j for all $k \neq j$, and then update the centers.

5. Calculate $T_m = \prod_{i=1,\ j=i+1}^{K} d_{i,j}$, where $d_{i,j}$ is the distance between center i and center j.

6. Repeat the steps above M times and select the K centers that give us maximum T_m.

7. Update the centers of the selected K centers until no longer change.

---

rithm, but it yields a high impact on the EE, and it is negligible if we compare it with the complexity of the power allocation problem. It is important to note that the proposed clustering algorithm requires the location of all users to be known. The users' locations depend on the channel knowledge at APs. Once the APs acquire the users' channels, the distances between users can be inferred using the equation of the channel model (1.1) [47]. Then, classical positioning and tracking can be used to determine the users' locations [98]. As a result, the users' locations would be known at AP side, where the clustering method can be implemented.

AP Association

It is plausible that increasing the number of APs in a cluster improves the EE of that cluster, but on the other hand, it increases the inter-cell interference in the other

clusters. This inspires us to propose a new cell formation technique that first involves all the APs in the network, then switches off the ones that are harmful (in terms of increasing the inter-cell interference) more than helpful (in terms of enhancing the EE inside the cell). Here, we distribute the APs to the clustered users, and in Section 3.5.3, we optimize the APs selection based on a given power allocation scenario. Our goal here is that for each AP, we select the best cluster that might serve the associated users or enhance the EE as possible as it can. Therefore, we propose two steps to associate the APs to the formed cells:

1. We assign for each user its closest AP by using the following steps: 1) In the channel matrix, find the maximum channel value, assign the corresponding AP to the corresponding user, then make the row and the column of the corresponding pair equal to zero, 2) Repeat Step (1) until the channel matrix equals the zero matrix.

2. For the remaining APs, for each cluster c, we first find the average channel of each AP to all users in the cluster c as follows

$$\hat{g}_{i,c} = \sum_{j \in c} h_{j,i}^2, \ c = 1, \ldots, K, i = 1, \ldots, N_A. \tag{3.6}$$

Then, we associate the AP i to the cluster that satisfies the following relation

$$I_i = \max_c (\hat{g}_{i,c}), \ c = 1, \ldots, K.$$

The target of the second step is to associate the AP to the cluster that would maximize

70

(a) User clustering. (b) Associating APs.
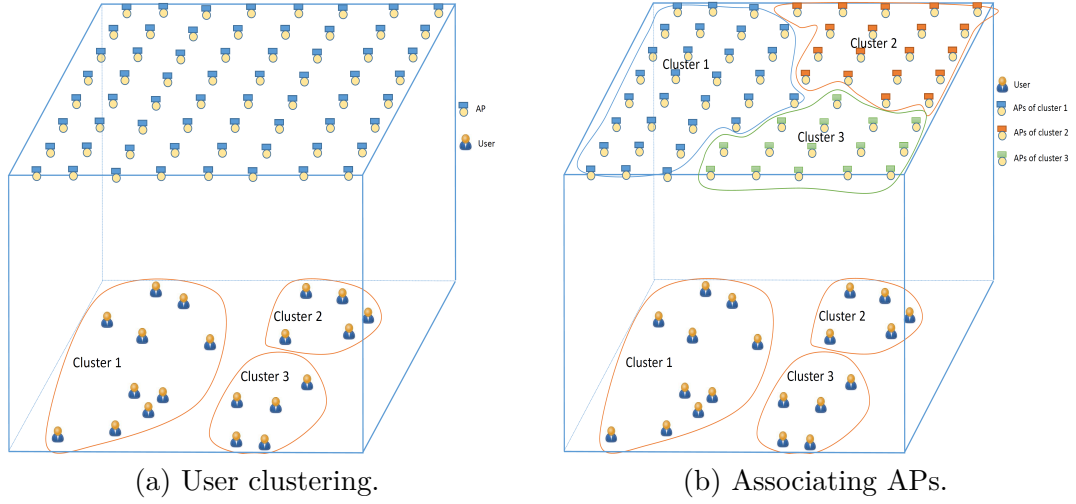
Figure 3.3: An example of cell formation a) User clustering using Algorithm 3, b) Associating APs using the proposed steps, when $K = 3$ and H-FoV=60°.

the cell capacity and minimize the inter-cell interference in the other cells.

In Fig. 3.3, we illustrate the cell formation by showing an example of clustering a given distributed users to a three clusters using our proposed Algorithm 3 in Fig. 3.3a. In addition, we show how the proposed steps in the APs association associate the APs to the clustered users in Fig. 3.3b. Fig. 3.3b shows that the number of APs associated to cluster c is directly proportional to the the number of the users in that cluster.

3.5.2 Power Allocation Scheme

Our goal in this section is how to allocate the power efficiently for the N_u users to maximize the EE. Specifically, the objective function is to maximize the EE of the whole network under certain QoS constraints and maximum available power constraints. These constraints are introduced to guarantee some fairness among users per cell and to achieve the required illumination, respectively. The EE function is defined as the

ratio of benifit provided by the system over the total consumed power [43]. In other words, if the system benefit is the sum rate, hence the energy efficiency is given by:

$$F_{EE} = \frac{R_T}{P_T},$$ (3.7)

where R_T is the sum rate, P_T is the total consumed power at the transmitters. In this chapter, we consider only the consumed power for communication in the formulated EE function. In the literature, two types of EE function have been introduced, which are the average per-cell EE and the global EE (GEE). For the average *per-cell* EE, let us define η_c as the EE at the cell c, hence, using Equations (3.2) and (3.3), the average per cell EE of the whole network is defined as

$$EE = \frac{1}{K} \sum_{c=1}^{K} \eta_c,$$ (3.8)

where

$$\eta_c = \frac{\beta \sum_{j=1}^{N_{u,c}} \log\left(1 + \frac{(\rho^2/2)P_{j,c}}{BN_0 + X_{c,j}}\right)}{\sum_{i=1}^{N_{A,c}} \sum_{j=1}^{N_{u,c}} g_{i,j}^2 P_{j,c}}.$$ (3.9)

The GEE is the summation of data rates of users in all clusters over the total power consumed at all APs, which can be expressed as

$$GEE = \frac{\beta \sum_{c=1}^{K} \sum_{j=1}^{N_{u,c}} \log\left(1 + \frac{(\rho^2/2)P_{j,c}}{BN_0 + X_{c,j}}\right)}{\sum_{c=1}^{K} \sum_{i=1}^{N_{A,c}} \sum_{j=1}^{N_{u,c}} g_{i,j}^2 P_{j,c}}.$$ (3.10)

Function (3.10) is usually optimized when the centralized approach is employed, while Function (3.8) supports an efficient distributed approach. We select to optimize

the average per-cell EE for its simplicity and for the reason that it can be implemented in each cell independently. The optimization problem can be formulated as follows:

$$\max_{P_{j,c}, \forall j,c} \quad EE, \tag{3.11a}$$

$$s.t. \quad R_{j,c} \geq \gamma, \ \forall j, c, \tag{3.11b}$$

$$\sum_{j=1}^{N_{u,c}} g_{i,j}^2 P_{j,c} \leq p_{max}, \ \forall j, c, \tag{3.11c}$$

$$P_{j,c} \geq 0, \quad \forall j, c, \tag{3.11d}$$

where γ is the minimum required data rate, and p_{max} is the maximum electronic transmit power available at the APs. It is important to note that the p_{max} must be selected to satisfy the illumination requirements and must be within the operational dynamic range of the LEDs. A detailed discussion about optimizing the value of p_{max} is provided in [47]. Problem (3.11) can be separated equivalently to K subproblems, where the optimization problem in cluster c can be expressed as follows:

$$\max_{P_{j,c}, j=1,\ldots,N_{u,c}} \quad \eta_c, \tag{3.12a}$$

$$s.t. \quad R_{j,c} \geq \gamma, \ j = 1, \ldots, N_{u,c}, \tag{3.12b}$$

$$\sum_{j=1}^{N_{u,c}} g_{i,j}^2 P_{j,c} \leq p_{max},$$

$$i = 1, \ldots, N_{A,c}, \tag{3.12c}$$

$$P_j \geq 0, \quad j = 1, \ldots, N_{u,c}. \tag{3.12d}$$

Problem (3.12) must be implemented in each cell independently aiming to maximize the summation of the cells' EE in the whole network. Problem (3.12) is not

73

easy to be solved because the inter-cell interference terms depend on the allocated powers and the power allocation problem depends on the interference terms. In order to simplify this problem, we first solve it under the worst case where the interference is considered to be at its highest value, which happens when all the APs are assumed to transmit at their maximum power. Then in Section 3.5.2, we provide an algorithm that solves the power allocation problem based on the exact or the approximate interference information. Even if we assume the interference information is available, Problem (3.12) is still not easy to solve since the objective function in (3.12) is a ratio of two functions (concave in the numerator and a linear function in the denominator), which is generally considered as a non-convex function. It is noted that there is no standard approach for solving non-convex optimization problems. However, this class of optimization problems, can be solved using fractional programming tools [99], [100] such as the Dinkelbach method [101] that transforms this problem into a successive concave functions. In the following, we decompose the solution of (3.12) into two loops:

Main Loop: Using Dinkelbach method, we can transform the objective function in (3.12) to be as

$$
\max_{P_{j,c}, j=1,\ldots,N_{u,c}} \beta \sum_{j=1}^{N_{u,c}} \log\left(1 + \frac{(\rho^2/2)P_{j,c}}{BN_0 + X_{c,j}}\right) - q_c \sum_{i=1}^{N_{A,c}} \sum_{j=1}^{N_{u,c}} g_{i,j}^2 P_{j,c}, \qquad (3.13a)
$$

$$
s.t. \quad (3.12a),\ (3.12b),\ (3.12c), \qquad\qquad\qquad\qquad (3.13b)
$$

where q_c is a positive variable introduced to be optimized or selected to have the objective function in (3.13) equal to zero at optimality. If q_c is given, Problem (3.13) is

concave and can be solved using the classic dual-decomposition method, since Slaters' conditions are satisfied [56], which means that the duality gap is zero. In order to find the optimal q_c, the Dinkelbach algorithm is used to find the optimal value of q_c by the following steps: Step 1) Put $q_c = 0$ as an initial value, Step 2) Solve Problem (3.13) using the approach provided in the inner loop, and let $P_{j,c}^*$ as the optimal solution, Step 3) update q_c by

$$q_c = \frac{\beta \sum_{j=1}^{N_{u,c}} \log \left(1 + \frac{(\rho^2/2)P_{j,c}^*}{BN_0 + X_{c,j}} \right)}{\sum_{i=1}^{N_{A,c}} \sum_{j=1}^{N_{u,c}} g_{i,j}^2 P_{j,c}^*}.$$

Step 4) Repeat Step 2 and Step 3 until the objective function of Problem (3.13) is less than ϵ, where ϵ is a small value close to zero.

Inner Loop: Here, we solve the optimization problem under the assumption that the value of q_c is given. Therefore, the optimization problem in (3.13) is a concave problem with one global optimal solution. Hence, we can use the dual problem to achieve the optimal solution, where the strong duality holds in the concave problems. Therefore, using the Lagrangian duality, the dual optimization problem of the problem in (3.12) can be expressed as follows:

$$\begin{aligned}
\zeta = k \sum_{j=1}^{N_{u,c}} \log \left(1 + \frac{(\rho^2/2)P_{j,c}}{BN_0 + X_{c,j}} \right) - q_c^* \sum_{i=1}^{N_{A,c}} \sum_{j=1}^{N_{u,c}} g_{i,j}^2 P_{j,c} \\
+ \sum_{j=1}^{N_{A,c}} \mu_{j,c}(R_{j,c} - \gamma) - \sum_{i=1}^{N_{A,c}} v_{i,c} \left(\sum_{j=1}^{N_{u,c}} g_{i,j}^2 P_{j,c} - P_{max} \right),
\end{aligned} \tag{3.14}$$

where $\mu_{j,c} \geq 0$, $j = 1, \ldots, N_u$ and $v_{i,c} \geq 0$, $i = 1, \ldots, N_{A,c}$ are the Lagrangian dual

variables. From the KKT conditions [56], we have

$$\frac{\partial \zeta}{\partial P_j} = 0. \tag{3.15}$$

Solving (3.15), we obtain

$$P_{j,c} = \frac{(1 + \mu_{j,c})k}{\ln(2)\left(\sum_{i=1}^{N_{A,c}}(v_{i,c} + q)g_{i,j}^2\right)} - \frac{2(N_0 B + X_{j,c})}{\rho^2}, \tag{3.16}$$

where the variable $\mu_{j,c}$ must be selected to guarantee that the Constraints in (3.11b) are feasible and $v_{i,c}$ must guarantee that the Constraints in (3.11c) are feasible too. Now, these dual variables must be found to obtain $P_{j,i} \; \forall \; j$. In [82], [84], [102], the authors used the subgradient method in similar problems to find the optimal dual variable. In brief, the subgradient method gives the dual variable initial values then finds $P_{j,c}$ using Equation (3.16). Then, the dual variables in each iteration can be updated as follows

$$v_{i,c}(n+1) = v_{i,c}(n) + \delta_v(\sum_{j=1}^{N_{u,c}} g_{i,j}^2 P_{j,c} - P_{max}), \; i = 1, \ldots, N_{A,c}, \tag{3.17}$$

$$\mu_{j,c}(n+1) = \mu_{j,c}(n) + \delta_\mu(\gamma - R_{j,c}), \; j = 1, \ldots, N_{u,c}, \tag{3.18}$$

where δ_μ and δ_v are steps size that should be sufficiently small to guarantee approaching the optimal solution at the steady state. The subgradient is an iterative algorithm that needs a large number of iterations to converge, a very careful selection of the step size, and a very careful selection of the initial values of the dual variables. Therefore,

76

in the following, we find a closed-form expressions for the $\mu's$ dual variables in terms of the $v's$ dual variables. By substituting (3.16) in Constraint (3.11b), $\mu_{j,c}$ must be

$$\mu_{j,c} \geq \frac{\ln(2)}{k} \left(\frac{P_{jmin}\rho^2 + 2(N_0 B + I_{j,c})}{\rho^2} \right) \\ \left(\sum_{i \in N_{A,c}} (v_{i,c} + q)\mathbf{g}_{j,i}^2 \right) - 1. \tag{3.19}$$

Hence, instead of updating the $\mu's$ dual variables using (5.34), we update them using (3.19). We show in details in our previous work [80] that the above substitution increases the rate of convergence significantly with less constraints violation compared to the sub-gradient method.

Finding the exact inter-cell interference information

In the literature, the power allocation problem was solved under the assumption that the inter-cell interference is in its maximum value [47], [1], [96]. The aim of this assumption is to simplify the power allocation problem and to guarantee that the required QoS of the users is achieved. However, this assumption yields a significant degradation in the objective function (EE), since the power is allocated based on inaccurate interference information. Therefore, we provide iterative steps that lead to find the actual interference information and enhance the EE as we increase the number of iterations. If the complexity is not an issue, we can increase the number of iterations to have a better EE. If not, we should decrease the number of iterations to avoid implementing the power allocation problem several times. The main idea is to implement the power allocation in the different clusters in a successive way and

update the inter-cell interference in each step. Thus, the steps are:

1. Implement the power allocation in Cell 1 under the assumption that the inter-ference at the users in that cell is in its maximum value, and then broadcast the allocated transmit powers to all clusters to update their inter-cell interference.

2. Implement Step 1 for Cells $2, 3, \ldots, K$ in a consecutive way with updating the interference information in each cell.

3. Repeat Step 2 for all cells (including Cell 1) until no improvement is achieved in the EE, or the number of iterations reaches its limit.

The above steps guarantee improving the EE and achieving the QoS constraints. This is because as we increase the number of iterations, each cell approaches to gather the exact interference information.

3.5.3   Joint Power Allocation and APs Selection

In the previous section, we provide a solution for allocating the power under a given participating APs. In this section, we first show how the power allocation and APs selection problems are interlinked, then we propose an iterative algorithm to solve both problems jointly. This iterative algorithm can be implemented after clustering the users and associating APs. To prove that the power allocation and the APs selection problems are interlinked, we should show that the allocated powers for the users' messages depend linearly on the transmit power at the APs. From (3.1), the relation between the transmit powers and the power assigned to the the users' messages in cluster c is given by $\mathbf{p}_c = \mathbf{G_c}^2 \mathbf{P}_c$, where $\mathbf{p}_c$ is the vector power at the APs, and

the square at $\mathbf{G}_c^2$ is the square of the elements in $\mathbf{G}_c$. Hence, we can find the powers assigned for the transmitted signals by

$$\mathbf{P}_c = \mathbf{F}_c \mathbf{p}_c, \tag{3.20}$$

where $\mathbf{F}_c = (\mathbf{G_c}^{2H} \mathbf{G_c}^2)^{-1} \mathbf{G_c}^{2H}$. Equation (3.20) means that switching off any AP (equating its transmit power by zero), affects the allocated power for users directly. Also, adding or inactivating an AP to cluster c affects the SNR of the users, belonging to the other cells, by changing the received interference. Therefore, selecting the participating APs in cell c affects the allocated power in that cell and in the other cells. This motivated us to deal with the power allocation and AP selection problems jointly.

The goal of optimizing the participating APs in communication is to minimize the inter-cell interference. It is clear that, under an optimal power allocation strategy, as we increase the participating APs in the cell c, the EE in that cell is improved. On the other hand, these added APs degrade the EE in the other cells by emitting interference. Therefore, first, we classify the APs into three categories: 1) the APs that have zero channels to all users, which must be switched off, 2) the APs that have channels to the associated users but zero channels to the users belonging to other cells (i.e. non-interfering APs), 3) the interfering APs that have LoS to their associated users and also have LoS to the users in the other clusters (i.e. interfering APs). The second category of the APs must be switched on because their participation in the communication improves the EE as long as the power allocation optimization

problem is applied. Our interest is in the third category, where each one of the APs has to be selected carefully to be switched on or switched off. Participating these APs definitely improves the EE in their own cells, but on the other hand, reduces the EE of the other cells by causing inter-cell interference. Thus, we first establish a metric that approximately measures the eligibility of each AP to participate in the communication (in case it causes non-zero inter-cell interference). This metric of the AP i in the cluster c can be given by

$$\Upsilon_{i,c} = \frac{\sum_{j \in c} h_{j,i}^2}{\sum_{j \notin c} h_{j,i}^2}. \quad \forall i \ \forall c \tag{3.21}$$

High value of $\Upsilon_{i,c}$ means that the quality of the information signal coming from the AP i to the intended users is much greater than the emitted interference from that AP and vice versa. The following algorithm solves the power allocation and APs selection alternatively until they converge.

The benefit behind sorting the APs ascendingly based on their $\Upsilon_{i,c}$ values is that we guarantee satisfying the condition that the number of active APs is greater than the number of users in each cluster with the APs that have highest $\Upsilon_{i,c}$. In addition, sorting the APs ascendingly increases the rate of convergence significantly. Condition in Step 4 in Algorithm 4 is needed to guarantee that the intra-cell interference is totally eliminated, since this cannot be guaranteed if the number of APs is less than the number of users. In addition, because of the assumption that the number of users in the system is much less than the number of APs, it is not wise to have some cells crowded with many users (number of users is greater than number of APs in the cell)

80

Algorithm 4 Joint APs selection and power allocation for EE maximization.

---

1. Specify all interfering APs and sort them ascendingly based on their $\Upsilon_{i,c}$ value. Let R be the number of interfering APs.

2. For $q = 1 : L$

3. For $i = 1 : R$

4. Change the AP i status (if it is on, switch it off and if it is off, switch it on) with keeping the condition that the number of the active APs is greater than the number of users in each cluster is satisfied.

5. Implement the power allocation problem and check if the EE is improved. If not, return the AP to its previous status.

6. End for

7. If $(EE(q-1) - EE(q) < \epsilon)$, break.

8. End for.

---

and some cells have only a few number of users. Therefore, we establish this condition to avoid or alleviate the effect of having unbalanced VLC systems and guarantee zero intra-cell interference.

Algorithm 4 is guaranteed to converge because with each change in the AP status in Step 3, the EE either improves or stays fixed. In addition, it is guaranteed to approach to the optimal solution as we increase the number of iterations. To show that, in each iteration, the proposed algorithm tests all the interfering APs by implementing the power allocation problem with each AP, which means that Algorithm 4 tries all the possible solution to have the best one. The reason to repeat testing the interfering APs is that the optimal state of AP i (on or off) depends on the given states of all other interfering APs, especially the ones that are close to the AP i.

81

Suboptimal Approach

Although Algorithm 4 approaches to the optimal joint power allocation and APs selection as we increase the number of iterations, it suffers from high computational complexity. In Algorithm 4, in each AP status change, we need to implement the power allocation problem. In other words, if we have L interfering APs, we need to implement the power allocation problem L times in each iteration. Therefore, in this section, we propose a suboptimal solution for the joint power allocation and APs selection optimization problem that is aimed at decreasing the complexity, by decreasing the number of times of implementing the power allocation problem, and minimizing the degradation in the EE as much as possible. This algorithm is based on estimating the APs that should be switched off. The main idea of this algorithm is first to implement the power allocation problem when all the APs are participating in communications, then we list all the interfering APs with sorting them ascendingly based on their eligibility factor. After that, we switch off all the APs that are contributing in the EE degradation without implementing the power allocation problem with each AP state change. Then, we can re-implement the power allocation problem after we finish switching off all the harmful APs. It is important to say that when we switch off the AP i in the cell c, we need to re-calculate the assigned power for the users in the cluster c using the relation $\mathbf{P}_c = \mathbf{F}_c \mathbf{p}_c$, where the ith term in $\mathbf{p}_c$ equal to zero. Algorithm 5 illustrates the steps to clearly provide a suboptimal solution for the joint power allocation and APs selection optimization problem. In Fig. 3.4, we show the difference between Algorithms 4 and 5 by applying them in the above example in Fig.

Algorithm 5 Joint APs selection and power allocation for EE maximization (suboptimal solution).

---

1. Find all interfering APs and sort them ascendingly based on their $\Upsilon_{i,c}$ value. Let R be the number of interfering APs.

2. Implement the power allocation problem when all APs are on.

3. For $q = 1 : L$

4. For $i = 1 : R$
   Check if switching off the AP i would increase the EE. If so, switch the AP i off; otherwise switch it on.

5. End for.

6. Implement the power allocation problem and check if the EE is improved.

7. If $(EE(q-1) - EE(q) < \epsilon)$, break.

8. End for.

3.3, and see what are the APs that should be switched off from both algorithms. It seems that both algorithms result in switching off the same APs with two added in Algorithm 5. This is because in Algorithm 5, once it switches off an AP, it does not return to test it again even if switching that AP on would be helpful in increasing the EE.

In the following we show the relationship of the proposed algorithms and steps by presenting a flowchart. Fig. 3.5 shows the whole proposed process for maximizing the EE based on the UC design. At Step 3 in Fig. 3.5, we can either use Algorithm 4 or 5, where the difference between them is that in Algorithm 4 the power allocation optimization problem is implemented with each AP status change, while in Algorithm 5 the power allocation is implemented after testing all the interfering APs.

(a) Algorithm 4.   (b) Algorithm 5.
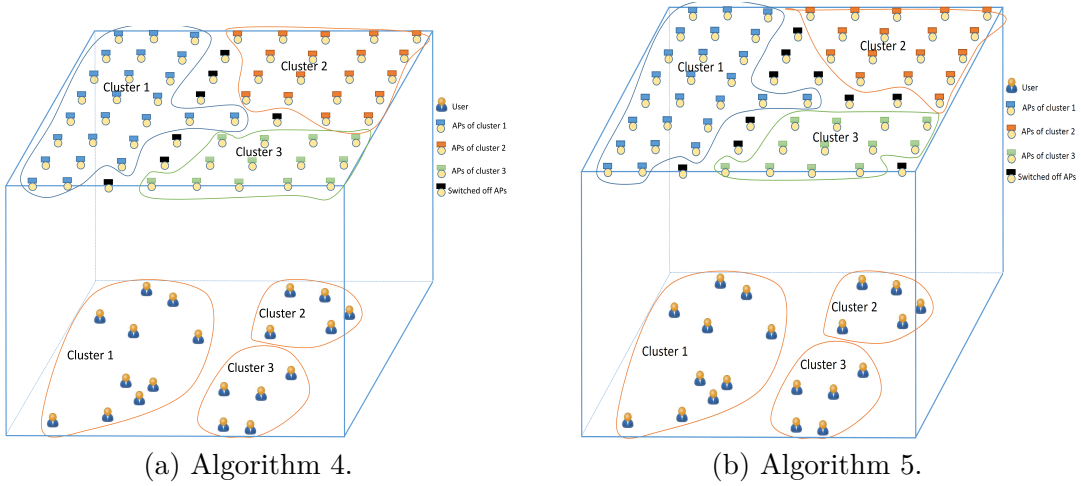
Figure 3.4: An example of switching off APs using a) Algorithm 4, b) Algorithm 5, when $K = 3$ and H-FoV $= 60^o$.
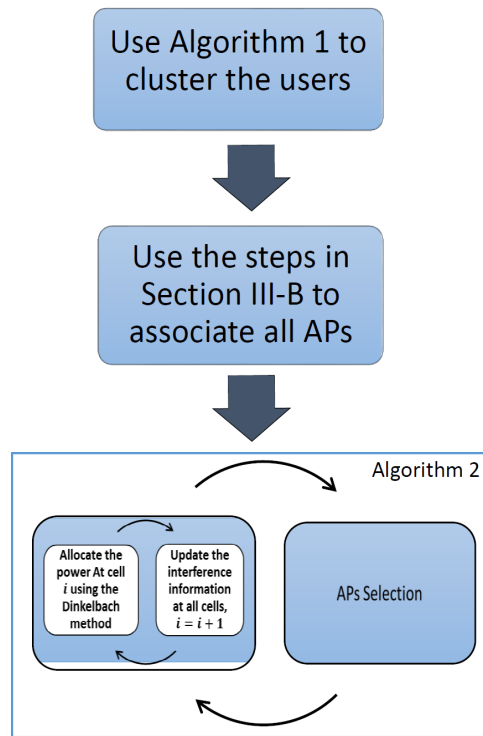
Figure 3.5: Flowchart showing how the proposed algorithms and steps would be arranged and implemented to maximize EE.

Table 3.1: Simulation Parameters

Name of the Parameter	Value of the Parameter
Maximum bandwidth of VLC AP, B	20 MHz
The physical area of a PD, A_p	0.1 cm^2
Half-intensity radiation angle, $\theta_{1/2}$	60°
H-FoV, semi-angle of PD,Θ	45$^o - 65^o$
Gain of optical filter, g_{of}	1
Refractive index, n	1.5
Efficiency of converting optical to electric, ρ	0.53 [A/W]
Maximum transmit power [1], p_{max}	0.386 Watt
Noise power spectral density of LiFi, N_0	10^{-22} A^2/Hz
Room size	16×16 m^2
Room height	3 m
User height	0.85 m
Number of APs	8×8
Number of users	20
Monte Carlo	150 iterations
M in the proposed clustering algorithm	5
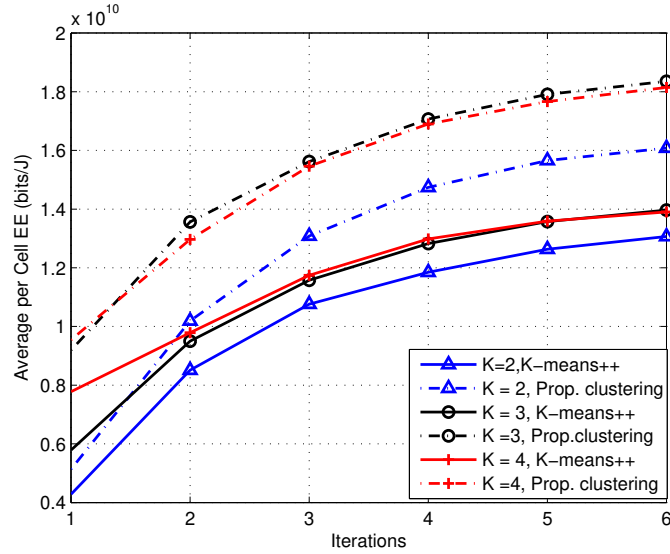
Figure 3.6: Energy efficiency versus number of iterations of updating the interference when all the APs are participating, H-FoV $= 55^o$.

3.6 Simulation Results

In the following, we verify the capability of the proposed algorithms for enhancing the performance of the VLC network. The values of all used parameters in the consid-
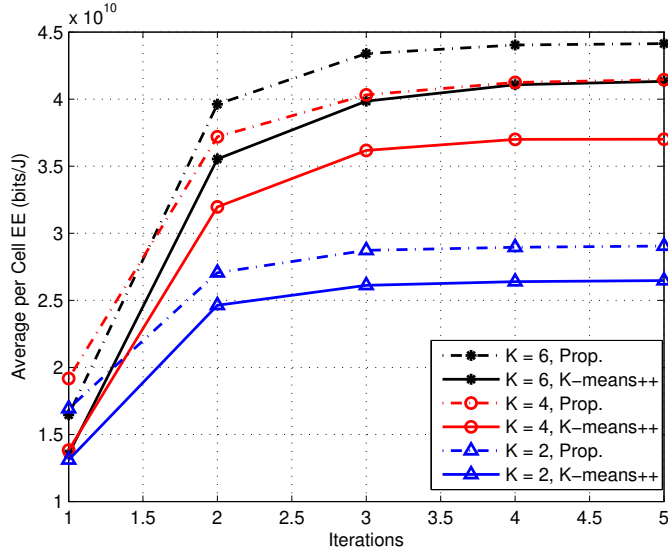
Figure 3.7: Energy efficiency versus number of iterations in Algorithm 4 with different number of clusters and different users clustering, H-FoV= 55°.
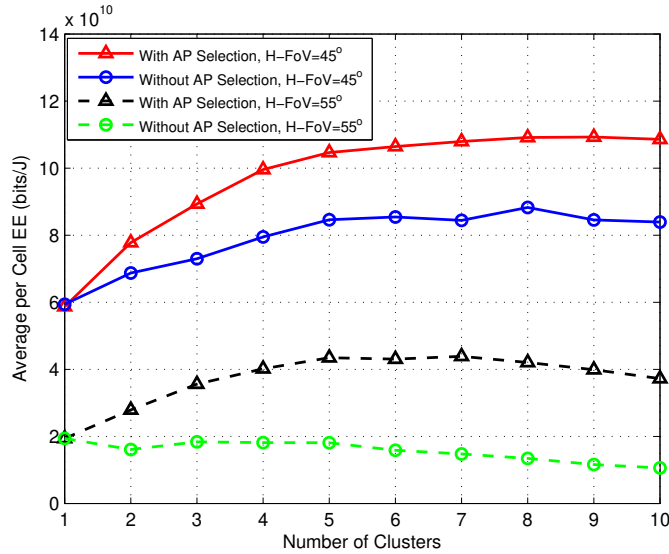
Figure 3.8: Comparison between applying Algorithm 4 for AP selection and participating all APs by plotting EE versus number of clusters with different H-FoV.

ered VLC system are given in Table I. Monte-Carlo simulation is used to assess the performance of the proposed algorithms where in each simulation iteration, a uniform random user distribution is generated. We show the convergence of the proposed algorithms and how they improve the system's EE. We compare our work with those in
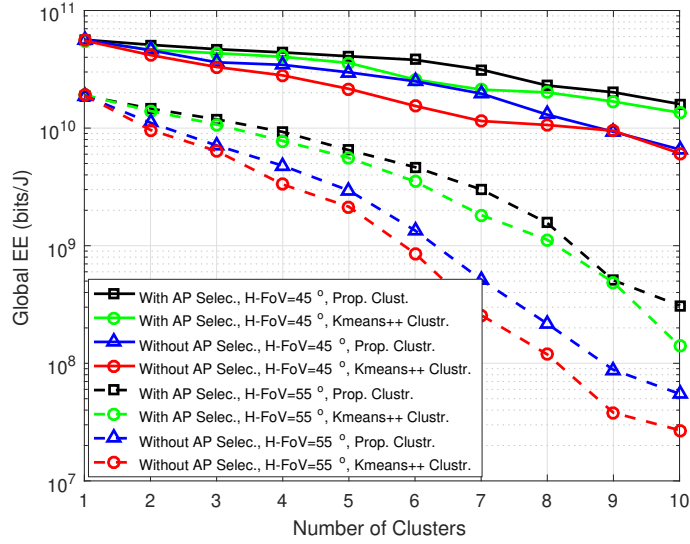
Figure 3.9: Comparison between applying Algorithm 4 for AP selection and participating all APs by plotting GEE versus number of clusters with different H-FoV.

the literature in general such as: 1) in Figures 6 and 10, we compare the approach of allocating the power based on the worst case interference, which is proposed in [47], [1], and [96], and our iterative algorithm that updates the interference information with each iteration, 2) in Figures 8-12, we consider the approach proposed in [47] of participating all APs (that have LoS to any user) in communication as a baseline and compare it with the proposed algorithm for the APs selection, where the approach in [47] is indicated by "without APs selection" in the figures, 3) in Fig. 14, we compare the proposed algorithm for APs selection and association with the one proposed in [1], 4) we also compare the proposed clustering method versus the Kmeans++ clustering method presented in [97].

In Fig. 3.6, we plot the EE versus the number of iterations of updating the interference when all the APs are involved in communications. As can be shown, as the number of iterations increases, the EE increases, and the rate of increasing gets smaller

with higher number of iterations. In each iteration, we need to implement the power allocation problem in each cluster which means that increasing the number of iterations would significantly increase the complexity but with a significant enhancement in the performance. Hence, the proposed algorithm for interference updating provides us with an optional decision whether to enhance the performance at the expense of the complexity or vice versa.
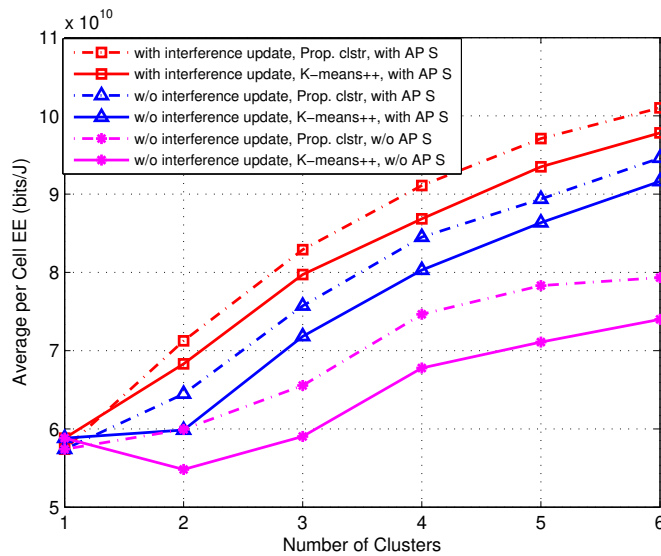
Figure 3.10: Comparison between the K-means++ and the proposed clustering methods with and without AP selection by plotting the EE versus number of cells when H-FoV = 45°.

Fig. 3.7 shows the convergence of Algorithm 4. It is clear that Algorithms 2 needs at most three iterations to converge. Furthermore, the number of iterations needed for convergence does not depend on the number of clusters in the system. In addition, it can be seen that only the first iteration yields a significant improvement in the EE of the system, especially when the number of clusters is large. Furthermore, this figure beside Fig. 3.6 fairly compare between the user clustering using the K-means++ and the proposed Algorithm 3. Both show the superiority of our proposed users' clustering

algorithm over the K-means++ algorithm with different number of clusters whether we implement one iteration or multiple iterations.

Fig. 3.8 illustrates how the EE behaves as we increase the number of cells. Besides, it shows the significant improvement in the EE when we apply Algorithm 4 compared to participating all the APs in the transmission. This figure shows unexpected results since as we know, as the number of cells increases, the inter-cell interference increases which degrades the EE. But, this figure shows that the average per-cell EE increases and then decreases with the number of cells, which means that there is another factor that helps in enhancing the average per-cell EE as the number of cells increases. This factor is the number of users per cell since as the number of clusters increases the average number of users per cell decreases. This means that the required transmit power per cell decreases as the number of clusters increases, which results in enhancing the average per-cell EE. Apparently, this factor has a great impact when the inter-cell interference is small which occurs when the number of clusters is small or when the H-FoV is small.

On the other hand, the GEE is decreasing with increasing the number of cells as shown in Fig. 3.9, because the GEE depends on the number of users in the whole system. It is important to note that in Fig. 3.9, we implement the proposed algorithms that are established to maximize the average per-cell EE and based on the output allocated power, we measure the GEE by calculating Equation (3.10). Fig. 3.9 also shows that the proposed user clustering algorithm outperforms the K-means++ algorithm in terms of GEE. Besides, Algorithm 4 provides a significant improvement in GEE as shown in Fig. 3.9.

89
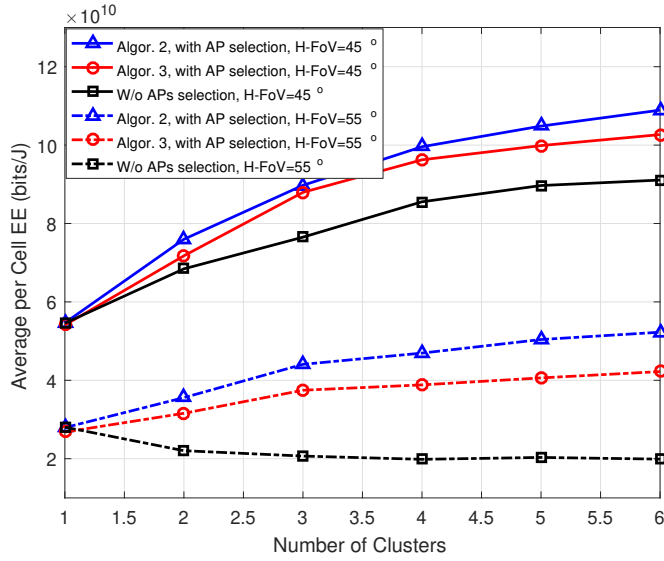
Figure 3.11: Comparison between the Algorithm 4 and Algorithm 5 with and without AP selection by plotting the average per cell EE versus number of cells with different H-FoV.
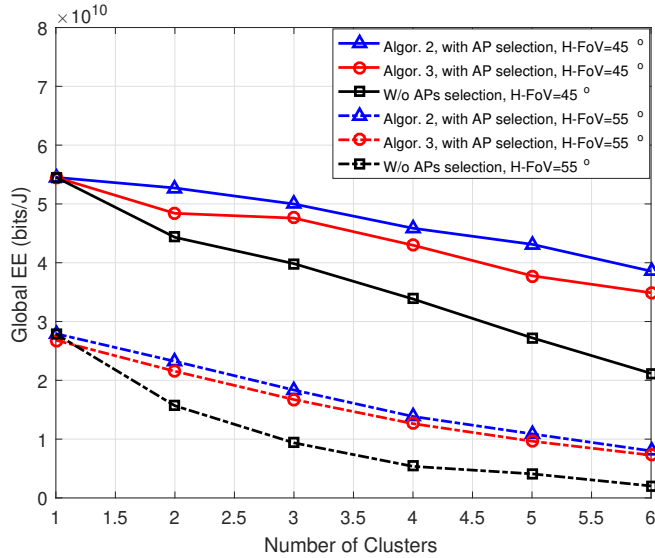
Figure 3.12: Comparison between Algorithm 4 and Algorithm 5 with and without AP selection by plotting the GEE versus number of cells with different FoV.

Fig. 3.10, shows the effectiveness of the proposed algorithms in improving the EE of the considered network. The best performance occurs when we apply the AP selection along with the proposed user clustering algorithm with updating the inter-
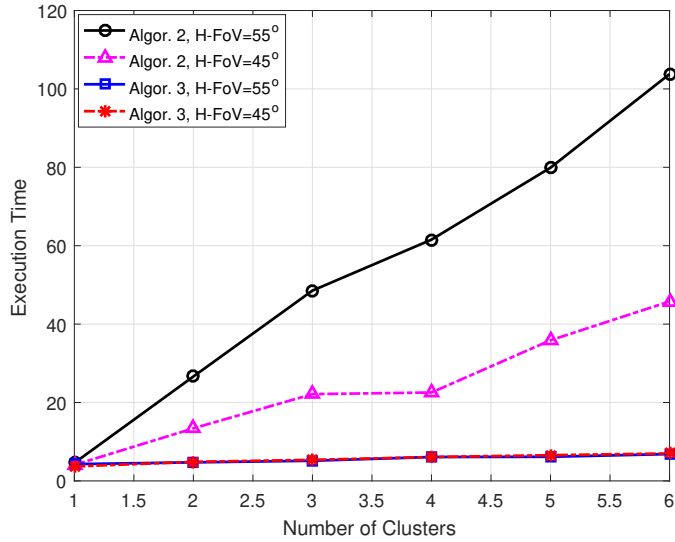
Figure 3.13: Comparison between complexity of Algorithms 4 and 5 by plotting the execution time versus number of cells when with different H-FoV.

ference, while the worst performance happens when the K-maens++ user clustering algorithm, all the APs participate in communication, and the powers are allocated based on the worst case interference. This figure shows that efficient user clustering methods leads to a significant improvement on the system's EE.

In Figs. 3.11 and 3.12, we conduct a fair comparison between Algorithm 4 and Algorithm 5 by plotting the average per cell EE and the GEE, respectively, versus number of cells. It can be shown that with different number of clusters and different H-FoV, Algorithm 4 is more energy-efficient than Algorithm 5. This is because in Algorithm 4, with each AP status change, we test the average per cell EE by re-implementing the power allocation problem, while in Algorithm 5, we implement the power allocation after we test all the interfering APs. In other words, if the number of interfering APs is L, in each iteration, we implement the power allocation problem in Algorithm 4 L times, while we implement the power allocation problem only once

in Algorithm 5 with each iteration.

On the other hand, in Fig. 3.13, we compare both Algorithms 4 and 5 in terms of complexity by plotting the execution time spent by both algorithms. Fig. 3.13 shows that Algorithm 5 needs much less time than Algorithm 4 to implement the joint power allocation and AP selection. This is because of the reason stated before that in Algorithm 4, with each AP status change, we test the average per cell EE by re-implementing the power allocation problem, while in Algorithm 5, we implement the power allocation after we test all the interfering APs. Because the number of interfering APs is increased as we increase H-FoV or the number of clusters, Fig. 3.13 shows that we need much time to test all the interfering APs and select the APs that must participate in communication.

In Fig. 3.14, we compare our algorithms for APs association with the algorithm that was proposed in [1]. The comparison is conducted under the same user clustering algorithm, the same power allocation algorithm, and with 200 Monte-Carlo simulations. The difference between them is that we deal with the power allocation problem and AP association jointly, while they solved both problems separately. In addition, we establish a metric for each AP based on its average channels to the clustered users aiming to select the best cell to serve and to mitigate the inter-cell interference. The algorithm proposed in [1] can be briefly explained by that, after selecting the anchor AP for each user, the rest of the APs are associated to the clusters within a certain range d_α. In other words, the AP i is assigned to the cluster c if the distance between that AP and the center of that cluster is less than or equal to d_α. If more than one cluster satisfy this condition for AP i, this AP must be switched off to mitigate the

interference. The disadvantages of this approach are: increasing or decreasing d_α may switch on the harmful APs and switch off the helpful ones because it depends only on the distance and not on the channel that is affected by different factors such as the receiver FoV, the transmitter coverage and so on; switching the APs off or on is not related to the transmit power at these APs, which is a crucial factor to consider. Therefore, as shown in Fig. 3.14, our proposed algorithms (Algorithms 4 and 5) significantly outperform the proposed algorithm in [1] for AP association in terms of the average per cell EE.
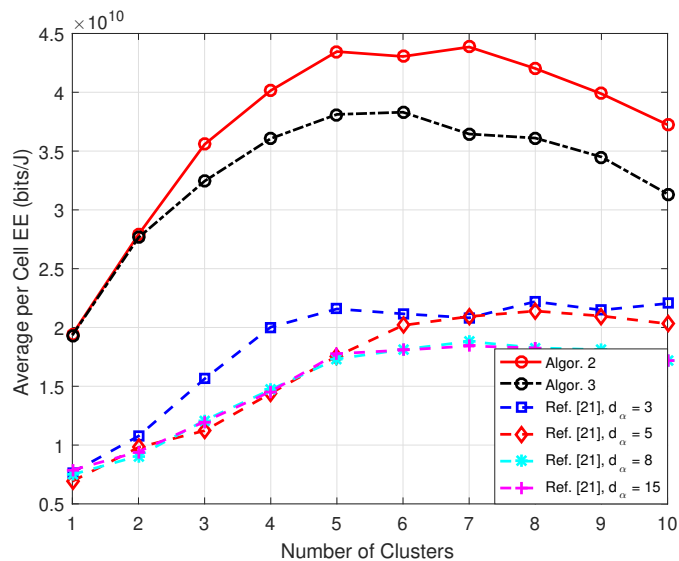
Figure 3.14: Comparison of our proposed algorithms (Algorithms 4 and 5) to the Algorithm proposed in [1] in terms of APs association to the clustered users, H-FoV = 55°.

In Fig. 3.15, we show how the average per cell EE behaves when we change the number of users in the system with different H-FoV. As shown in this figure, the EE is degraded as we increase the number of users. This is because the amount of required power needed by users to achieve the required QoS increases as we increase the number of users. It is also shown that the amount of improvement in the EE caused by APs

selection increases as we increase the number of users. This is because the number of interfering APs increases with higher number of users, which means that the AP selection is highly demanded when we have a high number of interfering APs. In other words, the AP selection algorithms have a slight impact on the EE if we have 10 users (small number of interfering APs), while the impact on the EE would be significant when we have 30 users (large number of interfering APs).
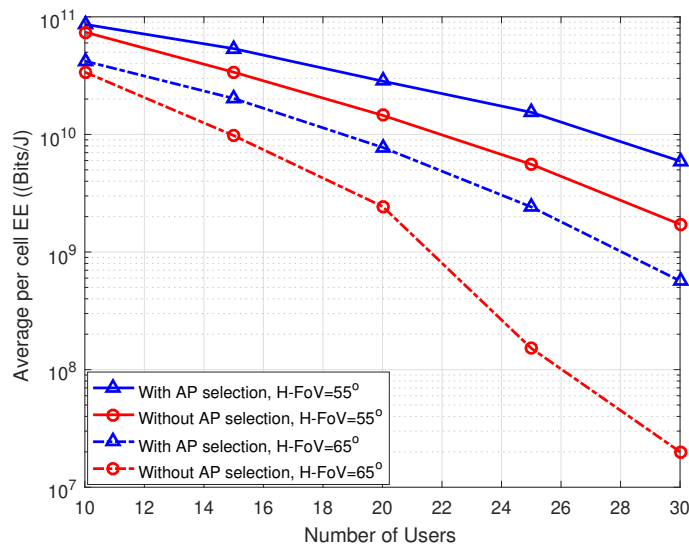
Figure 3.15: Energy efficiency versus the number of users in the system with different H-FoV when we have 5 clusters, Algorithm 5 is used for AP selection.

3.7 Conclusion

In this chapter, an energy-efficient VLC network was designed based on amorphous cell formation with jointly allocating the power and associating the APs. A new user clustering algorithm was proposed based on distances between users and separating the clusters as much as possible to mitigate the inter-cell interference. Also, two other algorithms were proposed to jointly allocate the power and select the APs in order to

maximize the EE. The aim of the first algorithm is to seek for the optimality of the EE maximization problem, while the aim of the second algorithm was to decrease the complexity of the first one with an acceptable degradation in the EE. We also proposed an iterative algorithm to find the optimal power allocation based on exact interference information, which significantly improved the EE. The results showed that designing an appropriate user clustering algorithm with considering the inter-cell interference, selecting the active APs based on the allocated power, and allocating the power based on the exact inter-cell interference information results a significant improvement in EE maximization problem.

CHAPTER 4

OPTIMIZING HYBRID VLC/RF COOPERATIVE NOMA FOR SUM-RATE AND FAIRNESS MAXIMIZATION

4.1 Introduction

It has been proved that VLC networks can provide data rates with several Giga-bits per second [103], [8] which makes them a powerful alternative or complementary to the existing RF networks. However, as discussed in the previous chapters, the main disadvantages of multi-user VLC networks is the limited coverage, fairness among users, and the blockages effect on the VLC link, resulting in unbalanced system containing high-serviced (strong) and poor-serviced (weak) users. The communication in

VLC networks mainly depends on line-of-sight (LoS) VLC links that can be blocked entirely by any opaque objects. In addition, the LoS link is significantly attenuated with distance between the transmitter and the receiver and this limits the coverage area, resulting a very small cells that are called attocells [104]. Furthermore, the users' field-of-view (FoV) has a great impact on the system coverage and on the channel quality which leads to unbalanced VLC systems [105]. This motivates us in this chapter to propose and evaluate a new scheme based on hybrid VLC/RF cooperative non-orthogonal multiple-access (Co-NOMA) to mitigate the aforementioned VLC disadvantages. This chapter addresses the problem of jointly allocating the power, pairing the users, and selecting links for weak users to maximize the weighted sum rate of a VLC system, consisting of one AP and multiple users.

NOMA scheme has been proposed for the future wireless networks which aims at increasing the throughput, decreasing the latency, and improving the fairness. The principle of NOMA is the use of a single resource component by multiple users, whether this component is a sub-carrier, a time slot, or a spreading code. This can be implemented by setting different power levels for different users. For instance, for two users served by the same access point (AP), and using the same resource block, the AP assigns a high power to the user with poor channel (weak user) and a low power for the user with a stronger channel (strong user). Then the weak user decodes the received signal and accepts the strong user's signal as a noise, whereas the strong user first decodes the signal of the weak user, and then removes it from the received signal, after that it decodes its own signal. This scheme improves the system performance in VLC networks but it cannot extend the system coverage or mitigate the blocking

effect.

In RF networks, one step further to improve NOMA is to propose Co-NOMA that can improve the fairness and strengthen the received SNR at the weak users [106] by exploiting the redundant information in NOMA systems. This can be implemented in RF networks, in which the strong user can also work as an energy harvesting relay to help the weak user. The weak user can use the maximal ratio combining (MRC) to combine the signal coming directly from the base station and the relayed signal coming from the strong user. This technique (Co-NOMA) has not been applied in VLC networks because it is not plausible to forward the light signal by the strong user to the weak user using light channel. However, the received light signal can be converted to RF signal and then forwarded to the weak user through a RF channel. The received visible light at the strong user can be used to charge a power storage and this can be used as a power source to forward the weak user's signal. The energy can be harvested in VLC networks using the received direct current (DC) without affecting the power of the transmitted signal [24], [107]. This chapter evaluates the benefits of implementing the hybrid VLC/RF Co-NOMA scheme and allocates the messages' power, selects the links, and pairs the users to improve the sum-rate and fairness in VLC systems.

4.2   Literature Review

Several techniques have been proposed in the literature and in this thesis to mitigate the SNR fluctuations, increase the system coverage probability, and improve the sys-

tem performance in terms of the total achievable data rates and the system fairness. The most common solutions are the Hybrid VLC/RF networks, coordinated transmissions, and the relay-assisted VLC transmission. The main idea in hybrid VLC/RF systems is to assign the users who suffer from interference, handover overhead, blockages, or uncovered to be served by RF AP(s) and maintain the rest users assigned to the VLC networks [105]. Authors in [69] formulated an optimization problem to jointly allocate the time slots and distributed the users among VLC APs and RF AP. Supplement VLC by RF AP(s) was shown to support mobility and decrease the handover overhead[61], [70]. Authors in [72] showed that the users that suffer from high rate of blockages should be served by the RF network.

APs cooperation was also proposed to alleviate the VLC limitations by merging the cells and providing more than one AP to serve a user [69], [47], [108]. The cooperating APs can coordinate their transmissions to cancel the interference [92], [47], [108], increase the cell size [69], and mitigate the blockages effect [94]. Relaying was also investigated in VLC networks to extend the VLC coverage [109], [110], [111]. In [109] and [110], a dual-hop hybrid VLC/RF links were proposed to serve an uncovered user. The authors showed that visible light was used in the first hop to transmit data and transfer the energy to the relay. The relay, could then forward the data to the destination, using the harvested energy.

From NOMA perspective, NOMA has been extensively investigated in RF networks to improve the spectral efficiency and enhance the system fairness[58], [59]. In VLC networks, authors of [112] showed the superiority of NOMA over OFDMA in terms of sum-rate. Authors of [113] evaluated the NOMA-VLC system and compare

it to orthogonal multiple-access (OMA)-VLC scheme in two cases: 1) when each user has a minimum required data rate, and 2) when the data rates of all users were assigned opportunistically according to their channels. Authors of [114] evaluated and compared the NOMA and OMA schemes, when the users change their locations and their vertical orientations. For multiple APs, the work in [115] proposed a gain ratio power allocation (GRPA) method and compared it with the fixed power allocation method, when the users' movement model was following the random walk model. For more than one cell in VLC networks, the users in [116] were classified based on the received interference. A special resource blocks were assigned for the interfered users, while NOMA was implemented for the remaining users.

Despite all the work conducted on NOMA-VLC networks, Co-NOMA, for our best knowledge, has not been studied before in VLC networks. Hence, this chapter introduces the concept of hybrid VLC/RF Co-NOMA as a new technique to mitigate the VLC drawbacks.

4.3 Contribution

Different from the aforementioned studies, this chapter introduces a cooperation among users in VLC networks based on hybrid VLC/RF Co-NOMA. In particular, this chapter studies a system model, consisting of one VLC AP and multiple users classified into two sets, strong and weak users. A transmission scheme based on hybrid VLC/RF Co-NOMA scheme is proposed, where the strong users can receive their own signals through the direct VLC link and then help the weak users by forwarding their

signal through RF links. This transmission scheme provides two options for the weak users, either to be served by the direct VLC link, or by the relayed hybrid VLC/RF link that is provided by a strong user. This technique extends the VLC coverage area and helps serving the blocked users, which leads to improving the fairness and balancing the load in VLC systems. For such kind of the proposed system mode, the chapter

- formulates an optimization problem that jointly pairs the users, selects the optimal link for each weak user, and allocates the messages' power by maximizing the weighted sum-rate of the system under maximum transmit power constraint.

- provides an efficient solution for the formulated mixed-integer non-convex optimization problem and compare the solutions to a proposed baseline simpler approach and to the optimal NOMA scheme. In the proposed solution, we first provide optimal closed-form solutions for the non-convex power allocation optimization problem, when the user pairing matrix and link selection vector are given. Second, we provide an efficient solution for joint link selection, user pairing, and power allocation. The solution also proposes that the weights can be updated in an outer loop to achieve a proportional fairness of the system, where in each iteration, the weight of each user is set to be inversely proportional to the long-term achievable data rate of that user.

- shows that both the system fairness and the sum-rate can achieve their own maximum values simultaneously if the weak users are served through the hybrid VLC/RF link.

- shows that the proposed formulation and solutions are also solving the problem in NOMA scheme for weighted sum-rate maximization which has not been solved before in VLC systems.

The rest of this chapter is organized as follows. System and channel models are presented and discussed in Section 4.4. Section 4.5 formulates the optimization problem and presents the proposed algorithms. Simulation results are shown and discussed in Section 4.6. Finally, the chapter is concluded in Section 4.7.

4.4 System and Channel Models

4.4.1 System Model

As shown in Fig. 5.1, the considered system model consists of a VLC AP and $N_u = 2K$ multiple users, where K is the number of pairs. The users are classified into two sets, a set of K users $\mathbb{U}_s$, defined as strong users, which are the users with best VLC channels, and a set of K weak users $\mathbb{U}_w$, which are the users with the worst VLC channels. We assume that the number of users are even to investigate the proposed cooperation technique, however, if the number of users are odd, we can dedicate a specific bandwidth for the remaining user and can be treated as an equivalent pair. Hybrid NOMA is adopted, where the available bandwidth is divided fairly into K blocks. Each spectrum block is shared by a pair (two users, one strong and one weak user). The weak user in each pair can be served either directly by the VLC AP through the VLC link, or by the dual-hop hybrid VLC/RF link through the paired strong user.
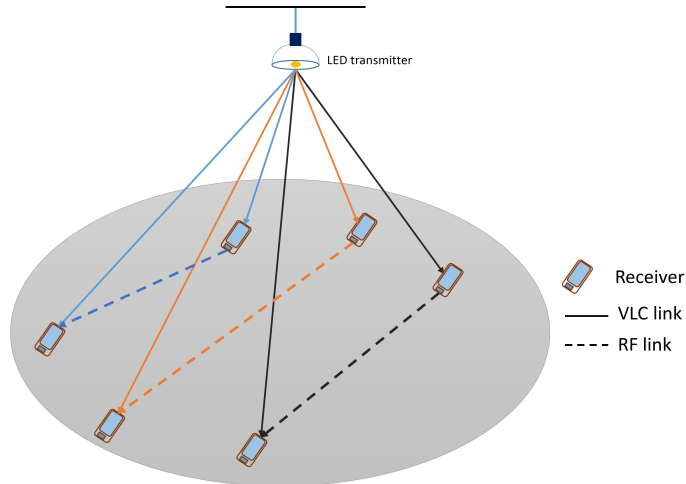
Figure 4.1: System model.

In the case where the weak user is not well served by the VLC, the strong user would act as an energy harvesting relay which harvests the energy from the VLC AP (using the received visible light), and would then use it to forward the information to the paired weak user using the RF link.

The channel between the transmitter LED and the jth user is denoted by h_j and is given by (1.1). We assume that when there is an opaque objects between the transmitter and a receiver, the channel is zero, otherwise the channel is given by (1.1).

4.4.2 RF Channel Model

The RF channel gain in indoor environment can be identified by the path loss model and the multipath propagation model. The path loss model depends on the distance between the transmitter and the receiver whether it is less than a breakpoint or greater than it. The path loss between the jth transmitter and the ith receiver is given by [117]

$$L(d_{i,j}) = L_{fs}(d_{i,j}) + a + X_\sigma, \tag{4.1}$$

where $L_{fs}(.)$ is the free space loss, X_σ is the shadow fading and it is a Gaussian random variable with zero mean and variance σ^2, $d_{i,j}$ is the distance between the jth transmitter and the ith receiver, and a is given by

$$a = \begin{cases} 0, & d_{i,j} \leq d_{BP}; \\ 35 \log_{10}(\frac{d_{i,j}}{d_{BP}}), & d_{i,j} > d_{BP}, \end{cases} \tag{4.2}$$

where d_{BP} is the breakpoint distance. The free space loss $L_{fs}(.)$ with central carrier frequency f_c is given by

$$L_{fs}(d_{i,j}) = 20 \log_{10}(d_{i,j}) + 20 \log_{10}(f_c) - 147.5. \tag{4.3}$$

According to [117], the RF multipath propagation channel is given by

$$H_{i,j}^{(RF)} = \sqrt{\frac{I}{I+1}} e^{j\psi} + \sqrt{\frac{1}{I+1}} h_s, \tag{4.4}$$

where I is the Ricean factor ($I = 1$ if $d_{i,j} \leq d_{BP}$ and $I = 0$ if $d_{i,j} > d_{BP}$), ψ is the angel of the departure/arrival of the LoS component, and h_s is a complex Gaussian variable with zero mean and variance one. The RF channel gain between the jth user and the i user can be expressed by

$$G_{i,j}^{RF} = |H_{i,j}^{(RF)}|^2 10^{-\frac{L(d_{i,j})}{10}}. \tag{4.5}$$

4.4.3 Transmission Scheme: Direct Links

Following the NOMA principle, suppose that the weak user i is paired with the strong user j (in the rest of this chapter, we associate the subscript i with the weak users and j with the strong users), the transmitted signal at the AP for i and j users is given by

$$y_{i,j} = \sqrt{P_j^{(s)}}s_j + \sqrt{P_i^{(w)}}s_i + P_{opt}b, \qquad (4.6)$$

where $P_j^{(s)}$ and $P_i^{(w)}$ are the powers of the strong and weak users assigned for s_j and s_i messages, respectively, b is the direct-current (DC) that must be added to guarantee that the transmitted signal is non-negative, and P_{opt} is the emitted optical power from the VLC AP. The observation at the jth and ith users, respectively, are given by

$$y_j = \rho h_j^{(s)}(\sqrt{P_j^{(s)}}s_j + \sqrt{P_i^{(w)}}s_i) + \rho h_j^{(s)}P_{opt}b + n_j, \qquad (4.7)$$

$$y_i = \rho h_i^{(w)}(\sqrt{P_j^{(s)}}s_j + \sqrt{P_i^{(w)}}s_i) + \rho h_i^{(w)}P_{opt}b + n_i, \qquad (4.8)$$

where $h_j^{(s)}$ and $h_i^{(w)}$ are the channels of the jth strong users and the ith weak user, respectively, ρ is the detector responsivity, and n_j or n_i are the noise, including both the thermal noise and the shot noise at the user, which can be modeled as zero-mean real-valued additive white Gaussian noise (AWGN) with variance $\sigma^2 = N_v B$, where B is the modulation bandwidth, and N_0 is the noise power spectral density. The received DC part $\rho h_j^{(s)}P_{opt}b$, at the strong user, can be blocked by a capacitor and forwarded to the energy harvesting circuit [24], while at the weak user, the DC part $\rho h_i^{(w)}P_{opt}b$ can be removed using a capacitor. The strong user first decodes the weak

user's signal s_i and removes or forwards it to the weak user, while the weak user decodes his own signal s_i with accepting the strong user's signal s_j as interference. Hence, the achievable data rate of the strong user signal can be approximated by [113]

$$R_j^{(s)}(P_j^{(s)}) = \frac{B_v}{2K} \log_2 \left(1 + \frac{\rho^2 h_j^{(s)2} P_j^{(s)}}{B_v N_v / K} \right),\qquad(4.9)$$

while the achievable data rate of the weak user at the strong user is given by

$$R_{j \to i}^{(w)}(P_i^{(w)}, P_j^{(s)}) = \frac{B_v}{2K} \log_2 \left(1 + \frac{\rho^2 h_j^{(s)2} P_i^{(w)}}{B_v N_v / K + \rho^2 h_j^{(s)2} P_j^{(s)}} \right),\qquad(4.10)$$

and the achievable data rate received at the weak user from the direct VLC link is given by

$$R_{i,DL}^{(w)}(P_i^{(w)}, P_j^{(s)}) = \frac{B_v}{2K} \log_2 \left(1 + \frac{\rho^2 h_i^{(w)2} P_i^{(w)}}{B_v N_v / K + \rho^2 h_i^{(w)2} P_j^{(s)}} \right),\qquad(4.11)$$

where B_v is the total modulation bandwidth at the VLC AP.

4.4.4 Transmission Scheme: Relayed Links

The chapter assumes that the strong user can work also as a relay that can harvest the energy from the received light and use it to forward the decoded weak user's signal. To harvest the energy, the DC component of the received signal is blocked by a capacitor and forwarded to the energy harvesting circuit [24], [107], [118]. The harvested energy is given by [55]

$$E = f I_{DC} V_{oc},\qquad(4.12)$$

where f is the fill factor (typically around 0.75), and I_{DC} is the received DC current which is at the jth user $I_{DC} = \rho P_{opt} h_j b$, and $V_{oc} = V_t \ln(1 + \frac{I_{DC}}{I_0})$, where V_t is the thermal voltage and I_0 is the dark saturation current of the PD. Hence, the harvested energy at user j is given by

$$E_j = f \rho P_{opt} V_t h_j b \ln(1 + \frac{\rho h_j P_{opt} b}{I_0}). \qquad (4.13)$$

Suppose that the amplitude of the transmitted signal is A, so the DC-bias and the signal amplitude $A + b$ must be within the maximum and minimum input currents that guarantee that the optical output power is a linear function of the input current. In other words, let I_H and I_L be the maximum and minimum limits of the input currents for the LEDs that guarantee a linear output optical power, the constraint $A \leq \min(b - I_L, I_H - b)$ must be achieved. The total transmit power at the AP is related to A and b by $P_{max} = P_{opt}^2 (A - b)^2$. This means that the total transmitted power P_{max} at the AP is a decreasing function of the DC-bias b, which also means that the harvested energy is also a decreasing function of P_{max}. The DC-bias can be optimized to balance between the received harvested energy and the transmit power, but this is out of the scope of this chapter. Hence, we assume that the DC-bias at the AP is fixed and is given by $b = \frac{I_H + I_L}{2}$ which maximizes the total transmit power [107]. Therefore, the transmit power is given by

$$P_{max} = P_{opt}^2 (\frac{I_H - I_L}{2})^2. \qquad (4.14)$$

The strong user is assumed to be able to receive the light signal and transmit the RF signal at the same time. However, the energy storage device cannot charge and discharge at the same time (i.e. the receiver cannot harvest the energy and transmit the data at the same time). Hence, suppose that T_1 is used to charge the battery and T_2 is used to re-transmit data through the RF link. Therefore, the RF re-transmission power is given by $P_{j,RF} = \frac{E_j T_1}{T_2}$. Under the assumption that $T_1 = T_2$, the achievable data rate of the weak user that can be offered by the strong user j through the RF link is given by

$$R_{i,j}^{RF} = \frac{B_{f,j}}{2} \log \left(1 + \frac{G_{i,j}^{RF} P_{j,RF}}{B_{f,j} N_{RF}} \right), \tag{4.15}$$

where $B_{f,j}$ is the RF modulation bandwidth at the user j and N_{RF} is the power spectral density of the RF signal. In case the number of users $2K > 2$, the RF interference should be considered if there are more than one pair of users connected through the RF link in the second hub. To avoid this interference, we assign orthogonal RF bandwidth for each pair connected through the RF link equally. Suppose that the number of weak users that are served through RF links is N_f and the total modulation bandwidth available for RF transmission is B_f, the modulation bandwidth at user j is $B_{f,j} = \frac{B_f}{N_f}$.

From (4.15) and (4.10), the achievable data rate at the weak user through the hybrid relayed link can be expressed as

$$R_{i,RL}^{(w)}(P_i^{(w)}, P_j^{(s)}) = \min \left(R_{i,j}^{RF}, R_{j \to i}^{(w)}(P_i^{(w)}, P_j^{(s)}) \right), \tag{4.16}$$

108

4.5 Problem Formulation and Solutions

To formulate and tackle the problem, we should answer the three interlinked questions: 1) how should the users be paired? 2) how should the weak user in each pair select the link to maximize its own data rate? 3) and how should the total power at the AP be allocated to all users?. These three question are interlinked, meaning that the answer of each question depends on the answers of the others. For the proposed system model, in this section, we formulate these questions as an optimization problem to find the power allocation vector $\mathbf{P}$, the pairing index matrix $\mathbf{Z}$, and the link selection index vector $\mathbf{x}$ to maximize the weighted sum of the achievable data rates of users.

Define the user pairing indication as $z_{i,j}$ matrix as

$$z_{i,j} = \begin{cases} 1, & \text{if user } i \text{ and user } j \text{ are multiplexed}, \\ 0, & \text{otherwise}, \end{cases} \tag{4.17}$$

where $\mathbf{Z} = \{z_{i,j}\}, i = 1, \ldots, K, \ j = 1, \ldots, K$. Define the link selection indicator x_i vector as

$$x_i = \begin{cases} 1, & \text{if user } i \text{ is served through the hybrid RF/VLC link}, \\ 0, & \text{if user } i \text{ is served through the direct VLC link}. \end{cases} \tag{4.18}$$

From (4.18), the number of weak users that are connected through RF link is given

by $N_f = \sum_{i=1}^{K} x_i$ and (4.15) becomes a function of $\mathbf{x}$ that can be re-written as

$$R_{i,j}^{RF}(\mathbf{x}) = \frac{B_f}{2 \sum_{x_i}^{K} x_i} \log \left(1 + \frac{G_{i,j}^{RF} P_{j,RF}}{B_f N_{RF} / \sum_{i}^{K} x_i} \right). \tag{4.19}$$

The received achievable data rate at the ith weak user through the hybrid VLC/RF link is given by

$$R_{i,RL}^{(w)}(P_i^{(w)}, P_j^{(s)}, \mathbf{x}) = \min \left(R_{i,j}^{RF}(\mathbf{x}), R_{j \to i}^{(w)}(P_i^{(w)}, P_j^{(s)}) \right). \tag{4.20}$$

The summation of the achievable data rate of the ith weak user and jth strong user is given by

$$R_{i,j}(P_i^{(w)}, P_j^{(s)}, z_{i,j}, \mathbf{x}) = z_{i,j} R_j^{(s)}(P_j^{(s)}) + z_{i,j}(1 - x_i) R_{i,DL}^{(w)}(P_i^{(w)}, P_j^{(s)})$$

$$+ z_{i,j} x_i R_{i,RL}^{(w)}(P_i^{(w)}, P_j^{(s)}, \mathbf{x}), \quad (4.21)$$

while the weighted sum-rate of all users in the system is given by

$$\sum_{i=1}^{K} \sum_{j=1}^{K} R_{i,j}(P_i^{(w)}, P_j^{(s)}, z_{i,j}, x_i, w_i^{(w)}, w_j^{(s)}) =$$

$$\sum_{i=1}^{K} \sum_{j=1}^{K} w_j^{(s)} z_{i,j} R_j^{(s)}(P_j^{(s)}) + w_i z_{i,j}(1 - x_i) R_{i,DL}^{(w)}(P_i^{(w)}, P_j^{(s)})$$

$$+ w_i^{(w)} z_{i,j} x_i \min \left(R_{i,j}^{RF}(\mathbf{x}), R_{j \to i}^{(w)}(P_i^{(w)}, P_j^{(s)}) \right), \quad (4.22)$$

where the weights $w_i^{(w)}$ and $w_j^{(s)}$ $\forall i, j$ are imposed to balance between the system sum-rate and the system fairness. These weights can be already given based on the

required application or can be updated in an outer loop to provide a proportional fairness.

The optimization problem to maximize the weighted sum-rate is given as follows

$$\max_{\mathbf{P},\mathbf{z},\mathbf{x}} \quad \sum_{i=1}^{K}\sum_{j=1}^{K} R_{i,j}(P_i^{(w)}, P_j^{(s)}, z_{i,j}, x_{i,j}, w_i^{(w)}, w_j^{(s)}) \tag{4.23a}$$

$$s.t. \quad \sum_{i=1}^{K}\sum_{j=1}^{K} z_{i,j}(P_i^{(w)} + P_j^{(s)}) \leq P_{max} \tag{4.23b}$$

$$\sum_{j=1}^{K} z_{i,j} = 1, \ \forall i, \tag{4.23c}$$

$$\sum_{i=1}^{K} z_{i,j} = 1, \ \forall j, \tag{4.23d}$$

$$z_{i,j} \in \{0,1\}, \ \forall i,j \tag{4.23e}$$

$$x_i \in \{0,1\}, \ \forall i \tag{4.23f}$$

$$0 \leq P_j^{(s)} \leq P_i^{(w)} \ \forall i,j. \tag{4.23g}$$

Constraint (4.23b) is imposed for the maximum transmit power. Constraints (4.23c), (4.23d), and (4.23e) guarantee that each strong user is paired only with one weak user. Constraint (4.23f) imposes that the weak user either receives the information from the direct VLC link or the relayed hybrid VLC/RF link.

The problem in (4.23) is a challenging mixed non-convex combinatorial optimization problem. In addition, the actual weak user's data rate from the relayed link cannot be determined without previous knowledge of the link selection vector $\mathbf{x}$ which makes the problem more difficult. Nevertheless, in the following, we develop two solutions, one is optimal with high complexity and the other is a simpler suboptimal

solution. The idea is that we first find optimal closed-form solutions for the power allocation problem with assuming that the pairing matrix $\mathbf{Z}$ and the link selection vector $\mathbf{x}$ are given. Then we provide optimal and suboptimal solutions for the joint user pairing, link selection, and power allocation problems.

4.5.1 Power Allocation for the Weighted Sum Maximization

This section solves the optimization problem (4.23), when the $\mathbf{Z}$ matrix and $\mathbf{x}$ vector are given. In particular, we find the optimal power allocation under the given pairing and link selection. Under the given $\mathbf{Z}$ and $\mathbf{x}$, the weighted sum maximization problem can be formulated as follows

$$\max_{\mathbf{P}} \ \sum_{i=1}^{K}\sum_{j=1}^{K} R_{i,j}(P_i^{(w)}, P_j^{(s)}, z_{i,j}, x_{i,j}, w_i^{(w)}, w_j^{(s)}) \tag{4.24a}$$

$$s.t. \ \sum_{i=1}^{K}\sum_{j=1}^{K} z_{i,j}(P_i^{(w)} + P_j^{(s)}) \leq P_{max} \tag{4.24b}$$

$$0 \leq P_j^{(w)} \leq P_i^{(s)} \ \forall i, j. \tag{4.24c}$$

Clearly, problem (4.24) is nonconvex since the objective function is not concave. However, in the following we provide closed-forms for the the optimal power allocation. Define a variable $q_{i,j}$ as the power budget of a pair consisting of the ith weak user and jth strong user and is given by $q_{i,j} = z_{i,j}(P_i^{(w)} + P_j^{(s)})$. Then, we can divide the problem (4.24) into K problems to find $P_i^{(w)}$ and $P_j^{(s)} \ \forall i, j$ and one main problem to find the power budgets $q_{i,j} \ \forall i, j$. Without loss of generality, suppose that the weak

user i is paired with the strong user j (i.e., $z_{i,j} = 1$). We have two cases:

Case 1: The users i and j are paired through the relayed hybrid VLC/RF link. The problem in this case can be formulated as follows

$$\max_{P_i^{(w)}, P_j^{(s)}} \quad w_j^{(s)} R_j^{(s)}(P_j^{(s)}) + w_i^{(w)} \min(R_{i,j}^{RF}(\mathbf{x}), R_{j \to i}^{(w)}(P_i^{(w)}, P_j^{(s)})) \quad (4.25a)$$

$$\text{s.t.} \quad P_i^{(w)} + P_j^{(s)} = q_{i,j} \quad (4.25b)$$

$$0 \leq P_j^{(s)} \leq P_i^{(w)}. \quad (4.25c)$$

Because of the min term in the objective function, the problem above must be carefully treated. It can be seen that function $R_{i,j}^{RF}(\mathbf{x})$ is given and not a function of the powers, which means it is fixed. In addition, by using constraint (4.25b) to re-write $R_{j \to i}^{(w)}(P_i^{(w)}, P_j^{(s)})$ and $R_j^{(s)}(P_j^{(s)})$ in terms of only $P_i^{(w)}$, we can show that $R_{j \to i}^{(w)}(P_i^{(w)})$ is increasing function, while $R_j^{(s)}(P_i^{(w)})$ is decreasing. By looking at the objective function in (4.25), increasing $R_{j \to i}^{(w)}(P_i^{(w)})$ to be greater than $R_{i,j}^{RF}(\mathbf{x})$ will decrease the objective function, because the min term will be fixed and the $R_j^{(s)}(P_i^{(w)})$ will decrease. This means that the resulted optimal function $R_{j \to i}^{(w)}(P_i^{(w)})$ must be less than or equal to $R_{i,j}^{RF}(\mathbf{x})$. To solve Problem (4.25), we first assume that $\min(R_{i,j}^{RF}(\mathbf{x}), R_{j \to i}^{(w)}(P_i^{(w)}, P_j^{(s)})) = R_{j \to i}^{(w)}(P_i^{(w)}, P_j^{(s)}))$ and solves the problem. If the re-sulted $R_{j \to i}^{(w)}(P_i^{(w)}, P_j^{(s)}) \leq R_{i,j}^{RF}(\mathbf{x})$, the assumption is correct and the resulted powers are the optimal solution. If not, (i.e. $R_{j \to i}^{(w)}(P_i^{(w)}, P_j^{(s)}) > R_{i,j}^{RF}(\mathbf{x})$) that means optimal solution is the value of the power $P_i^{(w)}$ that achieves that $R_{j \to i}^{(w)}(P_i^{(w)}, P_j^{(s)}) = R_{i,j}^{RF}(\mathbf{x})$ and $P_j^{(s)} = q_{i,j} - P_i^{(w)}$.

Proposition 4.1 *Under the assumption that* $\min(R_{i,j}^{RF}(\mathbf{x}), R_{j \to i}^{(w)}(P_i^{(w)}, P_j^{(s)})) =$

$R_{j\to i}^{(w)}(P_i^{(w)}, P_j^{(s)}))$, the optimal solution to (4.25) is given by $P_j^{(s)} = \frac{-1+\sqrt{1+q_{i,j}\Psi_j^{(s)}}}{\Psi_j^{(s)}}$ and $P_i^{(w)} = q_{i,j} - P_j^{(s)}$.

Proof. Define $\Psi_j^{(s)} = \frac{\rho^2 h_j^{(s)2}}{B_v N_v / K}$ and $\Psi_i^{(w)} = \frac{\rho^2 h_i^{(w)2}}{B_v N_v / K}$, the objective function in (4.25) can be rewritten as $R_{i,j} = w_j^{(s)} \frac{B_v}{2K} \log_2(1 + \Psi_j^{(s)} P_j^{(s)}) + w_i^{(w)} \frac{B_v}{2K} \log_2(\frac{\Psi_j^{(s)} q_{i,j}+1}{\Psi_j^{(s)} P_j^{(s)}+1})$. By deriving the function $R_{i,j}$, we obtain

$$\frac{dR_{i,j}}{dP_j^{(s)}} = \frac{\Psi_j^{(s)} B_v(w_j^{(s)} - w_i^{(w)})}{2K P_j^{(s)}}. \tag{4.26}$$

From (4.26), we can see that the objective function is an increasing function of $P_j^{(s)}$ if $w_j^{(s)} > w_i^{(w)}$, a decreasing function if $w_j^{(s)} < w_i^{(w)}$, and constant if $w_j^{(s)} = w_i^{(w)}$. This means that the sum-rate function is a constant function of $P_j^{(s)}$ and modifying the values of $w_i^{(w)}$ and $w_j^{(s)}$ just affects the weighted sum-rate but not the sum-rate itself. Hence, the maximum fairness can be implemented without any degradation in the sum-rate with setting $w_i^{(w)} = w_j^{(s)}$, and finding $P_j^{(s)}$, that results

$$\frac{B_v}{2K} \log_2(1 + \Psi_j^{(s)} P_j^{(s)}) = \frac{B_v}{2K} \log_2(\frac{\Psi_j^{(s)} q_{i,j}+1}{\Psi_j^{(s)} P_j^{(s)}+1}). \tag{4.27}$$

Solving (4.27), we obtain that $P_j^{(s)} = \eta_{i,j,1}$, where $\eta_{i,j,1}$ is given by

$$\eta_{i,j,1} = \frac{-1 + \sqrt{1 + q_{i,j}\Psi_j^{(s)}}}{\Psi_j^{(s)}}, \tag{4.28}$$

and

$$P_i^{(w)} = q_{i,j} - \eta_{i,j,1}. \tag{4.29}$$

Now, if (4.28) and (4.29) achieve that $\min(R_{i,j}^{RF}(\mathbf{x}), R_{j \to i}^{(w)}(P_i^{(w)}, P_j^{(s)})) = R_{j \to i}^{(w)}(P_i^{(w)}, P_j^{(s)})$, Proposition 4.1 provides the optimal solution for (4.25); otherwise, the values of $P_j^{(s)}$ and $P_i^{(w)}$ must be modified to have $R_{j \to i}^{(w)}(P_i^{(w)}, P_j^{(s)}) = R_{i,j}^{RF}(\mathbf{x})$, and this can be achieved with $P_j^{(s)} = \eta_{i,j,2}$, where $\eta_{i,j,2}$ is given by

$$\eta_{i,j,2} = \frac{q_{i,j}\Psi_j^{(s)} + 1 - A}{A\Psi_j^{(s)}}, \tag{4.30}$$

where $A = 2^{R_{i,j}^{RF}(\mathbf{x} - \frac{B_v}{2K})}$ and $P_i^{(w)}$ can be given by $P_i^{(w)} = q_{i,j} - \eta_{i,j,2}$. It is important to note that the values of both $w_i^{(w)}$ and $w_j^{(s)}$ must be selected carefully because as we will show later the budget $q_{i,j}$ is a function of both.

Case 2: The users i and j are paired and the user i is served through the direct VLC link (i.e. $x_i = 0$). The problem in this case can be formulated as follows:

$$\max_{P_i^{(w)}, P_j^{(s)}} \quad w_j^{(s)} R_j^{(s)}(P_j^{(s)}) + w_i^{(w)} R_{i,DL}^{(w)}(P_i^{(w)}, P_j^{(s)}) \tag{4.31a}$$

$$\text{s.t.} \quad P_i^{(w)} + P_j^{(s)} = q_{i,j} \tag{4.31b}$$

$$0 \leq P_j^{(s)} \leq P_i^{(w)}. \tag{4.31c}$$

Because of the interference term in $R_{i,DL}^{(w)}(P_i^{(w)}, P_j^{(s)})$, the optimization problem (4.31) is still nonconvex. However, the optimal solution can be obtained in a closed-form. Authors of [119] tackled such kind of problems and showed that the optimal solution is given by $P_j^{(s)} = \Omega_{i,j}$, where $\Omega_{i,j}$ is given by

$$\Omega_{i,j} = \frac{w_i \Psi_i^{(w)} - w_j^{(s)} \Psi_j^{(s)}}{\Psi_j^{(s)} \Psi_i (w_j^{(s)} - w_i^{(w)})}, \tag{4.32}$$

under the conditions that $w_i^{(w)}/w_j^{(s)} < \Psi_j^{(s)}/\Psi_i^{(w)}$ and $q_{i,j} > 2\Omega_{i,j}$.

Then, with the given closed-form solutions in (4.28), (4.30), and (4.32), we aim to find the optimal power budget $q_{i,j}$ $\forall i, j$. Using the above closed-form solutions, the problem can be formulated as

$$\max_{q_{i,j}} \sum_{i=1}^{K} \sum_{j=1}^{K} x_i z_{i,j} \left(w_j^{(s)} F_j^{(s)}(q_{i,j}) + w_i^{(w)} F_i^{(w)}(q_{i,j}) \right)$$

$$+ \sum_{i=1}^{K} \sum_{j=1}^{K} (1 - x_i) z_{i,j} w_i^{(w)} \frac{B_v}{2K} \log_2(1 + \Omega_{i,j} \Psi_j^{(s)})$$

$$+ \sum_{i=1}^{K} \sum_{j=1}^{K} (1 - x_i) z_{i,j} w_i^{(w)} \frac{B_v}{2K} \log_2 \left(\frac{q_{i,j} \Psi_i^{(w)} + 1}{\Omega_{i,j} \Psi_i^{(w)} + 1} \right) \tag{4.33a}$$

$$s.t. \quad \sum_{i=1}^{K} \sum_{j=1}^{K} q_{i,j} = P_{max}, \tag{4.33b}$$

where there are two possible expressions for $F_j^{(s)}(q_{i,j})$ and $F_i^{(w)}(q_{i,j})$ since they both have to be either

$$F_j^{(s)}(q_{i,j}) = R_j^{(s)}(\eta_{i,j,1}) = \frac{B_v}{2K} \log_2(\sqrt{\Psi_j^{(s)} q_{i,j} + 1}) \tag{4.34}$$

and

$$F_i^{(w)}(q_{i,j}) = R_{i,RL}^{(w)}(\eta_{i,j,1}) = \frac{B_v}{2K} \log_2(\sqrt{\Psi_j^{(s)} q_{i,j} + 1}) \tag{4.35}$$

116

or

$$F_j^{(s)}(q_{i,j}) = R_j^{(s)}(\eta_{i,j,2}) = \frac{B_v}{2K} \log_2\left(\frac{\Psi_j^{(s)} q_{i,j} + 1}{A}\right) \tag{4.36}$$

and

$$F_i^{(w)}(q_{i,j}) = R_{i,RL}^{(w)}(\eta_{i,j,2}) = R_{i,j}^{RF}(\mathbf{x}). \tag{4.37}$$

We cannot now decide what is the exact expression for $F_j^{(s)}(q_{i,j})$ and $F_i^{(w)}(q_{i,j})$ $\forall i, j$ because they depend on whether the optimal power allocation of the pair is given by (4.28) or (4.30) and this cannot be determined because $q_{i,j}$ is unknown. However, Proposition 4.2 finds a unique optimal closed-form solution for $q_{i,j}$ (if $x_i = 1$), for both possible expressions of $F_j^{(s)}(q_{i,j})$ and $F_i^{(w)}(q_{i,j})$.

Proposition 4.2 *The optimal solution to Problem (4.33) is given by*

$$q_{i,j} = \frac{wB_v}{2K\lambda} - \frac{1}{\Psi_j^{(s)}}, \tag{4.38}$$

where $w = w_i^{(w)}$ if $x_i = 0$ and $w = w_j^{(s)}$ if $x_i = 1$.

Proof. It can be seen that the Hessian matrix of the objective function in (4.33) is negative definite whether $F_j^{(s)}(q_{i,j})$ and $F_i^{(w)}(q_{i,j})$ are given by (4.34) and (4.35), respectively, or given by (4.36) and (4.37), respectively. In addition, the constraints in (4.33) are linear, which means that the optimization problem (4.33) is convex. To find an optimal closed-form solution for $q_{i,j}$ $\forall i, j$, we first find the Lagrangian dual

function that can be written as

$$\zeta = -\sum_{i=1}^{K}\sum_{j=1}^{K} x_i z_{i,j} \left(w_j^{(s)} F_j^{(s)}(q_{i,j}) + w_i^{(w)} F_i^{(w)}(q_{i,j}) \right)$$

$$-\sum_{i=1}^{K}\sum_{j=1}^{K}(1-x_i)z_{i,j}w_i^{(w)}\frac{B_v}{2K}\log_2(1+\Omega_{i,j}\Psi_j^{(s)})$$

$$-\sum_{i=1}^{K}\sum_{j=1}^{K}(1-x_i)z_{i,j}w_i^{(w)}\frac{B_v}{2K}\log_2\left(\frac{q_{i,j}\Psi_i^{(w)}+1}{\Omega_{i,j}\Psi_i^{(w)}+1}\right)+$$

$$\lambda\left(\sum_{i=1}^{K}\sum_{j=1}^{K}q_{i,j}-P_{max}\right), \quad (4.39)$$

where λ is a dual variable. Based on the first-order KKT conditions [56], we have

$$\frac{\partial\zeta}{\partial q_{i,j}} = 0, \ \forall i,j. \quad (4.40)$$

We have three cases, if $z_{i,j} = 0$ (i.e., users i and j are not paired), $q_{i,j} = 0$ whether $x_i = 1$ or $x_i = 0$. The second case if we have $z_{i,j} = 1$ and $x_i = 1$, we can reformulate (5.31), equivalently as

$$\frac{\partial}{\partial q_{i,j}}\left[-\left(w_j^{(s)}F_j^{(s)}(q_{i,j}) + w_i^{(w)}F_i^{(w)}(q_{i,j})\right) + \lambda(q_{i,j} - P_{max})\right] = 0. \quad (4.41)$$

If $F_j^{(s)}$ and $F_i^{(w)}$ are given by (4.34) and (4.35), respectively, (4.41) can be given by

$$\frac{\partial}{\partial q_{i,j}}\left[-2w_j^{(w)}\frac{B_v}{2K}\log_2(\sqrt{\Psi_j^{(s)}q_{i,j}+1}) + \lambda(q_{i,j} - P_{max})\right] = 0, \quad (4.42)$$

where $w_i^{(w)} = w_j^{(s)}$ because $F_j^{(s)} = F_i^{(w)}$ in this case. On the other hand, if $F_j^{(s)}$ and

$F_i^{(w)}$ are given by (4.36) and (4.37), respectively, (4.41) can be given by

$$\frac{\partial}{\partial q_{i,j}}\left[-w_j^{(w)}\frac{B_v}{2K}\log_2(\frac{\Psi_j^{(s)}q_{i,j}+1}{A}) - w_i^{(w)}R_{i,j}^{RF}(\mathbf{x}) + \lambda(q_{i,j} - P_{max})\right] = 0, \quad (4.43)$$

Solving (4.42) or (4.43), we obtain the same expression for $q_{i,j}$, which is given by

$$q_{i,j} = \frac{w_j^{(w)}B_v}{2K\lambda} - \frac{1}{\Psi_j^{(s)}}. \quad (4.44)$$

Similarly, the third case if we have $z_{i,j} = 1$ and $x_i = 0$ (the weak user is served through the direct VLC link), we can reformulate (5.31) equivalently as

$$\frac{\partial}{\partial q_{i,j}}\left[-w_i^{(w)}\frac{B_v}{2K}\log_2(\frac{q_{i,j}\Psi_i+1}{\Omega_{i,j}\Psi_i^{(w)}+1}) + \lambda(q_{i,j} - P_{max})\right] = 0 \quad (4.45)$$

Solving (4.45), we have

$$q_{i,j} = \frac{w_i^{(w)}B_v}{2K\lambda} - \frac{1}{\Psi_j^{(s)}}. \quad (4.46)$$

∎

The dual variable λ can be found by substituting (4.44) and (4.46) in constraint (4.33b), we then obtain

$$\sum_{i=1}^{K}\sum_{j=1}^{K}(x_iz_{i,j}(\frac{w_j^{(s)}B_v}{2K\lambda} - \frac{1}{\Psi_j^{(s)}}) + (1 - x_i)z_{i,j}(\frac{w_i^{(w)}B_v}{2K\lambda} - \frac{1}{\Psi_j^{(s)}})) = P_{max},$$

which results in

$$\lambda = \frac{B_v\sum_{k=1}^{K}(x_kw_k^{(w)} + (1-x_k)w_k^{(s)})}{P_{max} + \sum_{k=1}^{K}1/\Psi_k^{(s)}}. \quad (4.47)$$

To summarize the procedures of allocating the power, we present the following steps to allocate the power for users under given users' pairing and link selection:

- Find λ using (4.47).

- For each pair (when $z_{i,j} = 1$), if the corresponding $x_i = 0$, find $q_{i,j}$ using (4.46), $P_j^{(s)} = \Omega_{i,j}$, and $P_i^{(w)} = q_{i,j} - \Omega_{i,j}$.

- if the corresponding $x_i = 1$, find $q_{i,j}$ using (4.44) and find $F_i^{(w)}(q_{i,j})$ using (4.37). If $F_i^{(w)}(q_{i,j}) <= R_{i,j}^{(x)}$, the optimal $P_j^{(s)}$ is given by $\eta_{i,j,1}$; otherwise, the optimal $P_j^{(s)}$ is given by $\eta_{i,j,2}$, and the optimal $P_i^{(w)} = q_{i,j} - P_j^{(s)}$.

Updating the Weights: The weights can be modified to guarantee a proportional fairness of the system. We adopt the approach in [120] to find the weights. Simply, we update the weights in an outer loop by setting that $w_i^{(w)} = \frac{1}{R_i^{(w)}}$ and $w_j^{(s)} = \frac{1}{R_j^{(s)}}$, where $\overline{R}_i^{(w)}$ and $\overline{R}_j^{(s)}$ are the long term average rate of the ith weak user and the jth strong user, respectively, [120]. For the paired users i and j, if $x_i = 0$, we should be careful in updating the weights since the condition $w_i^{(w)}/w_j^{(s)} < \Psi_j^{(s)}/\Psi_i^{(w)}$ must be satisfied to have a positive power for the strong user. Hence, if $\overline{R}_j$ is dropped to be less than $\overline{R}_i$, we select $w_j^{(s)} = \alpha w_i^{(w)}$, where the value of α is very close but less than one.

4.5.2 Joint Power Allocation, User Pairing, and Link Selection

In Section 4.5.1, we found the optimal power allocation for given user pairing and link selection. In this section, we propose a heuristic solution for the joint power allocation, user pairing, and link selection. In addition the optimal solution can be found but with exponential complexity with respect to the number of users.

Optimal Approach

One important feature of VLC networks is that the covered area by a VLC AP is small due to the dramatic decrease in the channel with the distance. This means that each cell in VLC can serve only a small number of users. As a result, applying the exhaustive search approach for finding the joint $\mathbf{Z}$ matrix and $\mathbf{x}$ vector is not considered a complex approach if the number of users is small. To achieve the optimal solution, we calculate the powers of the users for each possible pairing and link selection combinations. The complexity of this approach depends on the number of users or pairs in the system. For instance, if the number of pairs in the system is K, we need to find the users' powers $2^K K!$ times and select the joint $\mathbf{Z}$ and $\mathbf{x}$ that maximize the objective function in (4.23).

Suboptimal Approach

Solving the considered optimization problem using exhaustive search is not an efficient approach especially if the number of users is high. Therefore, here, we propose an

iterative algorithm that finds the three variables in an alternative way. In particular, we first propose initial user pairing and link selection, we find the powers using the proposed closed-forms based on the given user pairing and link selection initial values. After that, we find the $\mathbf{Z}$ matrix under the given allocated power and link selection, then the link selection vector is updated to maximize the weighted sum objective function. These steps are repeated until the variables converge or a limit number of iteration is reached. In Section 4.5.1, we show how the power is allocated for the given user pairing and link selection combinations. In this section, we provide how to optimally pair the users under a given power allocation and link selection, and how to optimally select the links for the weak users under a given power allocation and user pairing.

- *User Pairing Optimization:* For the given power allocation and link selection, the optimization problem can be formulated as follows

$$\max_{\mathbf{Z}} \quad \sum_{i=1}^{K} \sum_{j=1}^{K} w_j^{(s)} z_{i,j} R_j^{(s)}(P_j^{(s)}) \tag{4.48a}$$
$$+ w_i^{(w)} z_{i,j} (1 - x_i) R_{i,DL}^{(w)}(P_i^{(w)}, P_j^{(s)})$$
$$+ w_i^{(w)} z_{i,j} x_i \min \left(R_{i,j}^{RF}(\mathbf{x}), R_{j \to i}^{(w)}(P_i^{(w)}, P_j^{(s)}) \right)$$

$$s.t. \quad \sum_{j=1}^{K} z_{i,j} = 1, \ \forall i, \tag{4.48b}$$

$$\sum_{i=1}^{K} z_{i,j} = 1, \ \forall j, \tag{4.48c}$$

$$z_{i,j} \in \{0, 1\}, \ \forall i, j \tag{4.48d}$$

The above problem is a mixed integer linear programming and can be considered

122

as a one-to-one assignment that can be solved using the Hungarian method [121].

- *Link Selection Optimization:* The problem of selecting the optimal links for the weak users even for the given power allocation and user pairing is not easy to be tackled. However, we provide an optimal solution by generating a $K \times K$ matrix that reduces the number of nominee $\mathbf{x}$ vectors from 2^K to K vectors. In particular, we find a matrix S, where the first row in S hosts the rates of the weak users coming from the relayed links subtracted form the rates coming from the direct link, when $\sum_{i=1}^{K} x_i = 1$ and the second row is the same when $\sum_{i=1}^{K} x_i = 2$ and so on until the Kth row where $\sum_{i=1}^{K} x_i = K$. After that we find $\mathbf{x}$ corresponding to each row, for example, at the kth row we set that $x_i = 1$ corresponding to the k highest values of the kth row. This results in having K different $\mathbf{x}$ vectors. Then we examine all the resulted vectors and select the one that maximizes the objective weighted sum function. This method is efficient if K is high since the computational complexity is of order $O(K \times K + K)$, while the computational complexity of the exhaustive search is of order $O(2^K)$.

4.5.3 Baseline Approaches

Baseline 1 (NOMA approach)

In this approach, we implement NOMA scheme to compare it with the proposed Co-NOMA. The difference between NOMA and Co-NOMA is that the Co-NOMA allows the strong users to forward the weak users' signal through RF links (i.e. there is cooperation among users) which provides two options for the weak users, to be

served by the VLC AP or by the paired strong user through the hybrid VLC/RF link. Whereas, the weak users in NOMA have only one option which is to be served through the direct VLC link (i.e., there is no cooperation among users in NOMA). NOMA is a special case of the formulated problem before, where it can be implemented when the link selection vector $\mathbf{x} = \mathbf{0}$. Therefore, the optimal NOMA scheme can be found by allocating the power using closed-forms (4.32) and (4.46) for all the possible user pairing. This approach cannot provide a service for the uncovered or the blocked users. It is important to note that if a strong user j is paired with a blocked or uncovered user i (that means $\Psi_i^{(w)} = 0$), the power allocation for this pair is distributed as $P_j^{(s)} = q_{i,j}$ and $q_{i,j}$ can be proved easily to be $q_{i,j} = \frac{w_j^{(s)} B_v}{2K\lambda} - \frac{1}{\Psi_j^{(s)}}$.

Baseline 2

In this approach we provide a very simple solution from the optimization perspective. Specifically, for pairing the users, we propose that the best strong user is paired with the worst weak user, the second best strong user is paired with the second worst weak user, and so on. This approach of pairing is proposed to improve the fairness among users. For the link selection vector, we propose that each blocked or uncovered user (i.e. has a zero VLC channel) must be served through the relayed VLC/RF link, while the rest weak users must be served through the direct VLC link. For the given user pairing and link selection, we allocate the power using the derived closed-forms in section 4.5.1.

Table 4.1: Simulation Parameters

Name of the Parameter	Value of the Parameter
Maximum bandwidth of VLC AP, B	20 MHz
The physical area of a PD, A_p	0.1 cm^2
Half-intensity radiation angle, $\theta_{1/2}$	60°
Gain of optical filter, g_{of}	1
Refractive index, n	1.5
Efficiency of converting optical to electric, ρ	0.53 [A/W]
Maximum input bias current, I_H	600 mA
Minimum input bias current, I_L	400 A
Fill factor, f	0.75
LEDs' power, P_{opt}	10 W/A
Thermal voltage, V_t	25 mV
Dark saturation current of the PD, I_0	10^{-10} A
Noise power spectral density of LiFi, N_0	10^{-21} A^2/Hz
LED height,	3 m
User height	0.85
Monte-Carlo for user distribution,	1000 different user distributions
RF	
The distance of breakpoint	5 m
Central carrier frequency	2.4 GHz
Bandwidth	16 MHz
Angle of arrival/departure of LoS	45°
Standard deviation of shadow fading (before the breakpoint)	3 dB
Standard deviation of shadow fading (after the breakpoint)	5 dB
Noise power spectral density	-174 dBm/Hz

4.6   Simulation Results

This section evaluates the performance of the proposed hybrid VLC/RF Co-NOMA

scheme and the proposed solutions in terms of the sum-rate and the system fairness.

We examine the effect of the FoV, number of users, blockage rate, and the cell size on

the system sum-rate and system fairness. All the simulation results are implemented
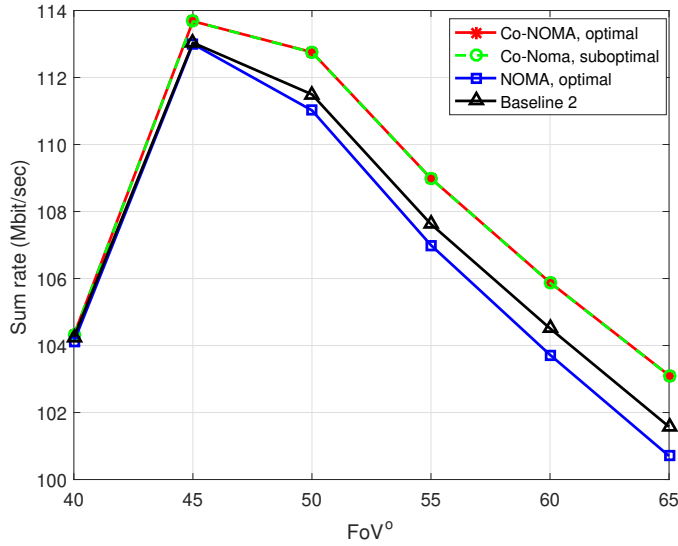
Figure 4.2: Sum-rate versus users' FoV when number of users is 6, the cell radius is 2.5 m, and the blockage rate 0.1.

under the given simulation parameters in Table 4.1. Monte-Carlo simulations are used to assess the performance of the proposed algorithms, where every point in the numerical results is the average of implementing 1000 different user distributions on the given cell size. The blockage rate is defined as the number of times that the user is blocked over the times of total simulation realizations.

Fig. 4.2 compares the proposed hybrid VLC/RF Co-NOMA scheme associated with the optimal and suboptimal solutions with the optimal NOMA and the baseline approaches by plotting the sum-rate versus the users' FoV. It can be seen that the sum-rate increases then decreases for all approaches with the users' FoV. This is because the very small users' FoV provides a potential for having some users uncovered or the LoS to these uncovered users is zero. As the users' FoV increases, the probability of coverage increases, but the channel quality decreases because of the relation (1.2) that affects equation (1.1). On the other hand, Fig. 4.3 compares the proposed hybrid
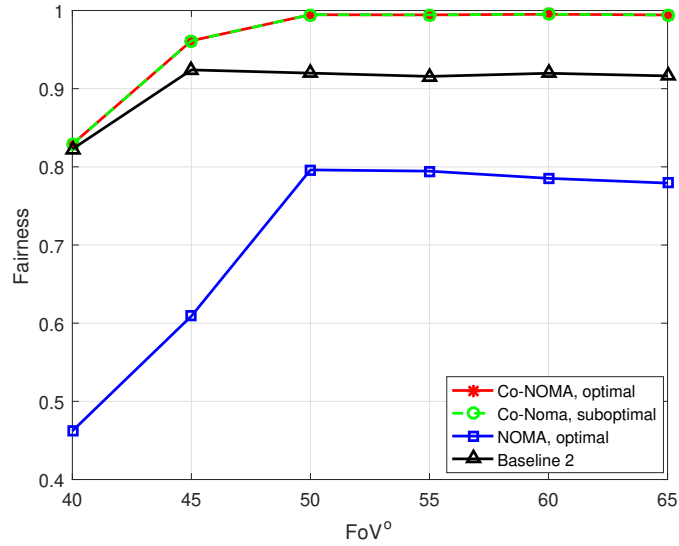
Figure 4.3: System fairness versus users' FoV when number of users is 6, the cell radius is 2.5 m, and the blockage rate 0.1.

VLC/RF Co-NOMA scheme associated with the optimal and suboptimal solutions with the optimal NOMA and the baseline approaches by plotting the sum-rate versus the users' FoV. It can be seen that the fairness is low when the users' FoV is low because the users that are far from AP would be out of the view (i.e. the LoS channel is zero), while the users that are close to the AP would get a good quality of service because of their channel quality. As the users' FoV increases, the probability that the number of covered users increases with a fixed certain area.

Figs. 4.2 and 4.3 show that the proposed hybrid VLC/RF Co-NOMA scheme (optimal or suboptimal) outperforms the NOMA and the proposed baseline 2 in terms of both the sum-rate and fairness. The improvement in terms of fairness is more than that in sum-rate because the NOMA scheme cannot reach the out-of-coverage or the blocked users, while the proposed hybrid VLC/RF Co-NOMA scheme can reach them through the hybrid VLC/RF relayed link. In addition, the hybrid VLC/RF links

can provide the maximum fairness (rather than the direct VLC link that provides proportional fairness) among the strong and weak users without affecting the sum-rate as we show in Section 4.5.1, Case 1.
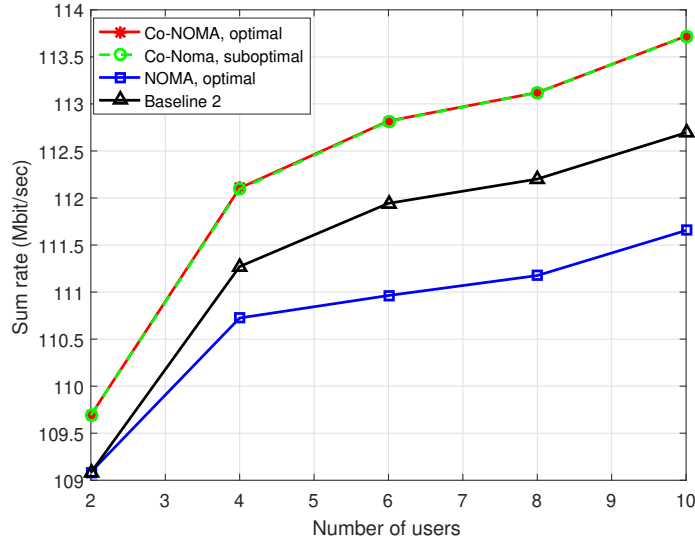
Figure 4.4: Sum-rate versus number of users in the system when the cell radius is 2.5 m, the blockage rate 0.1, and the user FoV= 50°.

Fig. 4.4 plots the sum-rate versus the total number of users located in the circle with radius 2.5 m, while Fig. 4.5 plots the fairness of the same users and with the same cell size. In general, Increasing the number of users in the system increases the sum-rate, but decreases the system fairness. However, this decrease in fairness (in Fig. 4.5) is significant in the NOMA scheme and negligible in the proposed hybrid VLC/RF Co-NOMA scheme. On the other hand, the sum-rate in the Co-NOMA scheme increases in a faster rate than in NOMA. Figs. 4.4 and 4.5 also show that the optimal and the suboptimal Co-NOMA scheme provide the same performance, which is much better than the proposed baseline approach.

Fig. 4.6 shows the effect of the blockage rate on the sum-rate. Increasing the
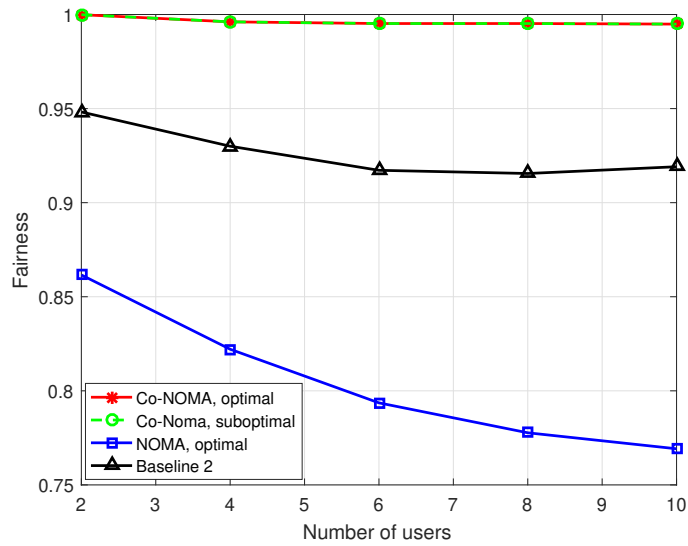
Figure 4.5: System fairness versus number of users in the system when the cell radius is 2.5 m, the blockage rate 0.1, and the user FoV= 50°.
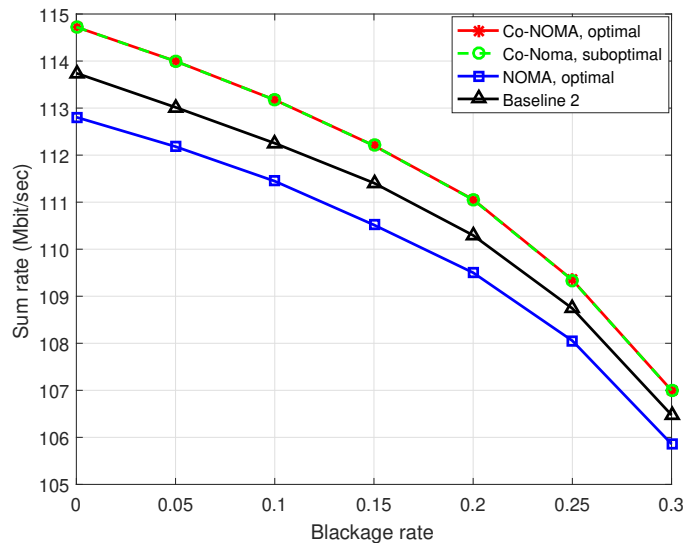
Figure 4.6: Sum-rate versus blockage rate when, $N_u = 6$, the cell radius is 2.5 m, and the and the users' FoV= 50°.

blockage rate decreases the probability of the availability of the VLC LoS to the users.

In other words, the number of blocked users increases which leads to decreasing the

sum-rate of the system. It can be seen that the proposed hybrid VLC/RF Co-NOMA

is better than NOMA for all the given blockage rate, even when there is no blockage

at all. This is because of the selection diversity at the weak user in Co-NOMA (the weak user in Co-NOMA can select the link that provides a maximum rate), while the weak user in NOMA has only one option.
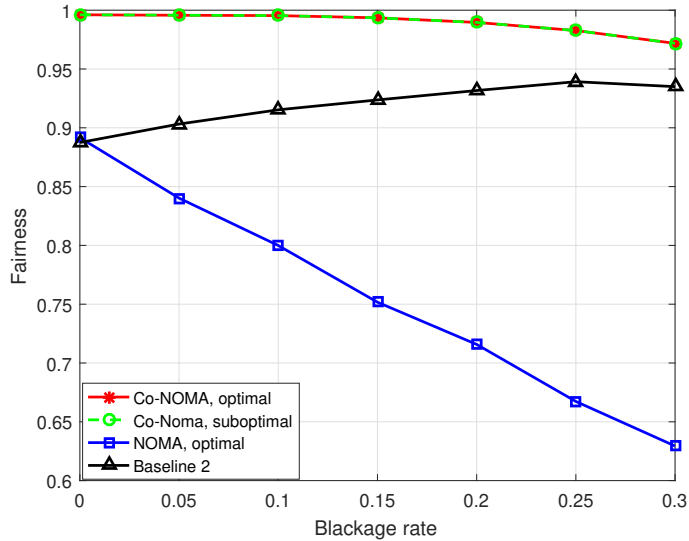
Figure 4.7: System fairness versus blockage rate when, $N_u = 6$, the cell radius is 2.5 m, and the users' FoV= 50°.

The effect of the blockage rate on the fairness is shown in Fig. 4.7. It can be seen that increasing the blockage rate has a very small impact on the fairness of the proposed hybrid VLC/RF Co-NOMA scheme until some point. This is because all the blocked users are considered as weak users and could be served through the paired strong users using the relayed link. But increasing the blockage rate further more may result in having the number of blocked users greater than the half of the total number of users, which affects also the fairness of the proposed Co-NOMA. The fairness of the baseline 2 increases with blocking rate because of that, when there is no blockage that means all the users in the baseline 2 approach are served through the direct link, which results to have a proportional fairness like NOMA. As the blockage rate

increases, the number of served users through the relayed link will increase, which results in approaching the maximum fairness like the proposed Co-NOMA.

Fig. 4.8 shows the impact of increasing the cell size that the AP must cover on the sum-rate. That means as the cell size increases the average channel quality decreases and the probability of having uncovered users increases. As a result, the sum-rate decreases as the cell size increases for Co-NOMA and NOMA and with different users' FoV. Whereas, the fairness, as shown in Fig. 4.9, is approximately
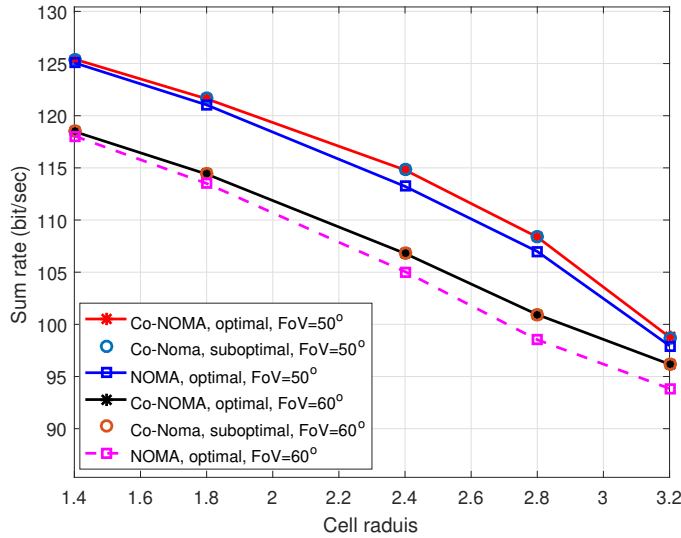
Figure 4.8: Sum-rate versus the cell size when, $N_u = 6$, blockage rate is 0.1, and with different users' FoV.

stay fixed with a slight decrease in case of the proposed hybrid VLC/RF Co-NOMA scheme. This is because such scheme extend the coverage area by the RF link and increases the probability of coverage. In contrast, the NOMA scheme cannot reach the out-of-coverage users, which leads to having a high rate of reduction in system fairness. However, increasing the users' FoV would increase the coverage probability, but at the expense of decreasing the channel quality, resulting in degrading the system
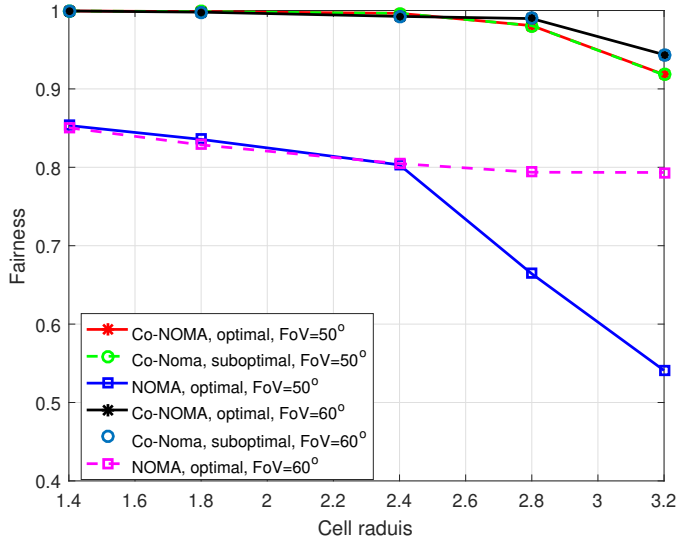
Figure 4.9: System fairness versus the cell size when, $N_u = 6$, blockage rate is 0.1, and with different users' FoV.

sum-rate as shown in Fig. 4.8.

4.7 Conclusion

VLC technology is expected to be one of the most participant tools in meeting the targeted metrics in the next wireless communication networks. This chapter introduced a novel cooperative scheme among users that contributed in extending the coverage, improving the sum-rate, and maximizing the fairness in VLC systems. This cooperation was based on Co-NOMA that can provide another chance for poor-serviced users to be served through a hybrid dual-hub VLC/RF link with the help of the good-serviced users. Furthermore, the chapter formulated an optimization problem for maximizing the weighted sum-rate by jointly allocating the power for users, pairing the users, and selecting the links for the weak users. An optimal and sub-optimal solutions were proposed and compared with a simpler baseline solution and with the traditional NOAM

scheme. Simulation results showed that a significant improvement in terms of sum-rate and fairness can be achieved by applying the proposed scheme and by optimizing the system jointly.

CHAPTER 5

DC-BIAS AND POWER ALLOCATION IN COOPERATIVE VLC NETWORKS FOR JOINT INFORMATION AND ENERGY TRANSFER

5.1 Introduction

Much attention has recently been paid to energy-harvesting techniques at user-equipment devices, either from exploiting the surrounding environment, or by trans-

134

ferring wireless power. Energy harvesting is the capability of converting the RF signals or light intensity into electrical voltage/current. With the advent of the era of the IoT, the demand for transferring the power and enabling IoT devices to harvest energy using light or RF transmission is increasing, especially in indoor applications where smart buildings, health monitoring, and sensors devices applications become abundant.

One important attractive VLC feature of valuable interest is its energy harvesting capabilities, which are best enabled through equipping the VLC receivers with solar panels, so as to directly convert the light intensity into current signals without the need for external power supply [24], and with up to 40% conversion efficiency [122]. In practical indoor environments, however, two different types of users can typically co-exist, i.e., information-users (IUs) (such as mobiles, laptops, or tablets) and energy-harvesting users (EHUs) (IoT devices, sensors, or relays). While IUs are data-hungry devices with specific data rate constraints, EHUs aim at harvesting visible light energy, which is especially feasible in indoor applications such as smart buildings, health monitoring, and sensors devices' applications. This motivates us in this chapter to evaluate the benefit of a particular VLC-based scheme which considers the coexistence of both IUs and EHUs, and addresses the problem of jointly optimizing and balancing the achievable sum-rate at the IUs and the total harvested energy by EHUs, by means of adjusting the DC-bias at the VLC access-points and the powers of the users' messages.

5.2 Literature Review

Investigating the harvesting of energy in VLC systems has been a timely topic of interest [55], [123], [109], [110], [124], [125], [126], [118]. A few papers recently published proposed to investigate systems that use the light to jointly transfer power, meet illumination requirements, and transmit data. Authors of [55] experimentally harvested the solar energy with mobile phone by equipping it with a commercial solar panel in an indoor environment. They showed that the devices directly exposed to the indoor light could be charged to a satisfactory level. Authors of [123] investigated the concept of indoor optical wireless power transfer to solar cells during darkness hours. By using laser diodes and a solar panel, they measured the power efficiency and showed an improvement over the inductive power transfer systems, of approximately 2.7 times. By using 42 laser diodes, they claimed to deliver 7.2 W of optical power to a solar panel 30 m distant from the diodes. Authors of [127] studied how much artificial indoor light could deliver an amount of energy, using different types of receiving cells.

In [109] and [110], a dual-hop hybrid VLC/RF communication system was studied as a means to reach out to the out-of-the-coverage user. The authors showed that visible light could be used, in the first hop, to transfer both data information and energy to the relay. The relay, could then forward the data to the destination, using the harvested energy. In [124], [125], authors maximized the sum-rate utility of a VLC system consisting of one AP and K users, subject to individual QoS constraints. Li *et al.* [124] assumed that a user k can receive the information in their assigned time slot, and the power within the time slots assigned to other users. In [125], on the

other hand, Abdelhady *et al.* proposed solving the problem by allocating the optical intensity and time slots, using an upper bound on the individual required harvested energy. Authors in [126] characterized the outage performance of a hybrid VLC-RF system, where the visible light is used for the downlink to transfer the energy and data to the users, who then use the harvested energy to transmit a RF signal in the uplink.

All the studies mentioned above use the alternating current (AC) component for harvesting the energy, where the DC component of the transmitted light is fixed and readily used to harvest energy [24]. In [24], authors designed an optical wireless receiver using a solar panel and enabled it to receive information and harvest energy simultaneously. Because the received current signal contains both DC-current and the AC-current components, authors in [24] suggested to attenuate the AC current, using an inductor to remove the ripples from the DC-current that is forwarded to energy harvesting branch, and to block the DC-current, using a capacitor, to obtain only an AC-current in the communication circuit. Sandalidis *et al.* [128] investigated the three functions of the LED lamp, i.e. the illumination, communication, and the energy harvesting, on a system consisting of a desk LED close to the receiver equipped with a solar cell. The authors divided the received optical power between the information signal and the harvested energy, using a splitter.

Diamantoulakis *et al.* [118] studied the lightwave information and power transfer for a system consisting of one transmitter and one receiver. They provided the two following protocols to maximize the harvested energy at the receiver, under data rate constraint: 1) Splitting the time into two portions, one dedicated to maximize

the user's SINR, and the second assigned purely to maximize the harvested energy by maximizing the DC component, 2) Optimization of the DC bias, in phase 1, to maximize the harvested energy under QoS constraints, with phase 2 assigned only to harvesting the energy. However, optimizing the DC bias for the whole time is more general, and there is no need to split the time between harvesting the energy and transmitting the data. In addition, the formulated problem would be more challenging if there were multiple receivers, since the fairness, in terms of data rate and harvested energy, is required.

5.2.1 Contributions

Different from the aforementioned references, this chapter considers a VLC network, where multiple APs cooperate to serve both EHUs (e.g. sensors or IoT devices), and IUs (e.g. laptops, mobile phones, etc.), so as to best capture the multi-diverse applications schemes expected in next generations of wireless networks. The chapter then investigates the problem of balancing the achievable sum-rate at the IUs and the total harvested energy by the EHUs, by means of adjusting the DC-bias at APs and allocating users' powers. For mathematical tractability, the chapter adopts the zero-forcing (ZF) precoding approach to cancel intra-cell interference, similar to [47], [129].

To balance between the performance of the IUs and the EHUs, the chapter formulates the optimization problem which maximizes a weighted sum of the IUs sum-rate and the EHUs total harvested energy, under QoS and illumination constraints. The performance of the system is a function of both the DC bias values allocated at each

AP, and the powers assigned to the users' messages. One of this work contributions is to solve such a difficult non-convex optimization problem using an iterative approach, which uses inner convex approximations of the objective and constraints. It then compensates for the approximations using proper outer-loop updates. The chapter also proposes a simpler sub-optimal baseline approach, which provides a feasible, yet simple, solution to the formulated problem based on equal DC-bias allocation. The chapter further considers solving the two special cases of the original optimization, i.e., the problem of maximizing the IUs sum-rate, and the problem of maximizing the EHUs total harvested energy, both subject to the same constraints as above. Simulation results highlight the performance and the convergence of our proposed algorithms. They particularly suggest that appreciable harvested energy and sum-rate improvement can be reached by optimizing the DC-bias and messages' powers in VLC systems.

The reminder of this chapter is organized as follows. The system model, VLC channel and the energy harvesting channel are presented in Section 5.3. In Section 5.4, we formulate the problem and present the proposed algorithms that solve the formulated problem. We introduce and discuss simulation results in Section 5.5. The chapter is then concluded in Section 5.6.
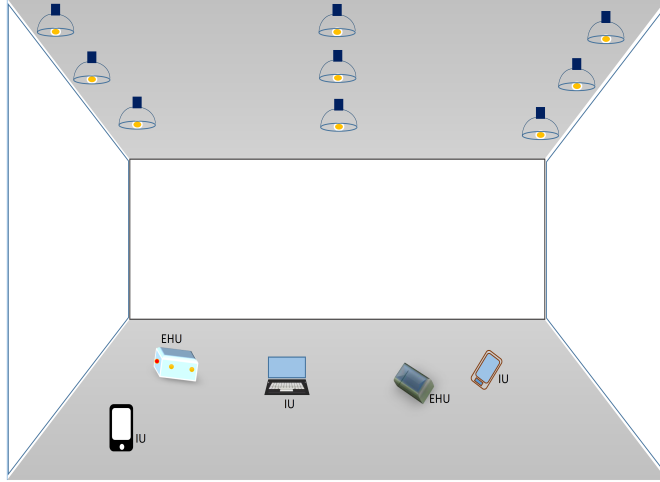
Figure 5.1: System model (an example of user distribution when $N_{u,1} = 3$, $N_{u,2} = 2$, and $N_A = 9$).
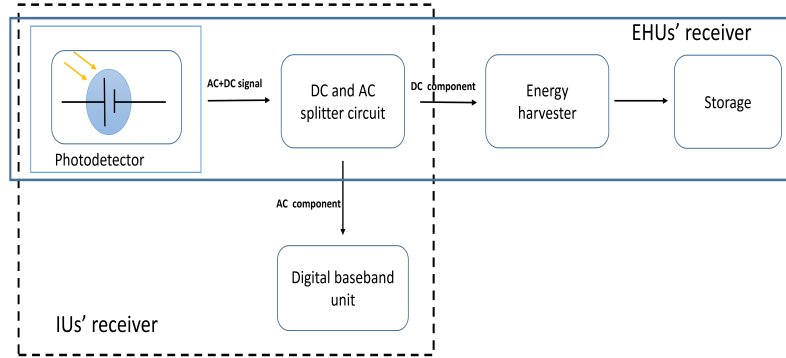
Figure 5.2: Receiver Model (The blocks inside the dashed square represent the receiver of the IUs, while the blocks inside the solid square represent the receiver of EHUs).

5.3 System and Channel Models

5.3.1 System Model

Consider an indoor VLC system consisting of N_A VLC access points (APs), which serve N_u users in total. Among the N_u users, $N_{u,1}$ users are IUs, and $N_{u,2}$ are EHUs, i.e., $N_u = N_{u,1} + N_{u,2}$. We assume that the EHUs are equipped with the functionality of energy harvesting as shown in Fig. 5.2. The chapter considers the case where $N_{u,1} <$

N_A, and adopts a zero-forcing (ZF) approach to cancel the intra-cell interference, so as to simplify the mathematical tractability of the problem. This assumption, i.e., $N_{u,1} < N_A$, emulates several indoor environments where the number of IUs are less than the number of lamps in the ceiling such as offices, labs, companies ,houses, etc. Let $\mathbf{s} \in \mathbb{R}^{N_{u,1} \times 1}$ be the vector hosting the information of the $N_{u,1}$ users, and let $\mathbf{G} \in \mathbb{R}^{N_A \times N_{u,1}}$ be the precoding matrix associated with $\mathbf{s}$. The matrix $\mathbf{G}$ can be written as $\mathbf{G} = [\mathbf{g}_1 \ldots \mathbf{g}_{N_A}]^T$, where $\mathbf{g}_i \in \mathbb{R}^{N_{u,1} \times 1}$ is the ith column of matrix $\mathbf{G}^T$. The AC input electrical signal to the AP i can be written as $x_i = \mathbf{g}_i^T \mathbf{s}$, where $\mathbf{s} \in \mathbb{R}^{N_{u,1} \times 1}$ is the message vector with unit power, $\quad = \text{diag}([\sqrt{P_1}, \sqrt{P_2}, \ldots, \sqrt{P_{N_{u,1}}}])$, and where P_j is the AC electrical power allocated to s_j (the jth user's message). The DC-bias of the ith AP is denoted by b_i and must be added to x_i to avoid the resulting non-positive signals [118]. The electrical signal, afterwards, modulates the optical intensity of the light-emitting diodes (LEDs) at AP i. The transmitted signal at AP i can, therefore, be written as

$$y_{t,i} = \rho_{se}(b_i + x_i), \tag{5.1}$$

where ρ_{se} is the slope efficiency of the LED or the electrical-to-optical conversion factor of the LED and measured in W/A. Let I_L and I_H be the minimum and the maximum input bias currents, respectively, i.e., $b_i \in [I_L, I_H]$. To guarantee that the output optical power is a linear function of the input current, the transmitter LED must be in its linear region. To this end, the peak amplitude of the modulated signal

x_i, denoted by A_i, must satisfy the following constraint

$$A_i \leq \min(b_i - I_L, I_H - b_i).$$ (5.2)

Constraint (5.2) implies that A_i must satisfy two constraints, which are $A_i + b_i \leq I_H$ and $b_i - A_i \geq I_L$, to guarantee that the input electrical current to the LED is within the range of the linear region LED operation. It is important to note that restricting the amplitude of the input signal to be lower than a given maximum current implies the eye safety constraint. This is because the eye safety constraint can be achieved by limiting the radiated optical power, which can be controlled by the maximum limit of the input current I_H.

After blocking the DC-bias at the receiver side, the signal vector received at the users from all APs ($\mathbf{Y}_r$ with size $N_{u,1} \times 1$) is given by

$$\mathbf{Y}_r = \rho_{oe}\rho_{se}\mathbf{H}\mathbf{G}\,\mathbf{s} + \mathbf{n},$$ (5.3)

where $\mathbf{H} \in \mathbb{R}^{N_u \times N_A}$ is the channel attenuation matrix that is assumed to be known at APs, ρ_{oe} is the optical-to-electric conversion factor, and $\mathbf{n}$ is the noise vector with size $N_{u,1} \times 1$, which includes the thermal noise and the shot noise at the user, and can be modeled as zero-mean real-valued AWGN with variance $\sigma^2 = N_0 W$, where W is the modulation bandwidth, and N_0 is the noise power spectral density. The precoding matrix $\mathbf{G}$ is used to cancel the inter-cell interference by diagonalizing the channel matrix, i.e., $\mathbf{G} = \mathbf{H}^T(\mathbf{H}\mathbf{H}^T)^{-1}$. This means that the received signal at the

jth user or the jth element of vector $\mathbf{Y}_r$ is given by

$$y_{r,j} = \rho_{oe}\rho_{se}\sqrt{P_j}s_j + n_j. \tag{5.4}$$

Since the power of s_j is normalized, a tight lower bound on the network sum-rate at the $N_{u,1}$ IUs can then be written as [130]

$$f_R(\mathbf{P}) = \beta \sum_{j=1}^{N_{u,1}} \log\left(1 + \frac{e\rho_{oe}^2\rho_{se}^2 P_j}{2\pi W N_0}\right), \tag{5.5}$$

where $\mathbf{P}$ is a vector with size $N_{u,1}\times 1$ hosting the messages powers of the IUs, $\beta = W/2$ is a constant, and e is the constant exponential (Euler's number). It is important to note that, from (5.3), we can define the relation between the electronic transmit power at AP i and the assigned powers of the messages as [1]

$$p_i = \sum_{j=1}^{N_{u,1}} g_{i,j}^2 P_j, \tag{5.6}$$

where $g_{i,j}$ is the (i,j)th element of matrix $\mathbf{G}$.

5.3.2 Energy Harvesting Signals

For the EHUs, the DC component of the received signal is blocked by a capacitor and forwarded to the energy harvesting circuit [24], [118]. The harvested energy (per unit-time) is given by [55]

$$E = fI_{sc}V_{oc}, \tag{5.7}$$

where f is the fill factor (typically around 0.75), and I_{sc} is the received DC current measured by shutting the solar panel charging circuit [55], which is given at the kth energy-harvesting user by

$$I_{sc,k} = \rho_{oe}\rho_{se}\mathbf{h}_k^T\mathbf{b}, \tag{5.8}$$

where $\mathbf{b} = [b_1, b_2, \ldots, b_{N_A}]^T$ is the DC-bias vector at APs, $\mathbf{h}_k$ is the channel vector from all APs to the user k with size $N_A \times 1$, and V_{oc} is the voltage that is measured by opening the solar panel charging circuit and is given by [118], [110]

$$V_{oc,k} = V_t \ln(1 + \frac{I_{sc,k}}{I_0}), \tag{5.9}$$

where V_t is the thermal voltage and I_0 is the dark saturation current of the PD. Hence, the harvested energy (per unit-time) at user k is given by

$$E_k(\mathbf{b}) = f\rho_{oe}\rho_{se}V_t\mathbf{h}_k^T\mathbf{b}\ln\left(1 + \frac{\rho_{oe}\rho_{se}\mathbf{h}_k^T\mathbf{b}}{I_0}\right), \tag{5.10}$$

and the total harvested energy at all $N_{u,2}$ users is given by

$$f_E(\mathbf{b}) = \sum_{k=1}^{N_{u2}} E_k(\mathbf{b}). \tag{5.11}$$

5.4 Problem Formulation and Algorithms

In order to jointly optimize the achievable sum-rate utility at the IUs and the total harvested energy utility at the EHUs, this section motivates and then considers

144

maximizing a weighted sum of both utilities under QoS constraints and maximum transmit power constraint. The section then proposes two different solutions to solve the formulated non-convex problem by efficiently adjusting the DC-bias vector and the users' powers. The section finally addresses the two individual optimization problems separately, i.e., maximizing the sum-rate utility, and then maximizing the total harvested energy utility, both under the same constraints.

5.4.1 Weighted Sum Utility Maximization and Constraints

The utility function for the IUs is the sum-rate that is given in (5.5), which is a function of the messages' powers, while the utility function for the EHUs, given in (5.11), is the total harvested energy, which is a function of the APs DC-bias.

The first constraint that should be considered is that the DC-bias at each AP should be within the maximum and minimum input currents (i.e., $I_L \leq b_i \leq I_H \ \forall i$). It is important to note that the DC-bias b_i at the ith AP must be greater than or equal to $\frac{I_H + I_L}{2}$. This is because decreasing b_i to be less than $\frac{I_H + I_L}{2}$ results in decreasing the harvested energy (5.10). It also decreases A_i (based on (5.2)), which decreases the transmit power of the signal that leads to a decrease in the sum-rate (5.5). b_i, therefore, should satisfy $b_i \geq \frac{I_H + I_L}{2}$, and $\min(I_H - b_i, b_i - I_L)$ becomes equal to $I_H - b_i$.

The second constraint that should be considered is that the input signal should be positive and within the maximum and minimum allowable limit currents. In other words, the input signal for the ith AP should satisfy the following

$$I_L \leq \mathbf{g}_i^T \, \mathbf{s} + b_i \leq I_H. \tag{5.12}$$

Constraint (5.12) can be written equivalently as

$$\mathbf{g}_i^T \mathbf{s} \leq I_H - b_i, \tag{5.13}$$

and

$$-\mathbf{g}_i^T \mathbf{s} \leq b_i - I_L. \tag{5.14}$$

Constraints (5.13) and (5.14) can be written equivalently as

$$|\mathbf{g}_i^T \mathbf{s}| \leq \min(I_H - b_i, b_i - I_L). \tag{5.15}$$

Constraint $\frac{I_H + I_L}{2} \leq b_i \leq I_H$ implies that $\min(I_H - b_i, b_i - I_L) = I_H - b_i$. Therefore, constraint (5.15) can be written equivalently as

$$|\mathbf{g}_i^T \mathbf{s}| \leq (I_H - b_i). \tag{5.16}$$

If the optimal b_i satisfies $b_i \leq I_H - |\mathbf{g}_i^T \mathbf{s}|$, b_i can be increased to have $b_i = I_H - |\mathbf{g}_i^T \mathbf{s}|$, which increases the objective function without violating the constraints. Hence, the inequality in (5.16) should be satisfied with equality. In order to represent constraint (5.16) in terms of power, we should find the expectation of the square of both sides [82]. Because $E(\mathbf{s}\mathbf{s}^T) = \mathbf{I}_{N_{u,1}}$, where $\mathbf{I}_{N_{u,1}}$ is the identity matrix with size $N_{u,1} \times N_{u,1}$, constraint (5.16) can be represented equivalently as

$$\mathbf{g}_i^T {}^T\mathbf{g}_i = (I_H - b_i)^2. \tag{5.17}$$

Since $\Lambda = \mathrm{diag}[\sqrt{P_1}, \ldots, \sqrt{P_{N_{u,1}}}]$, constraint (5.17) can be written as

$$\sum_{j=1}^{N_{u,1}} g_{i,j}^2 P_j = (I_H - b_i)^2, \ \forall i, \tag{5.18}$$

where $g_{i,j}$ is the jth component of $\mathbf{g}_i$ vector.

Expression (5.18) shows that the relation between both vectors is not one-to-one. More specifically, a unique DC-bias vector $\mathbf{b}$ can be calculated for a given messages' power vector. The messages' power vector $\mathbf{P}$ might, however, have several solutions from a given DC-bias vector. Expression (5.18) also shows that increasing the DC-biases increases the total harvested energy at the EHUs, but decreases the data rate at the IUs. Such conflicting impact of the DC-bias motivates the need for jointly optimizing both utilities by means of maximizing a weighted-sum under QoS and LEDs' linear operational region constraints. In this formulated problem, the weights of the utility functions can be controlled by a variable, called $\alpha \in [0, 1]$. In other words, α is the weight which balances between the sum-rate and harvested energy utilities. Mathematically, the considered optimization problem can be formulated as

follows

$$\max_{\mathbf{b},\mathbf{P}} \quad \alpha f_R(\mathbf{P}) + \frac{(1-\alpha)}{\omega} f_E(\mathbf{b}) \tag{5.19a}$$

$$\text{s.t.} \quad \beta \log\left(1 + \frac{e\rho_{oe}^2 \rho_{se}^2 P_j}{2\pi W N_0}\right) \geq R_{th,j}, \quad j = 1, \ldots, N_{u,1} \tag{5.19b}$$

$$f\rho_{oe}\rho_{se}V_t \mathbf{h}_k^T \mathbf{b} \ln(1 + \frac{\rho_{oe}\rho_{se}\mathbf{h}_k^T\mathbf{b}}{I_0}) \geq E_{th,k}, \quad k = 1, \ldots, N_{u,2} \tag{5.19c}$$

$$\sum_{j=1}^{N_{u,1}} g_{i,j}^2 P_j = (I_H - b_i)^2, \quad i = 1, \ldots, N_A \tag{5.19d}$$

$$\frac{I_H + I_L}{2} \leq b_i \leq I_H, \quad i = 1, \ldots, N_A, \tag{5.19e}$$

where $R_{th,j}$ and $E_{th,k}$ are the minimum required data rate at the jth user and the minimum required energy to be harvested by the kth user, respectively, and ω is a constant chosen to numerically equalize the order of magnitudes of the functions $f_R(\mathbf{P})$ and $\frac{1}{\omega}f_E(\mathbf{b})$. Constraints (5.19b) and (5.19c) are imposed to satisfy the minimum required fairness among IUs and the EHUs, while constraints in (5.19d) and (5.19e) are imposed to avoid any clipping and guarantee that the LEDs operate in their linear region. It is important to note that problem (5.19) solves three types of problems: 1) maximizing the sum-rate, which is achieved when we set $\alpha = 1$, 2) maximizing the total harvested energy, which can be achieved by setting $\alpha = 0$, 3) and maximizing a weighted sum of both utility functions for any $\alpha \in (0,1)$.

Problem (5.19) cannot be easily solved, since the objective function and the constraint (5.19c) are not concave, resulting in a difficult non-convex optimization problem. Specifically, $f_R(\mathbf{P})$ is a concave function in terms of $\mathbf{P}$, while $f_E(\mathbf{b})$ is a convex function in terms of $\mathbf{b}$, which makes their weighted sum a non-concave objective func-

tion. This chapter next solves problem (5.19) by first reformulating the problem in a more compact form, and then by proposing an numerical iterative approach.

The main idea of the proposed approach is that the problem is first formulated in terms of the messages' power vector $\mathbf{P}$ only, using the relation given in (5.18). The chapter then proposes a heuristic, yet efficient, algorithm to solve the reformulated problem through considering an approximated convex version of the problem, and then by correcting for the approximation in an outer loop update. For the sake of comparison, the chapter further proposes a simple baseline approach, which guarantees a feasible solution to (5.19).

5.4.2   Problem Reformulation

As discussed earlier, a unique DC-bias vector $\mathbf{b}$ can be calculated for a given messages' power vector. Thus, to reformulate problem (5.19) in a more compact fashion, we choose to formulate the objective function and constraints of problem (5.19) in terms of the vector $\mathbf{P}$ only. Using the relation in (5.18), the DC-bias vector can be expressed as

$$\mathbf{b} = I_H \mathbf{1}_{N_A} - \sqrt{\mathbf{G}\mathbf{P}}, \tag{5.20}$$

where $\mathbf{1}_{N_A}$ is the unity vector of length N_A with all entries set to 1, the matrix $\bar{\mathbf{G}}$ is defined as $\bar{\mathbf{G}} = [\bar{\mathbf{g}}_1, \bar{\mathbf{g}}_2, \ldots, \bar{\mathbf{g}}_{N_A}]^T$, with $\bar{\mathbf{g}}_i = [g_{i,1}^2, \ g_{i,2}^2, \ldots, g_{i,N_{u,1}}^2]^T$, and where the square root denotes the componentwise square root of the vector argument.

Plugging (5.20) in the energy harvesting functions (5.10) and (5.11), we obtain

$$E_k(\mathbf{P}) = f\rho_{oe}\rho_{se}V_t\mathbf{h}_k^T(I_H\mathbf{1}_{N_A} - \sqrt{\mathbf{GP}})\ln(1 + \frac{\rho_{oe}\rho_{se}\mathbf{h}_k^T(I_H\mathbf{1}_{N_A} - \sqrt{\mathbf{GP}})}{I_0}), \quad (5.21)$$

and

$$f_E(\mathbf{P}) = \sum_{k=1}^{N_{u,2}} E_k(\mathbf{P}). \quad (5.22)$$

Using (5.20), the constraints in (5.19e) can be rewritten as

$$0 \leq \mathbf{g}_i^T\mathbf{P} \leq \left(\frac{I_H - I_L}{2}\right)^2, \quad i = 1, \ldots, N_A. \quad (5.23)$$

Substituting (5.21), (5.22), and (5.23) in the optimization problem (5.19), the problem can then be formulated in terms of the messages' power vector as follows

$$\max_{\mathbf{P}} \quad \alpha f_R(\mathbf{P}) + \frac{(1 - \alpha)}{\omega} f_E(\mathbf{P}) \quad (5.24a)$$

$$\text{s.t.} \quad P_j \geq P_{j,min}, \quad j = 1, \ldots, N_{u,1} \quad (5.24b)$$

$$E_k(\mathbf{P}) \geq E_{th,k}, \quad k = 1, \ldots, N_{u,2} \quad (5.24c)$$

$$\mathbf{g}_i^T\mathbf{P} \geq 0, \quad i = 1, \ldots, N_A \quad (5.24d)$$

$$\mathbf{g}_i^T\mathbf{P} \leq (\frac{I_H - I_L}{2})^2, \quad i = 1, \ldots, N_A, \quad (5.24e)$$

where $P_{j,min} = \frac{(2^{\frac{R_{th,j}}{\beta}} - 1)2\pi WN_0}{e\rho_{se}^2\rho_{oe}^2}$. Because functions $f_E(\mathbf{P})$ and $E_k(\mathbf{P})$ are not concave, the problem in (5.24) is still a non-convex optimization problem. Hence, we next propose a novel method that solves problem (5.24) by using a proper convex approximation, and then by compensating for the approximation in the outer loop.

5.4.3 Problem Convexification

To convexify problem (5.24), we utilize a two-step iterative approach. At the first step, we fix the DC-bias vector values for specific terms of the non-concave functions, so as to get rid of the square root and the logarithm function expression in the energy functions. After solving the problem, the second step substitutes the updated value of the DC-bias vector in the terms of the non-concave functions. More specifically, in the first step (and at the very first iteration), let $\widehat{\mathbf{b}} = \frac{I_H + I_L}{2} \mathbf{1}_{N_A}$ (i.e., $\hat{b}_i = \frac{I_H + I_L}{2}$) be the initial DC-bias vector. Therefore, the relation in (5.18) can be approximated as follows

$$\mathbf{GP} \cong (I_H \mathbf{1}_{N_A} - \mathbf{b}) \circ (I_H \mathbf{1}_{N_A} - \widehat{\mathbf{b}}). \tag{5.25}$$

The DC-bias vector can be approximated as follows

$$\mathbf{b} \cong I_H \mathbf{1}_{N_A} - \mathbf{GP} \oslash (I_H \mathbf{1}_{N_A} - \widehat{\mathbf{b}}). \tag{5.26}$$

Define

$$\mathbf{G}_b = [\frac{1}{I_H - \hat{b}_1} \bar{\mathbf{g}}_1, \frac{1}{I_H - \hat{b}_2} \bar{\mathbf{g}}_2, \cdots, \frac{1}{I_H - \hat{b}_{N_A}} \bar{\mathbf{g}}_{N_A}]^T,$$

we can re-write (5.26) as follows

$$\mathbf{b} \cong I_H \mathbf{1}_{N_A} - \mathbf{G}_b \mathbf{P}. \tag{5.27}$$

To further convexify the energy functions, define $z_k(\widehat{\mathbf{b}})$ as $z_k(\widehat{\mathbf{b}}) = \ln(1 + \frac{\rho_{oe}\rho_{se}\mathbf{h}_k^T\widehat{\mathbf{b}}}{I_0})$, which is a constant that depends on $\widehat{\mathbf{b}}$.

Problem (5.24) can now be readily approximated as a convex optimization problem. For the completeness of presentation, define the following variables (which are all functions of the estimated DC-bias vector $\widehat{\mathbf{b}}$):

$\mathbf{x}_k = f\rho_{oe}\rho_{se}V_t z_k(\widehat{\mathbf{b}})\mathbf{h}_k, \ k = 1, \ldots, N_{u,2},$

$x = \sum_{k=1}^{N_{u,2}} \mathbf{x}_k^T(I_H \mathbf{1}_{NA}),$

$\mathbf{w} = \sum_{k=1}^{N_{u,2}} \mathbf{x}_k^T \mathbf{G}_b, \ m_k = I_H \mathbf{x}_k \mathbf{1}_{N_A} - E_{th,k},$ and

$\mathbf{w}_k = \mathbf{x}_k^T \mathbf{G}_b, \ k = 1, \ldots, N_{u,2}.$

Using the above notations, problem (5.24) can be approximated as follows

$$\max_{\mathbf{P}} \quad \alpha f_R(\mathbf{P}) + \frac{(1-\alpha)}{\omega}(x - \mathbf{w}^T\mathbf{P}) \tag{5.28a}$$

$$\text{s.t.} \quad P_j \geq P_{j,min}, \qquad j = 1, \ldots, N_{u,1} \tag{5.28b}$$

$$\mathbf{w}_k^T \mathbf{P} \leq m_k, \qquad k = 1, \ldots, N_{u,2} \tag{5.28c}$$

$$\mathbf{g}_i^T \mathbf{P} \geq 0, \quad i = 1, \ldots, N_A \tag{5.28d}$$

$$\mathbf{g}_i^T \mathbf{P} \leq (\frac{I_H - I_L}{2})^2, \quad i = 1, \ldots, N_A, \tag{5.28e}$$

Since the function $f_R(\mathbf{P})$ is concave and the function $x - \mathbf{w}^T\mathbf{P}$ is linear, the objective function in (5.28) is concave. Furthermore, all the constraints in (5.28) are linear, which means that the optimization problem (5.28) is convex and, thus, can be solved using efficient algorithms [56]. We next characterize the optimal solution of problem (5.28) by deriving the first-order Karush-Kuhn-Tucker (KKT) conditions, which helps iteratively finding the primal and dual variables associated with problem (5.28).

Proposition 5.1 *The solution of problem (5.28) is given by*

$$P_j = \frac{-\alpha\beta}{\ln(2)\left(-\frac{1}{\omega}(1-\alpha)\mathbf{w}(j) + \lambda_j - \sum_{k=1}^{N_{u,2}} \mu_k \mathbf{w}_k(j) - \sum_{i=1}^{N_A} d_i \mathbf{g}_i(j)\right)} - \frac{1}{\gamma}, \quad j = 1, \ldots, N_{u,1},$$

(5.29)

where $\gamma = \frac{e\rho_{oe}^2 \rho_{se}^2 P}{2\pi W N_0}$, λ_j, μ_k, *and* d_i *are the dual variables associated with constraints (5.28b), (5.28c), and (5.28e), respectively,* $p_{max} = (\frac{I_H - I_L}{2})^2$ *is the electrical maximum transmit power, and* $\mathbf{w}(j)$ *denotes to the jth element of the vector* $\mathbf{w}$.

Proof. The proof hinges upon the interpretation of the Lagrangian duality of problem (5.28). Observe first that constraints in (5.28d) are rather redundant, since all the elements in $\mathbf{g}_i$ are positive, $\forall i = 1, \ldots, N_A$, and since the values of the vector $\mathbf{P}$ are guaranteed to be positive by constraints (5.28b). The Lagrangian function of problem in (5.28) can, therefore, be expressed as follows

$$\zeta = -\alpha\beta \sum_{j=1}^{N_{u,1}} \log\left(1 + \gamma P_j\right) - \frac{(1-\alpha)}{\omega}(x - \mathbf{w}^T\mathbf{P}) - \sum_{j=1}^{N_{u,1}} \lambda_j(P_j - P_{j,min}) + \sum_{k=1}^{N_{u,2}} \mu_k(\mathbf{w}_k^T\mathbf{P} - m_k)$$

$$+ \sum_{i=1}^{N_A} d_i(\mathbf{g}_i^T\mathbf{P} - p_{max}).$$

(5.30)

Based on first-order KKT conditions [56], we have

$$\frac{\partial\zeta}{\partial P_j} = 0, \quad j = 1, \ldots, N_{u,1}.$$

(5.31)

Solving (5.31), we obtain

$$-\alpha\beta\frac{\gamma}{\ln(2)(1+\gamma P_j)} + \frac{1}{\omega}(1-\alpha)\mathbf{w}(j) - \lambda_j + \sum_{k=1}^{N_{u,2}}\mu_k\mathbf{w}_k(j) + \sum_{i=1}^{N_A}d_i\mathbf{g}_i(j) = 0. \quad (5.32)$$

Re-ordering (5.32) then gives (5.29), which completes the proof. ∎

The dual variables λ_j, μ_k, and d_i must be selected in such a way that the resulted allocated power vector achieves the associated constraints. For instance, the value of the dual variables λ_j must be selected to achieve the jth constraint in (5.28b). λ_j can in fact be found after substituting (5.29) in constraints (5.28b), which gives the following

$$\lambda_j \leq \frac{-\alpha\beta}{\ln(2)(P_{j,min} + \frac{1}{\gamma})} + \frac{1}{\omega}(1-\alpha)\mathbf{w}(j) + \sum_{k=1}^{N_{u,2}}\mu_k\mathbf{w}_k(j) + \sum_{i=1}^{N_A}d_i\mathbf{g}_i(j)). \quad (5.33)$$

The other dual variables, i.e., μ_k and d_i, can be found by using the subgradient method. More specifically, for a fixed value of P_j (i.e., using (5.29) based on preset dual variables values), the subgradient method iteratively updates the values of μ_k and d_i as follows

$$\mu_k(n+1) = \mu_k(n) + \delta_\mu(\mathbf{w}_k^T\mathbf{P} - m_k), \ j = 1,\ldots,N_k, \quad (5.34)$$

$$d_i(n+1) = d_i(n) + \delta_d(\mathbf{g}_i^T\mathbf{P} - p_{max}), \ i = 1,\ldots,N_A, \quad (5.35)$$

where δ_μ and δ_d are steps sizes, that are used to guarantee the algorithmic convergence.

5.4.4 Iterative Algorithm

In this section, we present the overall algorithm which is proposed to solve the original optimization problem (5.19). The algorithm compensates for the approximations made earlier while convexifying the optimization problem. Because the proposed solution of the reformulated problem iteratively updates the dual variables, the estimated DC-bias vector is also updated at each iteration, so as to reflect the newest update of the values of the dual variables. The steps of the proposed algorithm are summarized in Algorithm 6 description.

Algorithm 6 Find the vectors $\mathbf{b}$ and $\mathbf{P}$

---

1. Find the initial estimated DC-bias vector by choosing $\widehat{\mathbf{b}} = \frac{I_H + I_L}{2} \mathbf{1}_{N_A}$ and assign initial non-negative random values for the dual variables.

2. Set $n = 1$

3. Find P_j using (5.29) $\forall j = 1, \ldots, N_{u,1}$, and the corresponding $\mathbf{b}$ using (5.20).

4. Update the estimated DC-bias vector and update the corresponding values of $\mathbf{x}_k$ and $\mathbf{w}_k$ $\forall k = 1, \ldots, N_{u,2}$, $\mathbf{w}$, and x.

5. Update the dual variables, using (5.33), (5.34), and (5.35).

6. if $\|\mathbf{b} - \mathbf{b}\|^2 < \epsilon$, break;

7. Increment n and go to step 3).

Remark 1 *The main idea of Algorithm 6 is to update the dual variables along with the estimated DC-bias vector in each iteration by equating it with the resulted DC-bias vector from the previous iteration. This process continues until convergence. It is important to note that there is no unique values for the dual variables that can reach the optimal power. Such conclusion is due to the fact that the dual variables must be*

selected to achieve the corresponding constraints. Hence, in step 5) in Algorithm 6, we can find the $\lambda's$ using (5.33) by replacing the inequality with equality, which helps achieving the corresponding constraints.

5.4.5 Baseline Algorithm

For benchmarking purposes, we now propose a simple, yet feasible, solution to problem (5.19). In this approach, for simplicity, the DC-bias values are assumed to be equal across all APs, i.e., $b_i = b$. Based on this assumption and within the bounds of the DC-bias values, we find the maximum and minimum DC-bias values that achieve the constraints in (5.19). It can be noticed that the minimum feasible DC-bias value is the one that maximizes the sum-rate, while the maximum feasible DC-bias value is the one that maximizes the total harvested energy. Therefore, the idea of this approach is that, instead of weighting the utility functions, we weight the corresponding DC-bias values. In other words, we linearly combine the minimum and the maximum DC-bias vectors based on the given α value. After obtaining the fixed DC-bias vector, we formulate a linear optimization problem to find the corresponding messages' power vector. If we scrutinize the constraints in (5.19), we see that the value of the DC-bias b must be increased if at least one of the constraints in (5.19c) is violated, while it must be decreased if at least one of the constraints in (5.19b) is violated. That means the constraints in (5.19c) and the constraint $b \geq \frac{I_H + I_L}{2}$ specify the minimum DC-bias vector that achieves all the constraints. On the other hand, the constraints in (5.19b) and the constraint $b \leq I_H$ specify the maximum DC-bias vector that achieves all the constraints. If the value reached while searching for the maximum DC bias value is

156

found to be less than the value reached while searching for the minimum DC-bias value, the problem of finding equal DC-bias at all APs is then unfeasible.

To determine the minimum DC-bias vector, we solve all the equations in (5.19c) under the assumption that all the values in the vector $\mathbf{b}$ are equal. For the kth user, we find a solution for b_k from the following equation

$$b_k f \rho_{oe} \rho_{se} V_t \mathbf{h}_k^T \mathbf{1}_{N_A} \ln(1 + b_k \frac{\rho_{oe}\rho_{se}\mathbf{h}_k^T\mathbf{1}_{N_A}}{I_0}) \geq E_{th,k}. \quad k = 1, \ldots, N_{u,2} \tag{5.36}$$

Equations (5.36) can be solved using any numerical methods such as Newton method. Define $\mathbf{b} \in \mathbb{R}^{N_{u,2}\times 1}$ as the vector that hosts the solutions of equations (5.36), the minimum DC-bias vector can be given by

$$\mathbf{b}_{min} = \max\left(\frac{I_H + I_L}{2}, \max(\mathbf{b})\right) \mathbf{1}_{N_A}. \tag{5.37}$$

To determine the maximum DC-bias vector, we solve all the equations in (5.20) when $P_j = P_{j,min}, j = 1, \ldots, N_{u,1}$. Therefore, the maximum DC-bias vector is given by

$$\mathbf{b}_{max} = \min\left(I_H, I_H - \sqrt{\max(\mathbf{GP})}\right) \mathbf{1}_{N_A}. \tag{5.38}$$

Based on a predefined α, the DC-bias solution of the baseline approach is given by

$$\mathbf{b} = \alpha \mathbf{b}_{min} + (1 - \alpha)\mathbf{b}_{max}. \tag{5.39}$$

It can be seen that all the values in the solution vector $\mathbf{b}$ are equal. Because there is

more than one solution of the messages' power vector $\mathbf{P}$ for the given DC-bias vector, we formulate the following simple optimization problem to find an efficient power allocation

$$\max_{\mathbf{P}} \quad \sum_{j=1}^{N_{u,1}} \gamma P_j \tag{5.40a}$$

$$s.t. \quad P_j \geq P_{j,min}, \qquad j = 1, \ldots, N_{u,1} \tag{5.40b}$$

$$\mathbf{GP} \leq (I_H \mathbf{1}_{N_A} - \mathbf{b})^2, \ i = 1, \ldots, N_A \tag{5.40c}$$

$$\mathbf{P} \geq \mathbf{0}. \tag{5.40d}$$

Note that the vector $\mathbf{b}$ in the constraints (5.40c) is given by (5.39). Problem (5.40) is a linear programming (LP) and can be solved easily by the CVX solver [57]. All the baseline approach procedures are summarized in Algorithm 7.

Algorithm 7 Baseline approach to find the vectors $\mathbf{b}$ and $\mathbf{P}$

---

1. Find $\mathbf{b} \in \mathbb{R}^{N_{u,2} \times 1}$ by solving the $N_{u,2}$ equations in (5.36).

2. Find $\mathbf{b}_{min}$ and $\mathbf{b}_{max}$ using (5.37) and (5.38), respectively, then find the solution DC-bias vector using (5.39).

3. Using the given DC-bias vector, find the vector $\mathbf{P}$ by solving the linear optimization problem (5.40) using CVX solver [57].

5.4.6   Special cases

In this section, we consider the two special cases of the weighted-sum formulated problem. In these cases, we focus on solving the problem that considers maximizing

one of the two extreme utilities (i.e., either the total harvested energy or the sum-rate) under the same considered constraints.

Maximizing the total harvested energy $(\alpha = 0)$

To maximize the harvested energy instead of the weighted sum function, we set α to 0 for both Algorithm 6 and the baseline approach. For the proposed Algorithm 6, the problem is interestingly cast and approximated as the following linear optimization problem

$$\max_{\mathbf{P}} \quad (x - \mathbf{w}^T \mathbf{P}) \tag{5.41a}$$

$$s.t. \quad P_j \geq P_{j,min}, \qquad j = 1, \ldots, N_{u,1} \tag{5.41b}$$

$$\mathbf{w}_k^T \mathbf{P} \leq m_k \quad k = 1, \ldots, N_{u,2} \tag{5.41c}$$

$$\mathbf{g}_i^T \mathbf{P} \geq 0, \quad i = 1, \ldots, N_A \tag{5.41d}$$

$$\mathbf{g}_i^T \mathbf{P} \leq (\frac{I_H - I_L}{2})^2, \; i = 1, \ldots, N_A. \tag{5.41e}$$

Problem (5.41) can be solved efficiently using the CVX solver [57], without the need for the use of the dual decomposition method and the subgradient method. The steps of solving problem (5.41) are given in Algorithm 8.

For the baseline approach, the underlying algorithm (equal DC-bias allocation) for solving problem (5.41) is given by

$$\mathbf{b} = \min \left(I_H, I_H - \sqrt{\max(\mathbf{GP}_{min})} \right) \mathbf{1}_{N_A}, \tag{5.42}$$

Algorithm 8 Find the vector $\mathbf{b}$ that maximizes the total harvested energy

---

1. Find the estimated DC-bias vector by putting $\widehat{\mathbf{b}} = \frac{I_H + I_L}{2} \mathbf{1}_{N_A}$.

2. Solve problem (5.41) using CVX solver, with the given $\widehat{\mathbf{b}}$, and find the solution $\mathbf{b}$ using (5.20).

3. if $\|\widehat{\mathbf{b}} - \mathbf{b}\|^2 > \epsilon$ or the maximum iteration is not reached, update $\widehat{\mathbf{b}} = \mathbf{b}$ and go to step 2.

---

which is the maximum feasible DC-bias that achieves the constraints while maximizing the total harvested energy. The messages' power herein are given by $\mathbf{P} = \mathbf{P}_{min}$.

Maximizing the sum-rate ($\alpha = 1$)

The problem of sum-rate maximization under the established constraints can be obtained by setting $\alpha = 1$. The problem can be approximated as (5.28) with setting $\alpha = 1$, and Algorithm (6) can be used to find the joint DC-bias and power vector that maximize the sum-rate function. Similarly, the power vector in the baseline approach for the sum-rate maximization can be obtained by solving (5.40), where the DC-bias vector is given by

$$\mathbf{b} = \max\left(\frac{I_H + I_L}{2}, \max(\mathbf{b})\right) \mathbf{1}_{N_A}, \tag{5.43}$$

which is the minimum equal DC-bias that achieves the constraints while maximizing the sum-rate.

5.4.7 Computational Complexity

This section discusses the computational complexity of both the Algorithm 6 and the baseline approach. It is shown in [131], [82] that the complexity of the subgradient

approach is a polynomial function of the number of the dual variables, which is $M = N_{u,1} + N_{u,2} + N_A$. Besides, in each iteration, we need to update the estimated DC-bias and the corresponding variables $\mathbf{x}_k,\ k = 1, \ldots, N_{u,2}$ and $\mathbf{w}_k,\ k = 1, \ldots, N_{u,2}$. This means that for updating the DC-bias vector, the number of the updated variables in each iteration is $N_A \times N_{u,2} + N_A \times N_{u,1}$. Therefore, Algorithm 6 has a computational complexity in the order of $O(I_R(M + N_A \times N_{u,2} + N_A \times N_{u,1}))$, where I_R is the iterations' number needed for Algorithm 6 convergence.

On the other hand, the computational complexity of the proposed baseline approach is mainly due to solving a LP optimization problem, which is shown to be bounded by $O(n^2 l)$, where l is the number of constraints and $n = N_{u,1}$ is the number of variables [56].

5.5   Simulations

This section evaluates the performance of the proposed algorithms by illustrating how the weight α, the number of users (either IUs or EHUs), and the FoV affect the total harvested energy, sum-rate, and the weighted sum function. All the simulation results are implemented under the simulation parameters given in Table 5.1, similar to [118], [47], and [109]. Consider an $8 \times 8 \times 3$ m^3 room equipped with 16 VLC APs that are at ceiling level, and serve several IUs and EHUs. Monte-Carlo simulations are used to assess the performance of the proposed algorithms, where every point in the numerical results is the average of implementing 100 different user realizations.

Fig. 5.3 compares the proposed Algorithm 6 with the proposed baseline approach

Table 5.1: Simulation Parameters

Parameter Name	Parameter Value
VLC AP maximum bandwidth, W	20 MHz
The physical area of a PD for IUs, $A_p(IU)$	1 cm^2
The solar cell physical area for EHUs, $A_p(EHU)$	0.04 m^2
Gain of optical filter, g_{of}	1
Half-intensity radiation angle, $\theta_{1/2}$	60°
FoV semi-angle of PD, Θ	$40^o - 65^o$
Optical-to-electric conversion factor of IUs, $\rho_{oe}(IU)$	0.53 [A/W]
Optical-to-electric conversion factor of EHUs, $\rho_{oe}(EHU)$	0.4 [A/W]
Refractive index, n	1.5
Maximum input bias current, I_H	12 mA
Minimum input bias current, I_L	0 A
Fill factor, f	0.75
Electric-to-optical conversion factor, ρ_{se}	10 W/A
Thermal voltage, V_t	25 mV
Dark saturation current of the PD, I_0	10^{-10} A
Noise power spectral density, N_0	10^{-22} A^2/Hz
Room size	8×8 m
Room height	3 m
User height	0.85 m
Number of APs	4×4
Minimum IUs data rate, $R_{th,j}$, $j = 1, \ldots, N_{u,1}$	10 (Mbits/sec)
Minimum EHUs energy, $E_{th,k}$, $k = 1, \ldots, N_{u,2}$	1 μJoule

by plotting the weighted sum function versus α. The figure shows that the proposed

Algorithm 6 outperforms the proposed baseline approach for all different weights and

different users' FoV. The figure further shows that the weighted sum function is maxi-

mized when $\alpha = 0$ or 1, i.e., when the weighted sum function is just the total harvested

energy or the sum-rate function, respectively. Such performance behavior can be jus-

tified by the fact that when α is small (i.e. when $\alpha \leq 0.3$), the dominating function is

the total harvested energy, and hence the increase in α decreases the weighted sum,

while when α is large ($\alpha \geq 0.4$) the dominating function is the sum-rate and, hence,

the increase in α increases the weighted sum function.
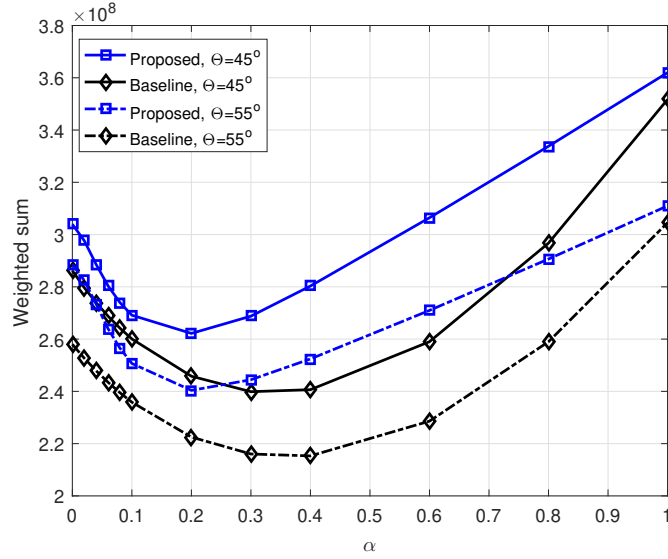
Figure 5.3: Comparison between the proposed algorithm and the proposed baseline by plotting the weighted sum function versus the weight α for different users' FoV, $N_{u,1} = 5$, $N_{u,2} = 5$, and $\omega = \frac{10^{-3}}{12 \times W}$.
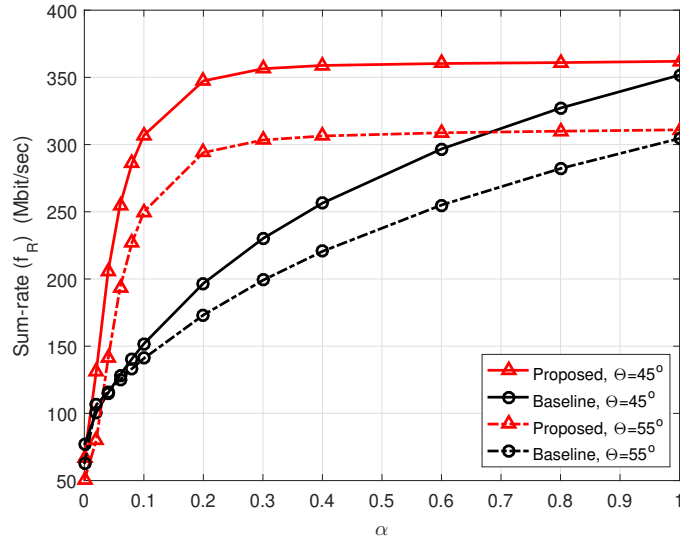
Figure 5.4: The sum-rate function versus α for different users' FoV.

To show how the weight α affects the sum-rate and the total harvested energy, we plot the sum-rate function versus α in Fig. 5.4, and the total harvested energy versus α in Fig. 5.5. It can be seen from both figures that as the weight increases, the sum-rate increases and the total harvested energy decreases, but with a decreased rate. The

figures also show that for the different values of α, as the sum-rate increases (as shown in Fig. 5.4), the total harvested energy decreases (as shown in Fig. 5.5). These results confirm that the sum-rate and the total harvested energy functions exhibit an opposite behavior, and can be controlled by allocating the DC-bias, since decreasing the DC-bias decreases the total harvested energy and preserves much power for transmitting data. Both figures further show that at some values of α, if the proposed baseline approach outperforms the proposed Algorithm 6 at one utility function (either the sum-rate or the total harvested energy), it provides much less performance at the same points at the other utility function. Both figures also show that in the proposed approach, the impact of α on sum-rate and harvested energy functions decreases as α increases from 0 to 1. We observed that the numerical choice of ω affects the decrease (and increase) rate of the sum-rate and the harvested energy. To decrease this rate of increasing (or decreasing), the value of ω should be adapted with α. However, this is not our interest, since we can confine our study in the range of α effectiveness.

Figs. 5.3, 5.4, and 5.5 show that the performance of the utility functions is better at lower values of FOVs, i.e., the 45° FOV case as compared to the 55° FOV case. Such result is further illustrated in Fig. 5.6 with different number of EHUs and IUs. Equation (1.2) further justifies this fact, since if the FoV (Θ) increases between 0° and 90°, the channel quality decreases significantly. On the other hand, from equation in (1.2), decreasing the user's FoV decreases the probability of coverage at that user. As a result, we can conclude that if the users' FoV is adjustable, decreasing its value subject to having at least one VLC AP in the FoV of that user would indeed increase the network harvested energy. The figures also show that the proposed iterative
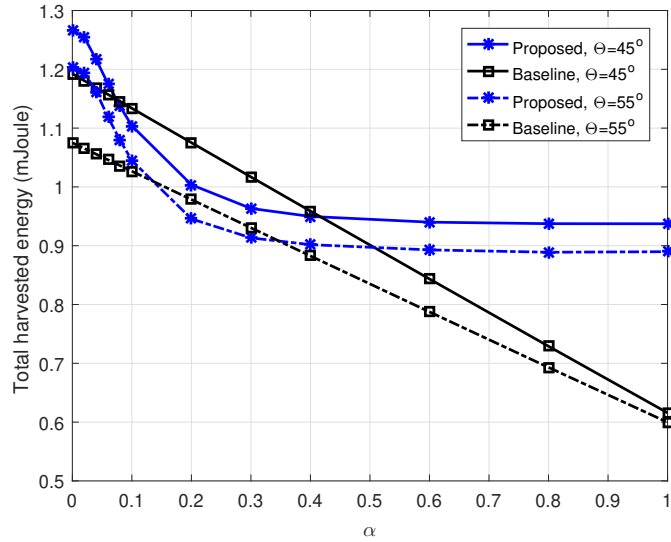
Figure 5.5: The total harvested energy function versus α for different users' FoV.

Algorithm 6 outperforms the proposed baseline approach with all the different users' FoV and different number of IUs and EHUs. To balance between the sum-rate and the total harvested energy functions, we select $\alpha = 0.1$, where as shown in Figs. 5.4 and 5.5 $\alpha = 0.1$ provides a sensible trade-off between the sum-rate and the total harvested energy functions. Fig. 5.6 further shows the behavior of the weighted sum function when the number of EHUs is dominating, when the number of both EHUs and IUs are equal, and when the number of IUs is dominating. It can be seen that the effect of increasing number of EHUs is higher than the effect of increasing the number of IUs. Increasing the number of EHUs would increase the total harvested energy linearly, while increasing the number of IUs would increase the sum-rate but at a decreasing rate. This is because the available bandwidth and power per information-user depends on the number of users, while the harvested energy is not a function of the bandwidth and the AC power. Another reason is because of the value of ω, which should be ideally adapted with changing the number of users.
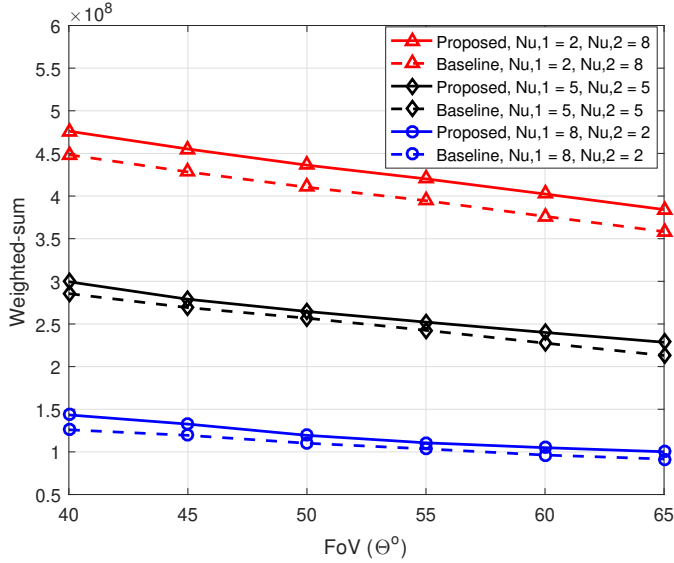
Figure 5.6: The weighted sum function versus users' FoV with different number of EHUs and IUs $\alpha = 0.1$ and $\omega = \frac{10^{-3}}{12 \times W}$.

Fig. 5.7 studies the effect of the users' FoV and the number of users on the sum-rate function. In this figure, we optimize the sum-rate under QoS constraints which can be implemented by setting $\alpha = 1$ in the weighted sum function. As expected, decreasing the users' FoV, increasing the IUs, or decreasing the number of EHUs improve the sum-rate as shown in Fig. 5.7. The figure also shows that the proposed Algorithm 6 outperforms the proposed baseline approach or the equal DC-bias allocation approach at the different scenarios considered in the figure, especially when the number of IUs is high.

Fig. 5.8 studies the effect of the users' FoV and the number of users on the total harvested energy function. In this figure, we use Algorithm 8 instead of Algorithm 6 to solve the optimization problem, which is a special case that can be implemented when $\alpha = 0$ in the weighted sum function. As expected, the figure shows that decreasing the users' FoV, increasing the IUs, or decreasing the number of EHUs lead to increasing
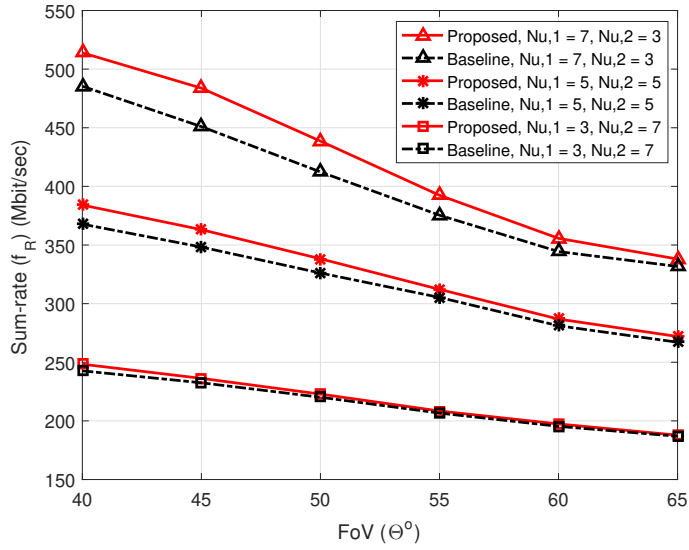
Figure 5.7: The sum-rate versus users' FoV with different number of EHUs and IUs, $\alpha = 1$.
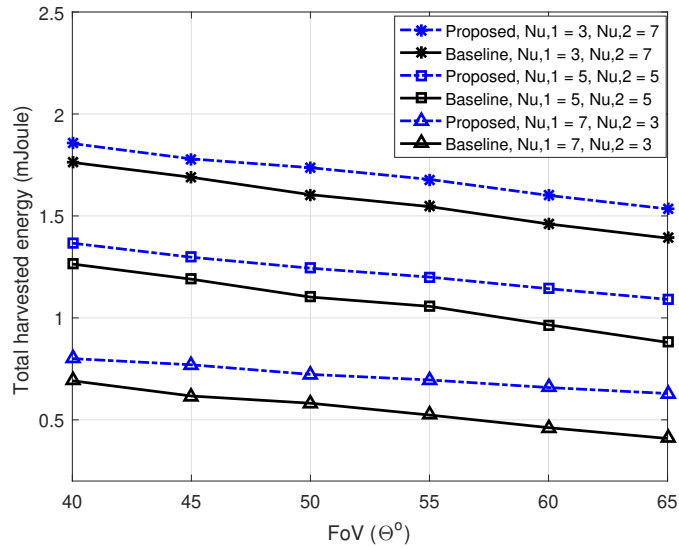
Figure 5.8: The total harvested energy versus users' FoV with different number of EHUs and IUs, $\alpha = 0$.

the total harvested energy. The figure also shows that the proposed Algorithm 8 outperforms the proposed baseline approach (i.e., the equal DC-bias allocation approach) at the different scenarios considered in the figure.

To illustrate the convergence of the iterative algorithm proposed to compensate for
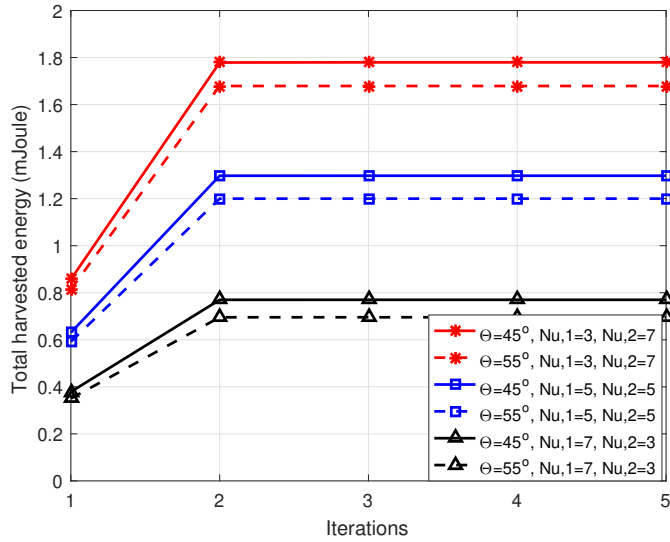
Figure 5.9: The total harvested energy versus number of iterations with different users' FoV and different number of IUs and EHUs, $\alpha = 0$.

the used approximations, Fig. 5.9 studies the behavior of Algorithm 8 and plots the total harvested energy at all EHUs versus the number of iterations, for two values of the FoV and different numbers of IUs and EHUs. The figure shows the fast convergence of Algorithm 8 for all values of FoV for the different number of users, which further highlight the numerical efficiency of our proposed algorithm.

Fig. 5.10 plots the sum-rate as a function of the percentage of number of EHUs out of the total number of users, also denoted by η (i.e. $\eta = \frac{N_{u,2}}{N_{u,2}+N_{u,1}}$). This figure shows that the sum-rate decreases as η increases, because increasing the EHUs or decreasing the IUs lead to decreasing the sum-rate. This figure also shows that increasing the total number of IUs increases the sum-rate but with a slower rate, since the rate achieved by increasing $N_u = 4$ to $N_u = 8$ is around double the rate achieved by increasing $N_u = 8$ to $N_u = 12$. This is because adding one user to the system decreases the assigned power (on average) for the existing users for a given fixed transmit power.
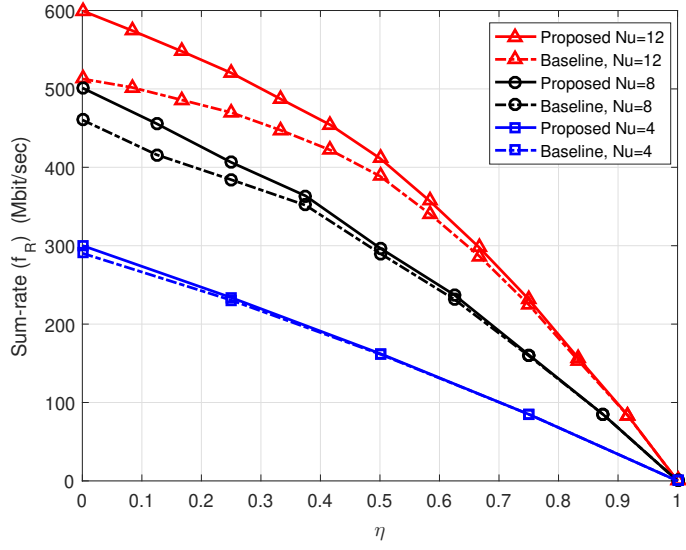
Figure 5.10: The sum-rate versus η (the percentage of EHUs out of total number of users N_u), with different total number of users, FoV$= 45^o$.
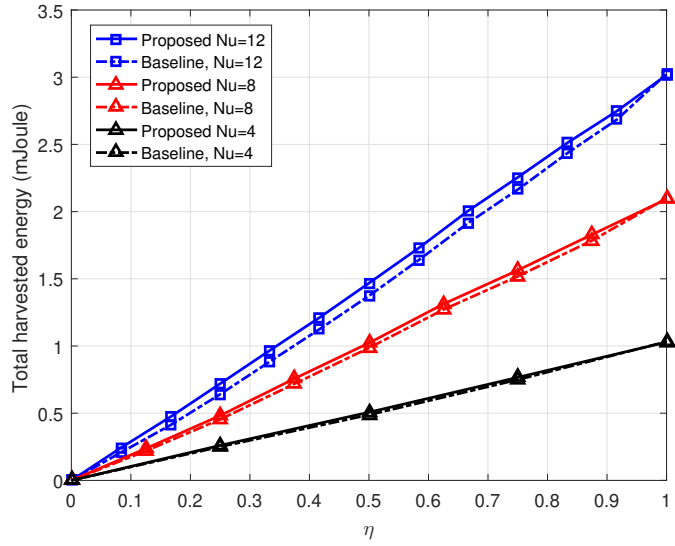
Figure 5.11: The total harvested energy versus η (the percentage of EHUs out of total number of users N_u) with different total number of users, FoV$= 45^o$.

Lastly, Fig. 5.11 shows that as the fraction of EHUs increases, the total harvested energy increases. As expected, this is mainly due to two main reasons. Firstly, for a fixed number of users N_u, as the fraction of EHUs increases, the number of EHUs increases, which adds to the total harvested energy. Secondly, decreasing the number

of IUs leads to decreasing the number of constraints in (5.19b), which increases the search space of (5.19b); thereby increasing the objective function. The figure further shows that, if $\eta = 1$ (i.e. when all users are EHUs), all the APs operate with a highest DC-bias (i.e. $b_i = I_H, \quad i = 1, \ldots, N_A$), and so both the iterative algorithm and the baseline achieve the same performance. On the other hand, if $\eta = 0$ (i.e., when all users are IUs), the total harvested energy becomes zero.

5.6 Conclusions

VLC-based systems are expected to play a major role in achieving the ambitious metrics of next generation indoor wireless networks. This chapter considered a VLC setup which considered the coexistence of both IUs and EHUs, and addressed the problem of maximizing a weighted sum of the total harvested energy and the sum-rate by means of properly adjusting the DC-bias values at the coordinating VLC APs and the messags' power vector subject to QoS constraints (minimum required data rate at IUs and minimum required harvested energy at EHUs). The chapter solved such a difficult problem using an iterative algorithm by first using an inner convex approximation, and then by properly compensating for the approximation in an outer loop. Simulation results showed that an appreciable, balanced performance improvement in both utility functions (the sum-rate and the total harvested energy) can be achieved by jointly optimizing the DC-bias vector and the messages' power vector.

<div align="center">

CHAPTER 6

CONCLUSION AND FUTURE

WORK

</div>

6.1 Conclusion

In this thesis, we considered and studied multiple types of VLC systems: hybrid VLC/RF systems, standalone VLC networks based on APs cooperation and user-centric design, cooperative NOMA-VLC networks, and VLC networks that contain energy-harvesting users. Different schemes and optimization techniques were proposed to improve the performance of VLC networks and to make them qualified for the future wireless communication networks.

Solving the power allocation and APs assignment problems jointly can provide an appreciable improvement in terms of achievable data rates and fairness in hybrid VLC/RF systems. When the number of users is less than the number of APs, it is appropriate to use the user-centric design to mitigate the inter-cell interference and improve the energy efficiency of standalone VLC networks. Based on user-centric

design, we proposed a new clustering method, a new metric for APs association, and algorithms to jointly allocate the power and select the APs for energy efficiency maximization.

For extending the VLC coverage and mitigating the blockage rate, we proposed a new users' cooperation approach based on cooperative NOMA. A problem to jointly allocate the power, select the links for poor users, and pair the users was formulated to maximize the weighted sum rate. For such formulated problem, an optimal and suboptimal solutions were proposed and compared with traditional NOMA scheme. It can be concluded that, the proposed scheme and solutions provide a significant improvement in sum-rate and fairness in VLC networks.

VLC networks might contain an energy-harvesting users such as sensors and IoT devices. Hence, we studied a VLC system that contains two types of users which are energy-harvesting users (EHUs) and information users (IUs). In such system, we used a cooperative transmission, DC-bias allocation, and power allocation to balance between the received harvested energy at EHUs and the received data rates at IUs. Simulation results showed that an appreciable, balanced performance improvement in both utility functions (the sum-rate and the total harvested energy) can be achieved by jointly optimizing the DC-bias vector and the messages' power vector.

6.2 Future Work and Open Research Problem

Based on the existing work in the literature, in this section, we outline different challenges and open research problems that need to be considered and investigated in

172

the future work.

6.2.1 Load Balancing, and CoMP Transmission

- Users' FoV alignment for balancing the load: we show before that many studies have been dedicated to balance the load in VLC or in hybrid VLC/RF networks. These studies focused mainly on optimizing the users' association, time or bandwidth resource allocation, and the power allocation. However, as we show in Section 1.2.1, the users' FoV parameter has a great impact on the system coverage, inter-cell interference, handover overhead, and on channel quality. Therefore, optimizing the users' FoV jointly with distributing the users and allocating the power would be more effective in balancing the load and in maximizing the system utilities.

- User-centric design in hybrid VLC/RF systems: different papers optimized the user-centric cell design in standalone VLC networks [47], [108]. However, optimizing the user-centric cell design in hybrid RF/VLC networks would be more challenging and leads to a high impact in improving the system utilities. The problem can be divided into two interlinked problems, which are assigning the users to networks (either RF or VLC) and clustering the users and assigning the APs in each network. These two problems can be solved alternatively to improve the system utility and to achieve the required constraints.

- Optimizing the joint cell formation and power allocation in user-centric VLC design: it was shown that the procedures user clustering, APs association, and

power allocation are interlinked problems [108], but only a subboptimal approach has been proposed for jointly associating the APs and allocating the power. However, formulating an optimization problem that considers the three procedures and proposing solutions for the formulated problem would be more efficient in improving the energy efficiency or the sum-rate. This problem can be formulated to optimize global energy efficiency of the system by jointly implementing the user clustering, APs association, and the power allocation.

- Extending the proposed hybrid VLC/RF Co-NOMA scheme to be applied in multi-cell VLC systems: In multi-cell VLC system the inter-cell interference shows up and the decision of classifying the users into weak and strong users does not depend only on the channel quality. It depends also on the received interference and on the load distribution in cells. Hence applying the proposed hybrid VLC/RF Co-NOMA scheme (proposed in Chapter 4) can be extended to balance the load in multi-cell and to improve the sum-rate and fairness of the system.

6.2.2 NOMA-VLC Networks

Despite all the aforementioned work on NOMA-VLC systems, numerous challenges remain, and important topics in this area of research are still to be investigated. Below is a list of some key open problems in NOMA-VLC networks:

- Hybrid NOMA-VLC systems: the hybrid NOMA is to group the users into multiple clusters, and assign to each cluster a designated resource block, following

the NOMA principle in each cluster. To our knowledge, the hybrid NOMA has not been studied yet in VLC systems. The rational for using the a hybrid NOMA is its ability to reduce the system's complexity. Indeed, having a large number of users in the VLC system, and assigning them to the same resource block can be problematic, since the user with the best channel must decode all the signals of all the users before decoding his/her own signal, creating delays the decoding and resulting in high complexity. Hybrid NOMA systems have been proposed in RF networks to take into account both the system performance and complexity. Therefore, we propose to study the hybrid NOMA-VLC system by finding the optimal user grouping, allocating the power to each group, the power inside each group, or grouping the users and allocating the power jointly, for sum-rate maximization purposes. This system can be extended to be a multi-cell system, in which the user-to-AP association problem also exists and should be considered. Hence, the problem would be then a two layer user grouping with power allocation.

- NOMA with different QoS requirements: In real life, not all users require the same amount of data rate. For example, some of them may stream videos, whereas others are texting or exploring websites. Also some receivers can be IoT devices that need low data rates. Allocating power, in the most effective way, to users with different needs still remain a challenge, and obtaining the required data rate for each user, even when some weak users (users with poor channels) require higher data.

- Modulation and coding for NOMA-VLC system: several papers studied the modulation and coding schemes in NOMA RF networks [132], [133]. As the modulation and coding in VLC networks is different (based on IM/DD), investigating the modulation and coding schemes in NOMA-VLC systems would be worthy for practical implementation.

- NOMA in coordinated multi-point (CoMP) VLC networks: CoMP VLC system means that multiple APs are cooperating to transmit the data for the users. The cooperation is for mitigating the inter-cell interference and enhancing the received data rate by optimizing the precoding matrix. Assume a VLC system consisting of N APs and M users, where $M > N$, the questions should be raised is that how the users should be sorted from the strongest user to the weakest user?, how should the users be grouped to be served by the cooperating APs?, and how should the power be allocated. Combining the two techniques NOMA and CoMP surly leads to having a significant performance improvement in VLC systems.

- Hybrid SDMA and NOMA: SDMA in VLC can be implemented using angle diversity transmitters that can generate several parallel narrow light beams directed to different directions using different LEDs. The goal of using SDMA is to mitigate inter-cell interference in VLC networks by directing the light to intended users and decreasing the overlap areas. However, some LEDs can be directed to non users, some to one user, and others to multiple users. The LEDs that are assigned or directed to serve multiple users can use the NOMA as a
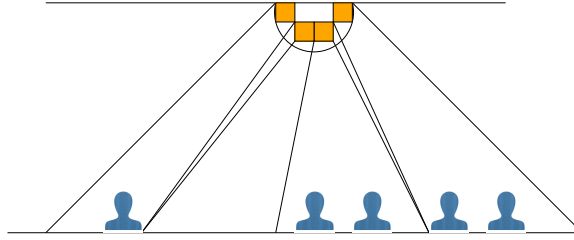
Figure 6.1: The proposed hybrid SDMA/NOMA system.

multiple access and to maximize the data rate. SDAM is used to mitigate or eliminate inter-cell interference, and NOMA is used to mitigate the intra-cell interference using SIC. By combining both of them, the system performance is significantly improved, in terms of data rate and system's fairness. Fig. 6.1 shows a system model in which SDMA and NOMA can coexist in VLC systems, where the NOMA can be used in LEDs that serve more than one user.

6.2.3 Harvesting the Energy in VLC Systems

Despite all the work conducted in the literature (see Introduction section in Chapter 5), there are several remaining challenges associated with the transfer of information and power, using a light wave. Here are below a few key issues that need to be investigated and optimized for obtaining the most efficient power and information transfer systems.

- *Simultaneous light-wave for information, illumination, and power transfer:* Several studies investigated VLC systems in which both energy and information could be transferred to users. However, achieving both functions in VLC networks might violate the illumination requirements. We therefore propose to study the three functions of the light simultaneously by formulating optimiza-

tion problems that allocate DC bias, available power, and available resources.

- *Joint DC-bias and resource allocation for sum rate with the presence of energy-harvesting users*: allocating both the DC bias and the available resources at the VLC APs leads to a significant improvement of the VLC performance under simultaneous lightwave information and power transfer (SLIPT). An effective allocation of resources (to the users) provides opportunities to preserve high energy that can be harvested by users.

- As proposed in the NOMA-VLC Section, a cooperative NOMA can be implemented in VLC systems; however, the strong user may do not want to consume some of his/her power by forwarding the signal to the weak user. We therefore suggest investigating ways for the strong user to harvest the energy from the light intensity, in the first phase, and then use it to forward the weak user's signal. This means that the transmitter should optimize the DC bias and the information power to maximize the sum rate and guarantee acceptable fairness.

- *Optimizing the MISO-VLC network with NOMA:* when the system consists of multiple VLC APs cooperating to transmit the information and power for multiple users, if the number of users is larger than the number of APs, the key issue that should be addressed is whether orthogonal multiple access (OMA) or NOMA is the best system for scheduling users and harvesting the energy. As previously reported in the literature, NOMA can provide better data rates than OMA. In other words, NOMA can achieve the required users' data rate with a small amount of transmit power (information power), which allow the DC bias

178

to increase, resulting in increasing the harvested energy.

- *Placing the energy harvesting users:* suppose that a VLC system consisting of multiple information users (users interested only in gathering the information), and IoT devices that work only in uplink (like sensors) and interested only in harvesting the energy (energy harvesting (EH) users). Optimizing the positions of the EH users in order to maximize the harvested energy and to achieve the required QoS at the information users is crucial in VLC systems. Yet, it remains challenging. Therefore, there is needed to investigate ways of implementing and simplifying this task.

6.2.4 Securing VLC Networks

Despite the significant number of studies already performed, there are still some important issues to tackle and still many challenges for researchers to overcome in the future. A few of them are highlighted below, together with potential solutions that may improve the physical layer security (PLS) in VLC systems:

- *Joint PLS and load balancing in hybrid RF/VLC systems with considering the illumination constraints*: All the conducted works on balancing the load in hybrid VLC/RF networks are implemented to maximize the system utilities (such as sum-rate and/or fairness) without considering the secrecy constraints. Hence, we propose to design and optimize the joint load balancing with secrecy and illumination constraints when single or multiple, known or unknown, eavesdroppers exist. This problem contains joint user-to-APs association and power allocation

to maximize the secrecy capacity and achieve the required illumination.

- How to optimize the beamforming vector in MISO-VLS systems when an active and passive eavesdropper exists. The common approach for the active eavesdropper is the zero-forcing preacoding approach, the common approach for the passive eavesdroppers is the design of protected zones, using an artificial noise or by steering the beamforming lobes. This raises an important question: what would the appropriate method be to improve the security, if the transmitters know the CSI of some eavesdroppers and they do not know the CSI of the others, or have a limited information about the eavesdropper (e.g. location only).

- PLS in NOMA-VLC system: Several recent papers investigated the PLS in NOMA RF networks for different system models [134], [135]. To this day, no paper has studied the PLS in NOMA-VLC systems. Because of the unique properties of VLC systems, the PLS in NOMA-VLC systems is required to be investigated, evaluated, and optimized.

- User-centric cell formation based in the presence of eavesdroppers: As shown above, the user-centric cell formation is an appropriate scenario when the number of users is much smaller than the APs. Suppose that the network contains some eavesdroppers (whether their CSI are available or not), the questions raised are: 1) how should the users be clustered? 2) how should the APs be associated to the clustered users? 3) which APs should participate in communication, and which should be switched off? 4) could the switched off APs help enhance the secrecy sum-rate in emitting jamming signals?

All the above questions indicate that the joint PLS and user-centric design should be investigated and optimized together.

6.2.5 Multi-User Outdoor VLC Networks

Toward developing smart cities, the street and park lamps can be utilized as VLC APs that can be used to serve multiple users. The feasibility and popularity of the VLC outdoor communication depends highly on defeating or mitigating the effect of the contaminating light stemming from the sun and the ambient lights [136]. Most of the optimization techniques proposed for indoor VLC networks cannot be applied directly in outdoor VLC networks. To extend the techniques which have been proposed for indoor VLC networks to be used in outdoor VLC networks, different issues should be considered in formulating and solving the optimization problems:

- Because of the sun light, the receivers might be blinded to detect the received light since the ambient light illuminance might be stronger than the transmitter illuminance. This contaminating light varies during the day time and can be mitigated using lens and filter at the receivers [136]. Islim *et al.* [137] showed that in the presence of the sun light, a reliable communication can be achieved at high speed data rates and by employing an optical bandpass blue filter that can reduce the effect of the sun light.

- The outdoor VLC channel is not stable and static like the ones in the indoor. The outdoor VLC channel is attenuated due to the atmosphere pressure and the inhomogeneities in the temperature, resulting in having the refractive index

varies along the transmission path [138].

- In outdoor VLC systems, the transmitters' distribution, transmitters' height, density of transmitters, and coverage area are different from those in indoor VLC systems [139]. In particular, the typical transmitters' height is 8 m, the cell radius is around 7 m, and the APs' distribution might be one dimensional in the street. Whereas, in indoor systems, the typical transmitters' height is 3 m, the cell radius is around 2-3 m, and the APs' distribution is two dimensional in the ceiling. These outdoor features lead to having a less inter-cell interference (because of the one dimensional distribution), lower channels quality (because of the longer distances between users and receivers), larger cell coverage (because of the APs heights), and less rate of blockages than the case in indoor VLC systems. In addition, the required illumination (in Lux) in the outdoor is less restricted than the one in the indoor environments [139].

REFERENCES

[1] X. Li, Y. Huo, R. Zhang, and L. Hanzo, "User-centric visible light communications for energy-efficient scalable video streaming," *IEEE Trans. Green Commun. Netw.*, vol. 1, no. 1, pp. 59–73, 2017.

[2] "Cisco global cloud index: Forecast and methodology, 2016–2021 white paper," 2017.

[3] J. G. Andrews, S. Buzzi, W. Choi, S. V. Hanly, A. Lozano, A. C. Soong, and J. C. Zhang, "What will 5G be?" *IEEE J. Sel. Areas Commun.*, vol. 32, no. 6, pp. 1065–1082, 2014.

[4] M. Shafi, A. F. Molisch, P. J. Smith, T. Haustein, P. Zhu, P. De Silva, F. Tufvesson, A. Benjebbour, and G. Wunder, "5G: A tutorial overview of standards, trials, challenges, deployment, and practice," *IEEE J. Sel. Areas Commun.*, vol. 35, no. 6, pp. 1201–1221, 2017.

[5] P. Pirinen, "A brief overview of 5g research activities," in *1st Int. Conf. 5G for Ubiquitous Connectivity (5GU)*.   IEEE, 2014, pp. 17–22.

[6] A. Al-Fuqaha, M. Guizani, M. Mohammadi, M. Aledhari, and M. Ayyash, "Internet of things: A survey on enabling technologies, protocols, and applications," *IEEE Commun. Surveys Tuts.*, vol. 17, no. 4, pp. 2347–2376, 2015.

[7] M. R. Palattella, M. Dohler, A. Grieco, G. Rizzo, J. Torsner, T. Engel, and L. Ladid, "Internet of things in the 5G era: Enablers, architecture, and business models," *IEEE J. Sel. Areas Commun.*, vol. 34, no. 3, pp. 510–527, 2016.

[8] D. Tsonev, S. Videv, and H. Haas, "Towards a 100 Gb/s visible light wireless access network," *Opt. Express*, vol. 23, no. 2, pp. 1627–1637, 2015.

[9] N. Bhushan, J. Li, D. Malladi, R. Gilmore, D. Brenner, A. Damnjanovic, R. Sukhavasi, C. Patel, and S. Geirhofer, "Network densification: the dominant theme for wireless evolution into 5G," *IEEE Commun. Mag.*, vol. 52, no. 2, pp. 82–89, 2014.

[10] X. Ge, S. Tu, G. Mao, C.-X. Wang, and T. Han, "5G ultra-dense cellular networks," *IEEE Wireless Commun.*, vol. 23, no. 1, pp. 72–79, 2016.

[11] Y. Tanaka, S. Haruyama, and M. Nakagawa, "Wireless optical transmissions with white colored LED for wireless home links," in *Proc. 11th Symp. Pers. Indoor and Mobile Radio Commun (PIMRC)*, vol. 2. IEEE, 2000, pp. 1325–1329.

[12] T. Kishi, H. Tanaka, Y. Umeda, and O. Takyu, "A high-speed LED driver that sweeps out the remaining carriers for visible light communications," *J. Lightw. Technol.*, vol. 32, no. 2, pp. 239–249, 2014.

[13] A. B. Siddique and M. Tahir, "Joint rate-brightness control using variable rate MPPM for LED based visible light communication systems," *IEEE Trans. Wireless Commun.*, vol. 12, no. 9, pp. 4604–4611, 2013.

[14] J. M. Kahn and J. R. Barry, "Wireless infrared communications," *Proc. IEEE*, vol. 85, no. 2, pp. 265–298, 1997.

[15] M. Kavehrad, "Sustainable energy-efficient wireless applications using light," *IEEE Commun. Mag.*, vol. 48, no. 12, pp. 66–73, 2010.

[16] H. Elgala, R. Mesleh, and H. Haas, "Indoor optical wireless communication: potential and state-of-the-art," *IEEE Commun. Mag.*, vol. 49, no. 9, 2011.

[17] I. Din and H. Kim, "Energy-efficient brightness control and data transmission for visible light communication," *IEEE Photon. Technol. Lett.*, vol. 26, no. 8, pp. 781–784, 2014.

[18] S. Dimitrov and H. Haas, "Information rate of OFDM-based optical wireless communication systems with nonlinear distortion," *J. Lightw. Technol.*, vol. 31, no. 6, pp. 918–929, 2013.

[19] ——, *Principles of LED light communications: towards networked Li-Fi.* Cambridge University Press, 2015.

[20] J. Miyakoshi, "Cellular and molecular responses to radio-frequency electromagnetic fields," *Proc. IEEE*, vol. 101, no. 6, pp. 1494–1502, 2013.

[21] A. Khalid, G. Cossu, R. Corsini, P. Choudhury, and E. Ciaramella, "1-Gb/s transmission over a phosphorescent white LED by using rate-adaptive discrete multitone modulation," *IEEE Photon. J.*, vol. 4, no. 5, pp. 1465–1473, 2012.

[22] G. Cossu, A. Khalid, P. Choudhury, R. Corsini, and E. Ciaramella, "3.4 gbit/s visible optical wireless transmission based on RGB LED," *Opt. Express*, vol. 20, no. 26, pp. B501–B506, 2012.

[23] P. H. Pathak, X. Feng, P. Hu, and P. Mohapatra, "Visible light communication, networking, and sensing: A survey, potential and challenges," *IEEE Commun. Surveys Tuts.*, vol. 17, no. 4, pp. 2047–2077, 2015.

[24] Z. Wang, D. Tsonev, S. Videv, and H. Haas, "On the design of a solar-panel receiver for optical wireless communications with simultaneous energy harvesting," *IEEE J. Sel. Areas Commun.*, vol. 33, no. 8, pp. 1612–1623, 2015.

[25] T. Komine and M. Nakagawa, "Fundamental analysis for visible-light communication system using LED lights," *IEEE Trans. Consum. Electron.*, vol. 50, no. 1, pp. 100–107, 2004.

[26] F. R. Gfeller and U. Bapst, "Wireless in-house data communication via diffuse infrared radiation," *Proc. IEEE*, vol. 67, no. 11, pp. 1474–1486, 1979.

[27] Y. Qiu, H.-H. Chen, and W.-X. Meng, "Channel modeling for visible light communications—a survey," *Wireless Communications and Mobile Computing*, vol. 16, no. 14, 2016.

[28] A. Al-Kinani, C.-X. Wang, L. Zhou, and W. Zhang, "Optical wireless communication channel measurements and models," *IEEE Commun. Surveys Tuts.*, vol. 20, no. 3, pp. 1939–1962, 2018.

[29] S. Rajagopal, R. D. Roberts, and S.-K. Lim, "Ieee 802.15. 7 visible light communication: modulation schemes and dimming support," *IEEE Commun. Mag.*, vol. 50, no. 3, 2012.

[30] H. Le Minh, D. O'Brien, G. Faulkner, L. Zeng, K. Lee, D. Jung, Y. Oh, and E. T. Won, "100-mb/s nrz visible light communications using a postequalized white LED," *IEEE Photon. Technol. Lett.*, vol. 21, no. 15, pp. 1063–1065, 2009.

[31] G. Ntogari, T. Kamalakis, J. Walewski, and T. Sphicopoulos, "Combining illumination dimming based on pulse-width modulation with visible-light communications based on discrete multitone," *IEEE J. Opt. Commun. Netw.*, vol. 3, no. 1, pp. 56–65, 2011.

[32] B. Bai, Z. Xu, and Y. Fan, "Joint LED dimming and high capacity visible light communication by overlapping PPM," in *19th Annu. Wireless and Optical Commun. Conf. (WOCC).* IEEE, 2010, pp. 1–5.

[33] H. Sugiyama and K. Nosu, "MPPM: A method for improving the band-utilization efficiency in optical PPM," *J. Lightw. Technol.*, vol. 7, no. 3, pp. 465–472, 1989.

[34] T. Ohtsuki, I. Sasase, and S. Mori, "Overlapping multi-pulse pulse position modulation in optical direct detection channel," in *Proc. Int. Conf. Commun.*

Technical Program, Conf. Record, ICC'93 Geneva, vol. 2.   IEEE, 1993, pp. 1123–1127.

[35] H. Elgala, R. Mesleh, H. Haas, and B. Pricope, "OFDM visible light wireless communication based on white LEDs," in *IEEE 65th Veh. Technol. Conf. (VTC2007)-Spring.*   IEEE, 2007, pp. 2185–2189.

[36] M. Z. Afgani, H. Haas, H. Elgala, and D. Knipp, "Visible light communication using OFDM," in *2nd Int. Conf. Testbeds and Research Infrastructures for the Development of Networks and Communities, TRIDENTCOM.*   IEEE, 2006, pp. 6–pp.

[37] J. Armstrong and A. Lowery, "Power efficient optical OFDM," *Electron. Lett.*, vol. 42, no. 6, pp. 370–372, 2006.

[38] A. Lapidoth, S. M. Moser, and M. A. Wigger, "On the capacity of free-space optical intensity channels," *IEEE Trans. Inf. Theory*, vol. 55, no. 10, pp. 4449–4461, 2009.

[39] J. G. Smith, "The information capacity of amplitude-and variance-constrained sclar gaussian channels," *Information and Control*, vol. 18, no. 3, pp. 203–219, 1971.

[40] A. A. Farid and S. Hranilovic, "Channel capacity and non-uniform signalling for free-space optical intensity channels," *IEEE J. Sel. Area. Commun.*, vol. 27, no. 9, 2009.

[41] K.-I. Ahn and J. K. Kwon, "Capacity analysis of M-PAM inverse source coding in visible light communications," *J. Lightw. Technol.*, vol. 30, no. 10, pp. 1399–1404, 2012.

[42] J.-B. Wang, Q.-S. Hu, J. Wang, M. Chen, and J.-Y. Wang, "Tight bounds on channel capacity for dimmable visible light communications," *J. Lightw. Technol.*, vol. 31, no. 23, pp. 3771–3779, 2013.

[43] S. Buzzi, I. Chih-Lin, T. E. Klein, H. V. Poor, C. Yang, and A. Zappone, "A survey of energy-efficient techniques for 5G networks and challenges ahead," *IEEE J. Sel. Areas Commun.*, vol. 34, no. 4, pp. 697–709, 2016.

[44] R. Jain, D.-M. Chiu, and W. R. Hawe, *A quantitative measure of fairness and discrimination for resource allocation in shared computer system.* Eastern Research Laboratory, Digital Equipment Corporation Hudson, MA, 1984, vol. 38.

[45] L. Li, M. Pal, and Y. R. Yang, "Proportional fairness in multi-rate wireless LANs," in *IEEE 27th Conf. Computer Commun. (INFOCOM).* IEEE, 2008, pp. 1004–1012.

[46] M. Uchida and J. Kurose, "An information-theoretic characterization of weighted alpha-proportional fairness," in *IEEE INFOCOM.* IEEE, 2009, pp. 1053–1061.

[47] R. Zhang, H. Claussen, H. Haas, and L. Hanzo, "Energy efficient visible light communications relying on amorphous cells," *IEEE J. Sel. Areas Commun.*, vol. 34, no. 4, pp. 894–906, 2016.

[48] J. Grubor, S. Randel, K.-D. Langer, and J. W. Walewski, "Broadband information broadcasting using LED-based interior lighting," *J. Lightw. Technol.*, vol. 26, no. 24, pp. 3883–3892, 2008.

[49] S. Dimitrov, S. Sinanovic, and H. Haas, "Clipping noise in OFDM-based optical wireless communication systems," *IEEE Trans. Commun.*, vol. 60, no. 4, pp. 1072–1081, 2012.

[50] J. Gancarz, H. Elgala, and T. D. Little, "Impact of lighting requirements on VLC systems," *IEEE Commun. Mag.*, vol. 51, no. 12, pp. 34–41, 2013.

[51] S. Lou, C. Gong, N. Wu, and Z. Xu, "Joint dimming and communication design for visible light communication," *IEEE Commun. Lett.*, vol. 21, no. 5, pp. 1043–1046, 2017.

[52] K. Lee and H. Park, "Modulations for visible light communications with dimming control," *IEEE Photon. Technol. Lett.*, vol. 23, no. 16, pp. 1136–1138, 2011.

[53] "IEEE standard for local and metropolitan area networks–part 15.7: Short-range wireless optical communication using visible light," *IEEE Std 802.15.7.2011*, pp. 1–309, Sep. 2011.

[54] C. Chen, S. Videv, D. Tsonev, and H. Haas, "Fractional frequency reuse in DCO-OFDM-based optical attocell networks," *J. Lightw. Technol.*, vol. 33, no. 19, pp. 3986–4000, 2015.

[55] C. Li, W. Jia, Q. Tao, and M. Sun, "Solar cell phone charger performance in indoor environment," in *IEEE 37th Annu. Northeast Bioengineering Conference (NEBEC)*. IEEE, 2011, pp. 1–2.

[56] S. Boyd and L. Vandenberghe, *Convex Optimization*. Cambridge University Press, 2004.

[57] M. Grant and S. Boyd, "Cvx: Matlab software for disciplined convex programming," 2008.

[58] Z. Ding, X. Lei, G. K. Karagiannidis, R. Schober, J. Yuan, and V. K. Bhargava, "A survey on non-orthogonal multiple access for 5G networks: Research challenges and future trends," *IEEE J. Sel. Areas Commun.*, vol. 35, no. 10, pp. 2181–2195, 2017.

[59] Y. Liu, Z. Qin, M. Elkashlan, Z. Ding, A. Nallanathan, and L. Hanzo, "Nonorthogonal multiple access for 5G and beyond," *Proc. IEEE*, vol. 105, no. 12, pp. 2347–2381, 2017.

[60] Z. Ding, Z. Yang, P. Fan, and H. V. Poor, "On the performance of non-orthogonal multiple access in 5G systems with randomly deployed users," *IEEE Signal Process. Lett.*, vol. 21, no. 12, pp. 1501–1505, 2014.

[61] Y. Wang and H. Haas, "Dynamic load balancing with handover in hybrid Li-Fi and Wi-Fi networks," *J. Lightw. Technol.*, vol. 33, no. 22, pp. 4671–4682, Nov. 2015.

[62] L. Li, Y. Zhang, B. Fan, and H. Tian, "Mobility-aware load balancing scheme in hybrid vlc-lte networks," *IEEE Commun. Lett.*, vol. 20, no. 11, pp. 2276–2279, 2016.

[63] Y. Wang, D. A. Basnayaka, and H. Haas, "Dynamic load balancing for hybrid Li-Fi and RF indoor networks," in *IEEE Int. Conf. Commun. Workshops (ICCW)*, London, UK, 2015, pp. 1422–1427.

[64] M. Kassab, J. M. Bonnin, and A. Belghith, "Fast and secure handover in WLANs: An evaluation of the signaling overhead," in *Consumer Commun. and Netw. Conf. (CCNC) 5th IEEE.* IEEE, 2008, pp. 770–775.

[65] H. Haas, L. Yin, Y. Wang, and C. Chen, "What is lifi?" *J. Lightw. Technol.*, vol. 34, no. 6, pp. 1533–1544, 2016.

[66] M. Ayyash, H. Elgala, A. Khreishah, V. Jungnickel, T. Little, S. Shao, M. Rahaim, D. Schulz, J. Hilt, and R. Freund, "Coexistence of WiFi and LiFi toward 5G: concepts, opportunities, and challenges," *IEEE Commun. Mag.*, vol. 54, no. 2, pp. 64–71, 2016.

[67] I. Stefan and H. Haas, "Hybrid visible light and radio frequency communication systems," in *IEEE 80th Veh. Technol. Conf. (VTC Fall).* IEEE, 2014, pp. 1–5.

[68] D. A. Basnayaka and H. Haas, "Hybrid RF and VLC systems: Improving user data rate performance of VLC systems," in *Proc. IEEE Veh. Technol. Conf. (VTC Spring)*, Glasgow, UK, May 2015, pp. 1–5.

[69] X. Li, R. Zhang, and L. Hanzo, "Cooperative load balancing in hybrid visible light communications and WiFi," *IEEE Trans. Commun.*, vol. 63, no. 4, pp. 1319–1329, 2015.

[70] Y. Wang, D. A. Basnayaka, X. Wu, and H. Haas, "Optimization of load balancing in hybrid LiFi/RF networks," *IEEE Trans. Commun.*, vol. 65, no. 4, pp. 1708–1720, 2017.

[71] X. Wu, M. Safari, and H. Haas, "Joint optimisation of load balancing and handover for hybrid LiFi and WiFi networks," in *Proc. Wireless Commun. and Netw. Conf. (WCNC).* San Francisco, USA: IEEE, 2017, pp. 1–5.

[72] X. Wu and H. Haas, "Access point assignment in hybrid LiFi and WiFi networks in consideration of LiFi channel blockage," in *IEEE 18th Int. Workshop Signal Processing Advances in Wireless Commun. (SPAWC).* IEEE, 2017, pp. 1–5.

[73] X. Wu, D. Basnayaka, M. Safari, and H. Haas, "Two-stage access point selection for hybrid VLC and RF networks," in *Proc. 27th Annual Int. Symp. Pers. Indoor, and Mobile Radio Commun. (PIMRC).* IEEE, 2016, pp. 1–6.

[74] X. Wu, M. Safari, and H. Haas, "Access point selection for hybrid Li-Fi and Wi-Fi networks," *IEEE Trans. Commun.*, vol. 65, no. 12, pp. 5375–5385, 2017.

[75] Y. Wang, X. Wu, and H. Haas, "Fuzzy logic based dynamic handover scheme for indoor Li-Fi and RF hybrid network," in *Proc. Int. Conf. Commun. (ICC).* IEEE, 2016, pp. 1–6.

[76] ——, "Load balancing game with shadowing effect for indoor hybrid LiFi/RF networks," *IEEE Trans. Wireless Commun.*, vol. 16, no. 4, pp. 2366–2378, Apr. 2017.

[77] Y. Wang and H. Haas, "A comparison of load balancing techniques for hybrid LiFi/RF networks," in *Proc. 4th ACM Workshop on Visible Light Commun. Syst.* ACM, 2017, pp. 43–47.

[78] J. Wang, C. Jiang, H. Zhang, X. Zhang, V. C. Leung, and L. Hanzo, "Learning-aided network association for hybrid indoor LiFi-WiFi systems," *IEEE Trans. Veh. Technol.*, 2017.

[79] M. Obeed, A. M. Salhab, S. A. Zummo, and M.-S. Alouini, "Joint load balancing and power allocation for hybrid VLC/RF networks," in *Proc. IEEE Global Commun. Conf. (Globecom)*, Singapore, 2017.

[80] ——, "Joint optimization of power allocation and load balancing for hybrid VLC/RF networks," *IEEE/OSA J. Opt. Commun. and Netw.*, 2018.

[81] F. Kelly, "Charging and rate control for elastic traffic," *Trans. Emerg. Telecommun. Technol.*, vol. 8, no. 1, pp. 33–37, 1997.

[82] M. Kashef, M. Ismail, M. Abdallah, K. A. Qaraqe, and E. Serpedin, "Energy efficient resource allocation for mixed RF/VLC heterogeneous wireless networks," *IEEE J. Sel. Areas Commun.*, vol. 34, no. 4, pp. 883–893, 2016.

[83] D. W. K. Ng, E. S. Lo, and R. Schober, "Energy-efficient resource allocation in multi-cell ofdma systems with limited backhaul capacity," *IEEE Trans. Wireless Commun.*, vol. 11, no. 10, pp. 3618–3631, 2012.

[84] H. Wang, A. Liu, and X. Pan, "Optimization of joint power and bandwidth allocation in multi-spot-beam satellite communication systems," *Mathematical Problems in Engineering*, vol. 2014, pp. 1–9, 2014.

[85] X. Wu, M. Safari, and H. Haas, "Bidirectional allocation game in visible light communications," in *Proc. IEEE Veh. Technol. Conf. (VTC Spring)*, Montreal, Canada, 2016, pp. 1–5.

[86] A. Yesilkaya, E. Basar, F. Miramirkhani, E. Panayirci, M. Uysal, and H. Haas, "Optical MIMO-OFDM with generalized LED index modulation," *IEEE Trans. Commun.*, vol. 65, no. 8, pp. 2429–3441, 2017.

[87] J. Armstrong, "OFDM for optical communications," *J. Lightw. Technol.*, vol. 27, no. 3, pp. 189–204, 2009.

[88] K. Chitti, Q. Kuang, and J. Speidel, "Joint base station association and power allocation for uplink sum-rate maximization," in *2013 IEEE 14th Workshop on Signal Processing Advances in Wireless Communications (SPAWC)*. IEEE, jun 2013.

[89] R. Jiang, Q. Wang, H. Haas, and Z. Wang, "Joint user association and power allocation for cell-free visible light communication networks," *IEEE Journal on Selected Areas in Communications*, vol. 36, no. 1, pp. 136–148, jan 2018.

[90] H. Shen, Y. Deng, W. Xu, and C. Zhao, "Rate-maximized zero-forcing beamforming for VLC multiuser MISO downlinks," *IEEE Photon. J.*, vol. 8, no. 1, pp. 1–13, 2016.

[91] A. Nuwanpriya, S.-W. Ho, and C. S. Chen, "Indoor MIMO visible light communications: Novel angle diversity receivers for mobile users," *IEEE J. Sel. Areas Commun.*, vol. 33, no. 9, pp. 1780–1792, 2015.

[92] C. Chen, D. Tsonev, and H. Haas, "Joint transmission in indoor visible light communication downlink cellular networks," in *Proc. Global Commun. Conf. (Globecom)*. IEEE, 2013, pp. 1127–1132.

[93] L. Chen, W. Wang, and C. Zhang, "Coalition formation for interference management in visible light communication networks," *IEEE Trans. Veh. Technol.*, vol. 66, no. 8, pp. 7278–7285, 2017.

[94] C. Chen and H. Haas, "Performance evaluation of downlink cooperative multipoint joint transmission in LiFi systems," in *Proc. Globecom Workshops (GC Wkshps)*. IEEE, 2017, pp. 1–6.

[95] R. Zhang, J. Wang, Z. Wang, Z. Xu, C. Zhao, and L. Hanzo, "Visible light communications in heterogeneous networks: Paving the way for user-centric design," *IEEE Wireless Commun.*, vol. 22, no. 2, pp. 8–16, 2015.

[96] X. Li, F. Jin, R. Zhang, J. Wang, Z. Xu, and L. Hanzo, "Users first: User-centric cluster formation for interference-mitigation in visible-light networks," *IEEE Trans. Wireless Commun.*, vol. 15, no. 1, pp. 39–53, 2016.

[97] D. Arthur and S. Vassilvitskii, "K-means++: The advantages of careful seeding," in *Proc. 8th Annu ACM-SIAM Sympo. Discrete Algorithms.* Society for Industrial and Applied Mathematics, 2007, pp. 1027–1035.

[98] S. Feng, X. Li, R. Zhang, M. Jiang, and L. Hanzo, "Hybrid positioning aided amorphous-cell assisted user-centric visible light downlink techniques," *IEEE Access*, vol. 4, pp. 2705–2713, 2016.

[99] A. Zappone and E. Jorswieck, "Energy efficiency in wireless networks via fractional programming theory," *Foundations and Trends® in Communications and Information Theory*, vol. 11, no. 3-4, pp. 185–396, 2015.

[100] A. Zappone, L. Sanguinetti, G. Bacci, E. Jorswieck, and M. Debbah, "Energy-efficient power control: A look at 5g wireless technologies," *IEEE Transactions on Signal Processing*, vol. 64, no. 7, pp. 1668–1683, apr 2016.

[101] W. Dinkelbach, "On nonlinear fractional programming," *Manage. Sci.*, vol. 13, no. 7, pp. 492–498, 1967.

[102] D. W. K. Ng, E. S. Lo, and R. Schober, "Energy-efficient resource allocation in multi-cell OFDMA systems with limited backhaul capacity," *IEEE Trans. Wireless Commun.*, vol. 11, no. 10, pp. 3618–3631, 2012.

[103] B. Schrenk, M. Hofer, F. Laudenbach, H. Hübel, and T. Zemen, "Visible-light multi-Gb/s transmission based on resonant cavity LED with optical energy feed," *IEEE J. Sel. Areas Commun.*, vol. 36, no. 1, pp. 175–184, 2018.

[104] L. Yin and H. Haas, "Coverage analysis of multiuser visible light communication networks," *IEEE Transactions on Wireless Communications*, vol. 17, no. 3, pp. 1630–1643, mar 2018.

[105] M. Obeed, A. M. Salhab, M.-S. Alouini, and S. A. Zummo, "On optimizing vlc networks for downlink multi-user transmission: A survey."

[106] Y. Liu, Z. Ding, M. Elkashlan, and H. V. Poor, "Cooperative non-orthogonal multiple access with simultaneous wireless information and power transfer," *IEEE Journal on Selected Areas in Communications*, vol. 34, no. 4, pp. 938–953, apr 2016.

[107] M. Obeed, H. Dahrouj, A. M. Salhab, S. A. Zummo, and M.-S. Alouini, "DC-Bias and power allocation in cooperative VLC networks for joint information and energy transfer," *arXiv preprint arXiv:1812.11791*, 2018.

[108] M. Obeed, A. M. Salhab, S. A. Zummo, and M.-S. Alouini, "New algorithms for energy-efficient VLC networks with user-centric cell formation," *IEEE Trans. Green Commun. and Netw.*, 2018.

[109] T. Rakia, H.-C. Yang, F. Gebali, and M.-S. Alouini, "Optimal design of dual-hop VLC/RF communication system with energy harvesting," *IEEE Commun. Lett.*, vol. 20, no. 10, pp. 1979–1982, 2016.

[110] ——, "Dual-hop VLC/RF transmission system with energy harvesting relay under delay constraint," in *Globecom Workshops (GC Wkshps)*. IEEE, 2016, pp. 1–6.

[111] R. C. Kizilirmak, O. Narmanlioglu, and M. Uysal, "Relay-assisted OFDM-based visible light communications," *IEEE Trans. Commun.*, vol. 63, no. 10, pp. 3765–3778, oct 2015.

[112] R. C. Kizilirmak, C. R. Rowell, and M. Uysal, "Non-orthogonal multiple access (NOMA) for indoor visible light communications," in *4th Int. Workshop Opt. Wireless Commun. (IWOW)*.   IEEE, 2015, pp. 98–101.

[113] L. Yin, W. O. Popoola, X. Wu, and H. Haas, "Performance evaluation of non-orthogonal multiple access in visible light communication," *IEEE Trans. Commun.*, vol. 64, no. 12, pp. 5162–5175, 2016.

[114] Y. Yapici and I. Guvenc, "Non-orthogonal multiple access for mobile VLC networks with random receiver orientation," *arXiv preprint arXiv:1801.04888*, 2018.

[115] H. Marshoud, V. M. Kapinas, G. K. Karagiannidis, and S. Muhaidat, "Non-orthogonal multiple access for visible light communications," *IEEE Photon. Technol. Lett*, vol. 28, no. 1, pp. 51–54, 2016.

[116] X. Zhang, Q. Gao, C. Gong, and Z. Xu, "User grouping and power allocation for NOMA visible light communication multi-cell networks," *IEEE Commun. Lett.*, vol. 21, no. 4, pp. 777–780, 2017.

[117] E. Perahia and R. Stacey, *Next Generation Wireless LANs.*   Cambridge University Press, 2013.

[118] P. D. Diamantoulakis, G. K. Karagiannidis, and Z. Ding, "Simultaneous light-wave information and power transfer (SLIPT)," *IEEE Trans. Green Commun. and Netw.*, 2018.

[119] J. Zhu, J. Wang, Y. Huang, S. He, X. You, and L. Yang, "On optimal power allocation for downlink non-orthogonal multiple access systems," *IEEE Journal on Selected Areas in Communications*, pp. 1–1, 2017.

[120] W. Yu, T. Kwon, and C. Shin, "Multicell coordination via joint scheduling, beamforming and power spectrum adaptation," in *2011 Proceedings IEEE IN-FOCOM.* IEEE, apr 2011.

[121] H. W. Kuhn, "The hungarian method for the assignment problem," *Naval research logistics quarterly*, vol. 2, no. 1-2, pp. 83–97, 1955.

[122] R. King, D. Bhusari, D. Larrabee, X.-Q. Liu, E. Rehder, K. Edmondson, H. Cotal, R. Jones, J. Ermer, C. Fetzer *et al.*, "Solar cell generations over 40% efficiency," *Prog. Photovoltaics Res. Appl.*, vol. 20, no. 6, pp. 801–815, 2012.

[123] J. Fakidis, S. Videv, S. Kucera, H. Claussen, and H. Haas, "Indoor optical wireless power transfer to small cells at nighttime," *J. Lightw. Technol.*, vol. 34, no. 13, pp. 3236–3258, 2016.

[124] Y. Li, N. Huang, J. Wang, Z. Yang, and W. Xu, "Sum rate maximization for VLC systems with simultaneous wireless information and power transfer," *IEEE Photonics Technol. Lett.*, vol. 29, no. 6, pp. 531–534, 2017.

[125] A. M. Abdelhady, O. Amin, A. Chaaban, and M. S. Alouini, "Resource allocation for outdoor visible light communications with energy harvesting capabilities," in *Proc. IEEE Globecom Workshops (GC Wkshps)*, Dec 2017, pp. 1–6.

[126] G. Pan, H. Lei, Z. Ding, and Q. Ni, "On 3-D hybrid VLC-RF systems with light energy harvesting and OMA scheme over RF links," 2017.

[127] C. Carvalho and N. Paulino, "On the feasibility of indoor light energy harvesting for wireless sensor networks," *Procedia Technol.*, vol. 17, pp. 343–350, 2014.

[128] H. G. Sandalidis, A. Vavoulas, T. A. Tsiftsis, and N. Vaiopoulos, "Illumination, data transmission, and energy harvesting: the threefold advantage of VLC," *Appl. Opt.*, vol. 56, no. 12, pp. 3421–3427, 2017.

[129] M. Obeed, A. M. Salhab, S. A. Zummo, and M.-S. Alouini, "Joint power allocation and cell formation for energy-efficient VLC networks," in *Proc. IEEE Int. Conf. Commun. (ICC)*, Kansas, USA, 2018.

[130] J.-B. Wang, Q.-S. Hu, J. Wang, M. Chen, and J.-Y. Wang, "Tight bounds on channel capacity for dimmable visible light communications," *J. Lightw. Technol.*, vol. 31, no. 23, pp. 3771–3779, 2013.

[131] M. S. Alam, J. W. Mark, and X. S. Shen, "Relay selection and resource allocation for multi-user cooperative ofdma networks," *IEEE Transactions on Wireless Communications*, vol. 12, no. 5, pp. 2193–2205, 2013.

[132] S.-L. Shieh, C.-H. Lin, Y.-C. Huang, and C.-L. Wang, "On gray labeling for downlink non-orthogonal multiple access without SIC," *IEEE Commun. Lett.*, vol. 20, no. 9, pp. 1721–1724, 2016.

[133] S.-L. Shieh and Y.-C. Huang, "A simple scheme for realizing the promised gains of downlink nonorthogonal multiple access," *IEEE Trans. Commun.*, vol. 64, no. 4, pp. 1624–1635, 2016.

[134] Y. Liu, Z. Qin, M. Elkashlan, Y. Gao, and L. Hanzo, "Enhancing the physical layer security of non-orthogonal multiple access in large-scale networks." *IEEE Trans. Wireless Communications*, vol. 16, no. 3, pp. 1656–1672, 2017.

[135] Y. Zhang, H.-M. Wang, Q. Yang, and Z. Ding, "Secrecy sum rate maximization in non-orthogonal multiple access," *IEEE Commun. Lett.*, vol. 20, no. 5, pp. 930–933, 2016.

[136] I. Lee, F. Kung, and M. Sim, "Performance enhancement of outdoor visible-light communication system using selective combining receiver," *IET Optoelectronics*, vol. 3, no. 1, pp. 30–39, feb 2009.

[137] M. S. Islim, S. Videv, M. Safari, E. Xie, J. J. D. McKendry, E. Gu, M. D. Dawson, and H. Haas, "The impact of solar irradiance on visible light communications," *J. Lightw. Technol.*, vol. 36, no. 12, pp. 2376–2386, jun 2018.

[138] Y.-J. Zhu, Z.-G. Sun, J.-K. Zhang, and Y.-Y. Zhang, "A fast blind detection algorithm for outdoor visible light communications," *IEEE Photon. J.*, vol. 7, no. 6, pp. 1–8, dec 2015.

[139] B. G. Guzman, V. P. G. Jimenez, M. C. Aguayo-Torres, H. Haas, and L. Hanzo, "Downlink performance of optical OFDM in outdoor visible light communication," *IEEE Access*, vol. 6, pp. 76 854–76 866, 2018.

VITAE

- Name: Mohanad Obeed

- Nationality: Yemen

- Date of Birth: 1 Jan. 1985

- Email: *mhndbaz@gmail.com, g201106250@kfupm.edu.sa*

- Permenant Address: Al-Ganad, Taiz, Yemen

- B.Eng. degree in computer and communication engineering, Taiz University, Taiz, Yemen, in 2008

- M.Sc. degree in electrical engineering, King Fahd University of Petroleum and Minerals (KFUPM), Dhahran, Saudi Arabia, in 2016.

- *Journal Papers (Published/Submitted)*

  [1] Mohanad Obeed, Anas M. Salhab, Mohamed-Slim Alouini, and Salam A. Zummo, "On Optimizing VLC networks for Downlink Multi-User Transmission: a Survey,", IEEE Commun. Survey & Tutorials, 2019.

[2] Mohanad Obeed, Anas M. Salhab, Salam A. Zummo, and Mohamed-Slim Alouini, "Joint Optimization of Power Allocation and Load Balancing for Hybrid VLC/RF Networks," J. Opt. Commun. Netw., OSA/IEEE, 10, 553-562 (2018).

[3] Mohanad Obeed, Anas M. Salhab, Salam A. Zummo and Mohamed-Slim Alouini "New Algorithms for Energy-Efficient VLC Networks with User-Centric Cell Formation" IEEE Trans. Green Commun. & Netw. 2018, doi: 10.1109/TGCN.2018.2886605

[4] Mohanad Obeed, and Wessam Mesbah. "Efficient algorithms for physical layer security in two-way relay systems." Physical Communication; Elsevier, 28 (2018): 78-88.

[5] Mohanad Obeed, and Wessam Mesbah. "Efficient algorithms for physical layer security in one-way relay systems." Wireless networks; Springer, 2018: 1-13.

[6] Mohanad Obeed, Hayssam Dahrouj, Anas M. Salhab, Salam A. Zummo and Mohamed-Slim Alouini, " DC-Bias and Power Allocation in Cooperative VLC Networks for Joint Information and Energy Transfer" to be appeared in IEEE Trans. Wireless Commun 2018.

- *Conference Papers (Published/Accepted)*

[1] Mohanad Obeed, and Wessam Mesbah. "An efficient physical layer security algorithm for two-way relay systems." Wireless Communications and Networking Conference (WCNC), 2016 IEEE.

[2] Mohanad Obeed, Anas M. Salhab, Salam A. Zummo, and Mohamed-Slim Alouini. "Joint Load Balancing and Power Allocation for Hybrid VLC/RF Networks." In Proc. GLOBECOM 2017-2017 IEEE Global Communications Conference, pp. 1-6. IEEE, 2017.

[3] Mohanad Obeed, Anas M. Salhab, Salam A. Zummo, and Mohamed-Slim Alouini, "Joint power allocation and cell formation for energy-efficient VLC networks," IEEE International conference on communications (ICC), 2018 (pp. 1-6).

[4] Mohanad Obeed, and Wessam Mesbah. "Improving physical layer security in two-way relay systems." International Conference on Telecommunication (ICT), IEEE, 2018.

[5] Mohanad Obeed, Hayssam Dahrouj, Anas M. Salhab, Salam A. Zummo and Mohamed-Slim Alouini, "DC-Bias Allocation in Cooperating VLC Networks for Information and Energy Transfer" In GLOBECOM 2018 IEEE Global Communications Conference, Abu Dhabi.

[6] Mohanad Obeed, Anas M. Salhab, Mohamed-Slim Alouini, and Salam A. Zummo, "Survey on Physical Layer Security in Optical Wireless Communication Systems," IEEE ComNet, 2018, Hammamet.

- *In Preparation*

[1] Mohanad Obeed, Hayssam Dahrouj, Anas M. Salhab, Salam A. Zummo and Mohamed-Slim Alouini, "User Pairing, Link Selection and Power Allocation for Cooperative NOMA Hybrid VLC/RF Systems".

206